A STUDY OF MOLECULAR STRUCTURE AND INTERNAL ROTATION IN AMIDES BY NUCLEAR MAGNETIC RESONANCE SPECTROSCOPY

Thesis for the Degree of Ph. D.
MICHIGAN STATE UNIVERSITY
LESTER REINHARDT ISBRANDT
1972

# This is to certify that the

# thesis entitled

A STUDY OF MOLECULAR STRUCTURE
AND INTERNAL ROTATION IN AMIDES
BY NUCLEAR MAGNETIC RESONANCE SPECTROSCOPY

presented by
LESTER REINHARDT ISBRANDT

has been accepted towards fulfillment of the requirements for

PH.D. degree in CHEMISTRY

Major professo

Date 10.27-72

O-7639



LIBRARY
Michigan State
University

#### ABSTRACT

# A STUDY OF MOLECULAR STRUCTURE AND INTERNAL ROTATION IN AMIDES BY NUCLEAR MAGNETIC RESONANCE SPECTROSCOPY

BY

#### Lester Reinhardt Isbrandt

High-resolution nuclear magnetic resonance (NMR) methods have been employed in a series of studies of molecular structure and internal motions in amides. A Varian HA-100 NMR spectrometer was used to obtain both proton and carbon-13 spectra.

Activation parameters for internal rotation about the central C-N bond in six previously studied N,N-dimethylamides, RCON(CH<sub>3</sub>)<sub>2</sub> (R=H,D,-CH<sub>3</sub>,-CH<sub>2</sub>CH<sub>3</sub>,Cl,CCl<sub>3</sub>), have been redetermined from proton NMR spectra by total lineshape analysis. The NMR method for carrying out the analysis has been improved by the digitization of the experimental spectra followed by computer curve fitting of the lineshapes to the theoretical lineshape equation containing all the NMR parameters as adjustable variables. The agreement between the activation parameters determined in this study and the literature values obtained by total lineshape analysis is quite good and establishes the reliability of the method.

Internal rotation about the central C-N bond in a series of four unsymmetrically N,N-disubstituted amides,  $CH_3CON(CH_3)R$  (R=ethyl, isopropyl,  $\underline{n}$ -butyl, and cyclohexyl), have been obtained by the proton NMR total lineshape technique developed for the study of the N,N-dimethylamides. Steric effects appear to be of particular importance and larger

groups, whether substituted on carbon or nitrogen, consistently reduce the rotational barrier.

Application of lanthanide shift reagents has been proven to be a reliable method of assigning the NMR resonances, proton or carbon-13, to substituents on the <u>cis</u> and <u>trans</u> rotational isomers of disubstituted amides. Assignments have been made in the proton NMR spectra for a representative series of amides and in the carbon-13 NMR spectrum of N,N-din-propylformamide.

The carbon-13 NMR chemical shifts of fifty monosubstituted and disubstituted amides have been measured. Assignments have been made by the use of model systems and the application of lanthanide shift reagents. The chemical shift difference between carbon atoms of groups  $\underline{cis}$  and  $\underline{trans}$  to carbonyl oxygen in disubstituted amides is greatest for the  $\alpha$ -carbon,  $\underline{ca}$ . 5.1 ppm in formamides and  $\underline{ca}$ . 3.5 ppm in alkylamides, and decreases for carbons farther away from the carbonyl group.

# A STUDY OF MOLECULAR STRUCTURE AND INTERNAL ROTATION IN AMIDES BY NUCLEAR MAGNETIC RESONANCE SPECTROSCOPY

Ву

Lester Reinhardt Isbrandt

# A THESIS

Submitted to

Michigan State University
in partial fulfillment of the requirements

for the degree of

DOCTOR OF PHILOSOPHY

Department of Chemistry

G19080

To Pamie

#### ACKNOWLEDGEMENTS

The author would like to express sincere appreciation to Professor Max T. Rogers for his guidance, encouragement, and patience during the course of this study.

The financial support of the Dow Chemical Company, the National Science Foundation, and the Chemistry Department during the various parts of this study are gratefully acknowledged.

To Pamela, my wife, whose ever-present smile, encouragement, and self-sacrifice enabled me to complete this phase of my education, I offer my deepest appreciation.

# TABLE OF CONTENTS

	Page
INTRODUCTION	1
HISTORICAL	3
Determination of Barriers in Amides	4
Assignments of Resonances in Amides	
Application of Carbon-13 NMR Spectroscopy to Amides	
Additivity of Carbon-13 Chemical Shifts	
THEORETICAL	14
• • • • • • • • • • • • • • • • • • •	1/
Introduction	
Spin-Spin and Spin-Lattice Relaxation	
NMR Lineshape Theory	
The Lineshape Equation with Exchange	
Chemical Shifts	
Nuclear Spin-Spin Coupling	
Proton Decoupling	
Nuclear Overhauser Enhancement	
Lanthanide Induced Chemical Shifts	
Zanchanida inadada onemidal bullab ///////////////////////////////////	-
EXPERIMENTAL	34
Preparation of Compounds	34
Physical Constants of Compounds Studied	
Spectrometer	
Time Averaging and Digitization of Spectra	
Sample Preparation	
Bulk Diamagnetic Susceptibility Corrections	45
Determination of Energy Barriers of Hindered	
Internal Rotations	46
RESULTS	48
KESULIS	40
Hindered Internal Rotation in Tertiary Amides	48
Symmetrically Disubstituted Amides	48
N,N-Dimethylacetamide	48
N,N-Dimethylcarbamylchloride	55
N,N-Dimethylformamide	55
$N, N-Dimethylformamide-d_1 \dots \dots$	55
N, N-Dimethylpropionamide	62
N, N-Dimethyltrichloroacetamide	62

# TABLE OF CONTENTS - Continued

	Page
Unsymmetrically Disubstituted Amides	
N-Ethyl-N-methylacetamide	
N- <u>n</u> -Butyl-N-methylacetamide	
N-Cyclohexyl-N-methylacetamide	. 62
N-Isopropyl-N-methylacetamide	. 73
Resonance Assignments in the Proton NMR Spectra of	
Several Tertiary Amides	. 73
1-Methyl-2-pyrrolidinone	
N, N-Dimethylformamide	
N, N-Diethylformamide	
N, N-Diisopropylformamide	
N, N-Dimethylacetamide	
N,N-Dimethylcarbamylchloride	
N, N-Dimethyltrichloroacetamide	
N,N-Dimethyltrifluoroacetamide	
Ethyl-N,N-dimethylcarbamate	
N-Isopropyl-N-methylformamide	
Carbon-13 Chemical Shifts of Aliphatic Amides	
Monosubstituted Amides	. 93
Symmetrically Disubstituted Amides	
	-
Unsymmetrically Disubstituted Amides	. 100
DISCUSSION	. 103
Hindered Internal Rotation	• 103
Total Lineshape Analysis	• 103
The Frequency Factor in the Arrhenius Equation	• 104
Rotational Barriers in N, N-Disubstituted Amides	
Resonance Assignments in Tertiary Amides by	
Lanthanide-induced Shifts	. 111
Carbon-13 Chemical Shifts of Amides	
SUMMARY	. 119
LIST OF REFERENCES	. 120

# LIST OF TABLES

ABLE		Page
1.	Reported activation parameters for hindered rotation in N,N-dimethylformamide	. 5
2.	Reported activation parameters for hindered rotation in some other dimethylamides	. 7
3.	Substituent parameters correlating alkane carbon-13 chemical shifts in ppm	. 12
4.	Shielding effects of some common substituents in aliphatic systems	. 13
5.	N-monosubstituted amides studied	. 36
6.	N,N-Dimethylamides studied	. 37
7.	Other symmetrically N, N-disubstituted amides studied	. 38
8.	Unsymmetrically N,N-disubstituted amides studied	. 39
9.	Volume magnetic susceptibilities and bulk magnetic susceptibility corrections for several compounds	. 45
10.	Experimental data and calculated activation parameters for the internal rotation about the central C-N bond in neat N,N-dimethylacetamide	. 53
11.	Experimental data and calculated activation parameters for the internal rotation about the central C-N bond in neat N,N-dimethylcarbamylchloride	. 56
12.	Experimental data and calculated activation parameters for the internal rotation about the central C-N bond in neat N,N-dimethylformamide - Method I	. 58
13.	Experimental data and calculated activation parameters for the internal rotation about the central C-N bond in neat N,N-dimethylformamide - Method II	• 60
14.	Experimental data and calculated activation parameters for the internal rotation about the central C-N bond in neat N.N-dimethylformamide-d <sub>1</sub>	. 63

# LIST OF TABLES - Continued

<b>CABLE</b>		Page
15.	Experimental data and calculated activation parameters for the internal rotation about the central C-N bond in neat N,N-dimethylpropionamide	65
16.	Experimental data and calculated activation parameters for the internal rotation about the central C-N bond in neat N,N-dimethyltrichloroacetamide	67
17.	Experimental data and calculated activation parameters for the internal rotation about the central C-N bond in neat N-ethyl-N-methylacetamide	69
18.	Experimental data and calculated activation parameters for the internal rotation about the central C-N bond in neat N-n-butyl-N-methylacetamide	71
19.	Experimental data and calculated activation parameters for the internal rotation about the central C-N bond in neat N-cyclohexyl-N-methylacetamide	74
20.	Experimental data and calculated activation parameters for the internal rotation about the central C-N bond in neat N-isopropyl-N-methylacetamide	76
21.	Proton chemical shifts, observed and calculated, in 1-methyl-2-pyrrolidinone with increasing amounts of Eu(fod) <sub>3</sub>	79
22.	Proton chemical shifts, observed and calculated, in N,N-dimethylformamide with increasing amounts of Eu(fod) <sub>3</sub>	80
23.	Proton chemical shifts, observed and calculated, in N,N-diethylformamide with increasing amounts of Eu(fod) <sub>3</sub>	81
24.	Proton chemical shifts, observed and calculated, in N,N-diisopropylformamide with increasing amounts of Eu(fod) <sub>3</sub>	83
25.	Proton chemical shifts, observed and calculated, in N,N-dimethylacetamide with increasing amounts of Eu(fod) <sub>3</sub>	84
26.	Proton chemical shifts, observed and calculated, in N,N-dimethylacetamide with increasing amounts of Pr(fod) 2	85

# LIST OF TABLES - Continued

rable		Page
27.	Proton chemical shifts, observed and calculated, in N,N-dimethylcarbamylchloride with increasing amounts of Eu(fod) <sub>3</sub>	87
28.	Proton chemical shifts, observed and calculated, in N,N-dimethyltrichloroacetamide with increasing amounts of Eu(fod) <sub>3</sub>	88
29.	Proton chemical shifts, observed and calculated, in N,N-dimethyltrifluoroacetamide with increasing amounts of Eu(fod) <sub>3</sub>	89
30.	Proton chemical shifts, observed and calculated, in ethyl-N,N-dimethylcarbamate with increasing amounts of Eu(fod) <sub>3</sub>	90
31.	Proton chemical shifts, observed and calculated, in N-isopropyl-N-methylformamide with increasing amounts of Eu(fod) <sub>3</sub>	92
32.	Carbon-13 chemical shifts of some N-monosubstituted amides	94
33.	Carbon-13 chemical shifts of some N,N-dimethylamides	96
34.	Carbon-13 chemical shifts of some other symmetrically N,N-disubstituted amides	97
35.	Assignments of carbon-13 chemical shifts for the N-alkyl substituents of N,N-di-n-propylformamide in carbon tetrachloride	99
36.	Carbon-13 chemical shifts of some unsymmetrically N,N-disubstituted amides	101
37.	Activation parameters for hindered internal rotation in some symmetrically N,N-disubstituted amides	106
38.	Activation parameters for hindered internal rotation in some unsymmetrically N,N-disubstituted amides	107
39.	Conformer equilibria in unsymmetrically N,N-disubstituted amides	111
40.	△Eu values for some N,N-disubstituted amides	113
41.	Proton resonance assignments in some N,N-disubstituted amides	114

# LIST OF FIGURES

FIGURE	3	Page
1.	Resonance in amides	. 1
2.	The amide group and conformers of substituted amides	. 3
3.	Energy-level diagram for an AX two-spin system in presence of a magnetic field	. 29
4.	Carbon-13 NMR spectrum of N,N-diethylpropionamide	. 42
5.	Observed (X) and calculated (O) signals of the N-methyl protons in neat N,N-dimethylacetamide at $T = 325.7$ °K	. 49
6.	Observed (X) and calculated (O) signals of the N-methyl protons in neat N,N-dimethylacetamide at T = 340.1°K	. 50
7.	Observed (X) and calculated (O) signals of the N-methyl protons in neat N,N-dimethylacetamide at T = 343.0°K	. 51
8.	Observed (X) and calculated (O) signals of the N-methyl protons in neat N,N-dimethylacetamide at $T=348.5^{\circ}K$	. 52
9.	Plot of $ln(1/2\tau)$ against $10^3/T^{\circ}K$ for neat N,N-dimethylacetamide	. 54
10.	Plot of $\ln(1/2\tau)$ against $10^3/\text{T}^{\circ}\text{K}$ for neat N,N-dimethyl-carbamylchloride	. 57
11.	Plot of $ln(1/2\tau)$ against $10^3/T^\circ K$ for neat N,N-dimethylformamide - Method I	. 59
12.	Plot of $\ln(1/2\tau)$ against $10^3/T^\circ K$ for neat N,N-dimethylformamide - Method II	. 61
13.	Plot of $\ln(1/2\tau)$ against $10^3/T^\circ K$ for neat N,N-dimethylformamide-d <sub>1</sub>	. 64
14.	Plot of $\ln(1/2\tau)$ against $10^3/T^\circ K$ for neat N,N-dimethyl-propionamide	. 66
15.	Plot of $\ln(1/2\tau)$ against $10^3/T^\circ K$ for neat N,N-dimethyltrichloroacetamide	. 68
16.	Plot of $ln(1/2\tau)$ against $10^3/T^{\circ}K$ for neat N-ethyl-N-methylacetamide	. 70

# LIST OF FIGURES - Continued

FIGURE	Page
<pre>17. Plot of ln(1/2τ) against 10<sup>3</sup>/T°K for neat N-n-butyl-N- methylacetamide</pre>	72
18. Plot of ln(1/2τ) against 10 <sup>3</sup> /T°K for neat N-cyclohexyl-N-methylacetamide	75
19. Plot of ln(1/2τ) against 10 <sup>3</sup> /T°K for neat N-isopropyl-N-methylacetamide	77

#### INTRODUCTION

Amides have been studied more extensively by nuclear magnetic resonance (NMR) spectroscopy than nearly any other class of compounds. Substantial stimulus arises from the importance of amide linkages in peptide chains and proteins, as well as interest in the electronic structure of a carbonyl group partially conjugated with a nitrogen lone pair. Most of the NMR studies are concerned with this partial double-bond character in the central C-N bond. The double-bond character resulting from a contribution of resonance structure II to the ground state of amides (1) leads to restricted rotation about the C-N bond.

Figure 1. Resonance in amides.

As a result of the nonequivalence, geometrically and magnetically, of the nitrogen substituents, even when  $R_1 = R_2$ , the NMR spectra provide a great deal of information about the amide structure. The NMR investigations of amides have largely involved identification and assignment of conformers, measurements of scalar coupling constant and chemical shift values and their interpretation, and study of hindered internal rotation.

A comprehensive presentation of the subject including preparations and molecular properties of amides, may be found in "The Chemistry of Amides", edited by Zabicky (2).

The research reported in this thesis consists of the following:

(1) re-examination of the proton NMR method for determining rotational energy barriers of several N,N-dimethylamides by total lineshape analysis; (2) examination of the rotational energy barriers of a series of unsymmetrically N,N-disubstituted amides by proton NMR using total lineshape analysis; (3) assignment of the proton NMR resonances of amides by the application of lanthanide shift reagents; (4) the investigation of carbon-13 chemical shifts in a series of N-monosubstituted, symmetrically N,N-disubstituted and unsymmetrically N,N-disubstituted amides.

# HISTORICAL

The present knowledge of the molecular structure of the amide group is

$$\begin{array}{c|c}
C - N & R_1 (A) & O \\
R_3 & C - N & R_2 (B) & R_3 & R_1 (B)
\end{array}$$
III IV

Figure 2. The amide group and conformers of substituted amides.

founded largely upon the results of x-ray and electron diffraction analysis, while that of the electronic structure is derived from spectroscopic experiments (ultraviolet, infrared, nuclear magnetic resonance, microwave) and the results of various semi-empirical and <u>ab initio</u> quantum mechanical calculations (2).

X-ray structure analyses of a variety of crystalline amides established the planarity of the amide framework (3-5). Formamide (6) has been shown by microwave spectroscopy to have a slightly pyramidal conformation about the nitrogen atom in the gas phase while N,N-dimethylformamide is essentially planar (7). However, the pyramidal conformations will invert very rapidly, so that formamide and simple substituted amides, even if slightly non-planar, would appear effectively planar in NMR studies.

Pauling (1) postulated that the rotation about the central C-N bond of amides would be restricted due to the partial double-bond character in this bond. As a result of this double-bond character, the environments of the nitrogen substituents are not averaged, and should be observed separately by NMR spectroscopy. This was confirmed by Phillips (8) from a proton NMR study of N,N-dimethylformamide and N,N-dimethylacetamide. Gutowsky and Holm (9) developed the first application of NMR signal analysis to the determination of energy barriers in a study of internal rotation in N,N-dimethylformamide and N,N-dimethylacetamide. They obtained the rotation rates,  $2\tau$ , as a function of temperature and fit them to an Arrhenius-type equation,  $1/2\tau = A \exp(-E_A/RT)$ , to obtain an energy barrier  $E_A$  and frequency factor A; a single parameter, the apparent peak separation for the N-methyl peaks, was used.

Woodbrey and Rogers (10,11) followed with an extensive study of dimethylamides, and were able to correlate the activation energy of the barrier with structure. A single parameter, the ratio of maximum to central minimum in the partially coalesced peaks, was used in the analysis.

#### Determination of Barriers in Amides

These early investigations were the beginning of numerous examinations and re-examinations of the hindered internal rotation problem in amides by NMR spectroscopy. Table 1 shows that the barrier for N,N-dimethylformamide has been determined over and over again, producing random numbers between the extremes of 6.3 and 28.2 kcal/mole for the activation energy, E<sub>2</sub>, and 4.6 and 17.2 for the logarithm of the frequency

Table 1. Reported activation parameters for hindered rotation in N,N-dimethylformamide.

Solvent	E a kcal/mole	Log A (A = sec <sup>-1</sup> )	Method <sup>a</sup>	Reference
Hexachloro- ethane	6.3 ± 0.3	4.60 ± 0.01	A	32
Neat	7 ± 3	3-7	A	9
Hexamethyl- disiloxane	9.4 ± 1.0		A	33
Neat	9.6 ± 1.5	6.5	A,B,C	34
CFC1 <sub>3</sub>	11.3 ± 2.0		A	33
Neat	15.9 ± 2.0	16.8 ± 2.0	A	33
Acetone-d <sub>6</sub>	16.8 ± 2.0		A	33
Neat	18.3 ± 0.7	10.8 ± 0.4	С	11
Neat	18.7 ± 0.9	11.8 ± 0.6	С	35
CC1 <sub>4</sub>	20.5 ± 0.2	12.7 ± 0.5	D	25
Neat	22.0	13	$A,B,C^{b}$	36
Neat	26	16	A,B,C	37
Neat	27.4	16	$A,B,C^{C}$	36
Neat	28.2 ± 2	17.2	A	38
Formamide	26.3 ± 2.6	15.5 ± 1.5	С	35

 $<sup>^{\</sup>mathbf{a}}\mathbf{A}$  - Peak separation approximation.

B - Line width approximation.

C - Other approximate treatment.

D - Total line-shape analysis.

<sup>&</sup>lt;sup>b</sup>Spectra taken at 100 MHz.

<sup>&</sup>lt;sup>C</sup>Dimethylformamide-d<sub>1</sub>.

factor, log A. It was shown (12) that all the approximate NMR methods tended to introduce systematic errors into the values of the rotational barriers, and the results of Table 1 dramatize the shortcomings of applying approximate formulas and single-parameter methods. The entire subject of the barrier to rotation in amides has been reviewed extensively by Johnson (13), Binsch (14), Stewart and Siddall (15,16), Kessler (17), and Lowe (18). The conclusion drawn by these authors is that the best method for the determination of energy barriers in amides is by total lineshape analysis and all other methods must be viewed with suspicion. In the total lineshape method, the experimental spectrum is compared point by point with the theoretical spectrum calculated from modified Bloch equations; the rotation rate  $\tau$ , chemical shift in the absence of exchange  $\delta \nu$ , fractions of conformers  $p_A$ ,  $p_R$ , and linewidths in the absence of exchange  $T_{2A}$ ,  $T_{2R}$ , are taken to be adjustable parameters and a computer method employed to obtain best values of each of them from the These authors point out that extreme care is required in measuring the high-resolution NMR spectrum at each temperature. The radiofrequency field must be set well below saturation, the sweep rate must be extremely slow to insure minimal distortion in the lineshape, and the temperature at which the spectrum is recorded must be very stable. If these measures are not taken into account, the recorded lineshapes will be non-Lorentzian and curve-fitting to the theoretically calculated lineshape will lead to erroneous NMR parameters. Total lineshape analysis has now been used by several research groups (19-31) for the determination of barriers in various amides and the activation parameters which have been reported for the amides that have been re-examined in this research are listed in Table 2.

Table 2. Reported activation parameters for hindered rotation in some other dimethylamides.

Compound	E a kcal/mole	$\frac{\text{Log A}}{\text{(A = sec}^{-1})}$	$\Delta G^{\sharp d}$ kcal/mole	∆H <sup>‡</sup> kcal/mole	*8	Reference
N,N-Dimethylacetamide	10.6 ± 0.4 12 ± 2 23.0 20.2 19.6 16.8 26 19.0 ± 0.1	7.8 ± 0.2 7-10 16.0 16.1 13.8	17.4 19 18.7 15.7 18.2 17.8 21 18.1 ± 0.1	19.0 16.3 18.3 ± 0.1	+2.7 -3.6 0.7 ± 1	11 9 37 38 30a 21b 45 113
N,N-Dimethylpropionamide	$9.2 \pm 0.7$ $21.0$ $16.6 \pm 0.1$	7.3 ± 0.5 15.0	16.7 16.6 17.2 ± 0.1	20.4 16.0 ± 0.1	12.7 -4.1 ± 1	11 37 113
N,N-Dimethylcarbamylchloride	7.3 ± 0.5 14.0 ± 0.9 16.9 ± 0.5 17.6 ±	6.1 ± 0.3 10.9 ± 0.6 12.9 ± 0.4	16.4 16.6 16.8 16.8	6.7 ± 0.5 13.4 ± 0.9 16.3 ± 0.5 17.0 ± 0.5	-27.1 ± 2 -10.6 ± 2.7 -1.6 ± 2.0 0.8 ± 1.6	11 39 <sup>c</sup> 40 21
N,N-Dimethyltrichloroacetamide	9.9 ± 0.3 14.6 ± 0.6 15.7 ± 0.1 16.6 ± 0.8	9.1 ± 0.2 12.5 ± 0.4 13.3	14.9 15.0 17.6	15.1 ± 0.1	0.3 ± 0.3	11 39 <sup>c</sup> 26 30

aN,N-Dimethylacetamide-ds.

bl4.9 mole % in CCl4.

CAnalyzed by spin-echo method.

dSee page 22, Equations (22) and (23).

Although symmetrically N,N-disubstituted amides have been rather intensively investigated, relatively few measurements have been made on unsymmetrically substituted compounds. Rotational barriers in three formamides,  $HCON(CH_3)R[R = \phi CH_2$ -,  $\phi_2CH$ - and  $\phi C(CH_3)H$ -] were determined by Franconi (41) who found no significant difference among the three within the rather large errors involved. Gehring et al. (38) reported activation parameters for five compounds and showed that a large decrease in the barrier occurs when one of the substituents is the vinyl group. Gutowsky et al. (29) made a study of N-methyl-N-benzylformamide, Weil et al. (42) of N-methyl-N-picrylacetamide, and Mannschreck et al. (43,44) of N-mesityl substituted amides.

# Assignment of Resonances in Tertiary Amides

Except in a few cases where there is chemical shift degeneracy, the <a href="cis">cis</a> (to oxygen) and the <a href="trans">trans</a> substituents on nitrogen give well separated NMR signals whenever rotation around the C-N bond is slow on the NMR time scale. The principal cause of the chemical shift between the <a href="cis">cis</a> and <a href="trans">trans</a> NMR signals is the anisotropy of the magnetic susceptibility of the amide grouping (46). The chemical shift is observed whether substitution on the nitrogen atom is symmetrical or unsymmetrical. Assignment of the observed resonances to protons at sites A,B has been of considerable interest and is particularly important in the case of unsymmetrical substitution, when it serves to identify the isomers, III and IV (Figure 2). Also, the values of the proton chemical shifts for groups <a href="cis">cis</a> or <a href="trans">trans</a> to oxygen yield information on the structure of the amide molecule, as well as the nature of the adducts and complexes that it forms with other molecules.

Several criteria have been used to identify the proton resonances for  $R_1$  and  $R_2$  as <u>cis</u> or <u>trans</u>. These include: (a) inequality of the <u>cis</u> and <u>trans</u> coupling constants (47) for the protons of  $R_3$  with those of  $R_1$  and  $R_2$ , (b) differential solvent shifts in an aromatic solvent (48,49), (c) the nuclear Overhauser effect (50,51), and (d) contact shifts induced by complex formation with paramagnetic metal ions (124). Most of these methods are quite limited in scope of application and the assignments may not be unequivocal (51), particularly when  $R_3, R_1, R_2$  are larger groups.

# Application of Carbon-13 NMR Spectroscopy to Amides

Very limited attention has been given to the carbon-13 NMR spectroscopy of amides compared to proton NMR since the low natural abundance (1.1%) of the carbon-13 isotope and the reduced magnetogyric ratio ( $\gamma_{\rm C}/\gamma_{\rm H}=0.251$ ) combine to greatly reduce the detectability of the carbon-13 NMR signal. The signal-to-noise ratio may be significantly enhanced with proton decoupling techniques, increased sample size, and utilization of time-averaging techniques. The instrumentation necessary for, and chemical applications of, carbon-13 NMR spectroscopy have been recently discussed by Stothers (52) and by Randall (53).

The first reported observation of the carbon-13 resonance in amides was made by Lauterbur (54), who observed the carbon-13 chemical shifts in N,N-dimethylformamide. McFarlane (55) reported the carbon-13 chemical shift difference between N-methyl carbons in N,N-dimethylformamide, N,N-dimethylacetamide, and N,N-dimethylcarbamylchloride in five different solvents of various dielectric strengths. The chemical shift differences were invariant to the choice of solvent. He pointed out that the

principal contribution to the carbon-13 chemical shift differences between the N-methyl carbons in these amides arises from an intramolecular electric field. This field will also affect the proton chemical shifts, although to a smaller extent, since it is the paramagnetic contribution to the shielding which is involved.

Levy and Nelson (56) studied the spin-lattice relaxation times in N,N-dimethylformamide, N,N-di-n-butylformamide, and N,N-di-n-butylacetamide by carbon-13 Fourier transform NMR spectroscopy. They found significant carbon steric compression shifts for the four aliphatic carbons trans to the formyl hydrogen and eclipsing the carbonyl oxygen in N,N-di-n-butylformamide. These steric shifts range from over 5 ppm for the α-carbon to ca. 0.1 ppm for the δ-carbon on the same chain. Carbon spin-lattice relaxation behavior in N,N-di-n-butylformamide indicated that the ends of both butyl chains have significantly increased motional freedom.

Gansow, Killough, and Burke (31) studied hindered internal rotation in N,N-dimethyltrichloroacetamide by carbon-13 NMR spectroscopy. Their results are comparable to the best activation parameters by proton NMR. However, they pointed out several experimental shortcomings of the technique. First, the reported spectra were the absolute limit of the carbon-13 NMR sensitivity and several thousand scans were necessary. Second, as lines broaden or as measurements are performed at higher temperature, sensitivity drops dramatically for two reasons: (a) Boltzmann populations readjust, and (b) as a result of the large low-temperature chemical shift difference, broadening and coalescence occur over a large spectral area.

# Additivity of Carbon-13 Chemical Shifts

Grant and Paul (57) found that alkanes absorb over a range of approximately 45 ppm and also discovered that the chemical shifts could be described by the relation

$$\delta_{c}^{i} = B + \sum_{j} A_{j}^{n}_{ij} , \qquad (1)$$

where  $\delta_c^i$  is the ith carbon-13 shift, A an additive shift parameter for the jth position,  $n_{ij}$  is the number of atoms in the jth positions, and B is a constant. For linear alkanes five parameters (A,) correlate 30 shifts ranging over 37 ppm, with a standard deviation ( $\sigma$ ) of 0.2 ppm. For the branched alkanes additional parameters are required to account for the shieldings of highly substituted carbons and their immediate neighbors. With a total of 13 parameters, 53 measured chemical shifts are correlated with  $\sigma$  = 0.3 ppm. Five of these parameters, labeled  $\alpha$ ,  $\beta$ ,  $\gamma$ ,  $\delta$ , and  $\epsilon$  factors, represent the effect of replacing a hydrogen atom in the indicated position with a methyl group while the remainder account for the effects of branching; for example, a factor for methyl carbons bonded to a tertiary carbon is denoted 1°(3°). These substituent parameters are listed in Table 3. The constant B has the value -2.5 ppm. illustrate the manner in which these parameters may be employed, consider C-2 of 3-methylpentane for which  $\delta_c$  is given by [B +  $2\alpha$  +  $2\beta$  +  $\gamma$  + 2°(3°)] = 29.5 ppm, while  $\delta_c^{OBS}$  = 29.3 ppm (57).

Several families of substituted hydrocarbons have been examined by this empirical method and the general trends follow those found for hydrocarbons, with the additional feature that polar substituents exhibit

Table 3. Substituent parameters correlating alkane carbon-13 chemical shifts<sup>a</sup> in ppm<sup>b</sup>.

α	9.1 ± 0.1	1°(3°)	-1.1 ± 0.2
β	9.4 ± 0.1	1°(4°)	$-3.4 \pm 0.4$
γ	-2.5 ± 0.1	2°(3°)	$-2.5 \pm 0.2$
δ	0.3 ± 0.1	3°(2°)	$-3.7 \pm 0.2$
E	0.1 ± 0.1	4°(1°)	$-1.5 \pm 0.1$

aReference 57

rather larger inductive deshielding effects at the immediate neighbors (i.e., the  $\alpha$  and  $\beta$  effects) while the  $\gamma$  effects are comparable to those of methyl groups. To illustrate the effects produced by a selection of substituents, some representative results are given in Table 4 most of which were obtained from the data for 1-substituted alkanes.

Perhaps the most distinctive feature of these substituent parameters is the change for the effect of a  $\gamma$ -methyl carbon with respect to the  $\alpha$  and  $\beta$  effects. The original proposal by Grant and Paul (57) that the  $\gamma$  effects are caused by conformational interactions appears to be sound, since it is generally observed that carbon atoms in sterically congested environments tend to absorb at higher fields than those in otherwise comparable orientations.

In this and the following Table, a positive value indicates a shift to low field. Values from single observations: 2°(4°), -7.2; 3°(3°), -9.5; 4°(2°), -8.4. Symbols are defined in the text.

Table 4. Shielding effects a of some common substituents in aliphatic systems.

	_α_	_β_	<u> </u>	δ	<u> </u>	Reference
C1	31.2	10.5	-4.6	0.1	0.5	58
Br	20.0	10.6	-3.1	0.1	0.5	58
I	-6.0	11.3	-1.0	0.2	1.0	58
NH <sub>2</sub>	29.3	11.3	-4.6	0.6	0.6	58
1° OH ,	48.3	10.2	-5.8	0.3	0.1	59
2°b	40.8	7.7	-3.7	0.2	0.3	59
СООН	20.9	2.5	-2.2	1.0	1.2	60
coo	24.4	4.1	-1.6	1.2		60
RCO	30	1	-2	1		61

<sup>&</sup>lt;sup>a</sup>In ppm.

bExcluding 2-alcohols, RCHOHCH<sub>3</sub>.

#### THEORETICAL

## Introduction

Nuclear magnetic resonance is a spectroscopic phenomenon observed only for nuclei which possess a magnetic moment,  $\widehat{\widetilde{\mu}}$ , given by

$$\widetilde{\widetilde{\mu}} = \gamma \widetilde{\widetilde{p}} = \gamma \widetilde{\widetilde{I}} h/2\pi \quad , \tag{2}$$

where  $\gamma$  is the magnetogyric ratio of the nucleus,  $\widetilde{p}$  is the angular momentum of the nucleus, h is Planck's constant,  $\widetilde{I}$  is the nuclear spin vector, given by  $\widetilde{I} = I(I+1)$ , and I is the spin quantum number. When the nucleus is placed in a uniform magnetic field, there are (2I+1) energy levels available, each corresponding to a different component of the angular momentum with values I, I-1,...-I+1, -I. The absorption or emission of an appropriate quantum of energy,

$$\Delta E = h_{\nu} = \gamma h H_{O} / 2\pi = \mu H_{O} / I , \qquad (3)$$

will enable the nucleus to make a transition from one energy level to an adjacent level.

In order to observe an energy transition the population of the energy levels must be different. For an ensemble of nuclei the relative populations are given by the Boltzmann factor

$$\frac{N_{+}}{N} = \exp[(2I+1)m\mu H_{o}/IkT] \simeq \frac{1}{2I+1}(1 - \frac{m\mu H_{o}}{IkT}) , \qquad (4)$$

where m is the nuclear magnetic quantum number with values I, I-1,...

-I+1, -I, k is the Boltzmann constant, and T is the absolute temperature.

After the nuclei have undergone a transition, some mechanism is required whereby nuclei in an upper spin state can relax to a lower state so that the absorption of energy may continue.

# Spin-Spin and Spin-Lattice Relaxation

Spin-lattice relaxation is a process by which a nucleus in an upper spin state may give up energy to the lattice in the form of translational or rotational energy. Random molecular motions of magnetic nuclei result in fluctuating magnetic fields, which may have an oscillating component whose frequency will match the precessional frequency of the magnetic nuclei in the upper spin state. When the two are in phase, the nucleus will be able to lose its extra energy to the lattice and drop to a lower energy level.

The rate that magnetic nuclei of spin I=1/2 approach their equilibrium distribution,  $n_0$ , is given by

$$\frac{\mathrm{d}n}{\mathrm{d}t} = \frac{1}{\mathrm{T}_1} (\mathrm{n}_0 - \mathrm{n}) \quad , \tag{5}$$

where  $T_1$  is the spin-lattice relaxation time, and n is the excess population of the lower energy state at time t. The magnitude of  $T_1$  depends on the magnetogyric ratio of the nucleus and on the nature of the molecular

motions. The reciprocal of  $T_1$  gives an approximate measure of the line width due to spin-lattice relaxation.

Another type of relaxation is by spin-spin interaction. The precession of a magnetic nucleus about the fixed axis of a uniform magnetic field,  $\widetilde{\mathbb{H}}_0$ , may be resolved into a static component parallel to  $\widetilde{\mathbb{H}}_0$  and a rotating component parallel to  $\widetilde{\mathbb{H}}_0$ . When the rotating component is at the correct frequency, there is an exchange of spin energy between two neighboring nuclei. Spin-spin relaxation thus results in no net change of spin state. The spin-spin relaxation time is further decreased by the small variation in the local field at each nucleus due to the fields of neighboring nuclei. The small local magnetic fields will add to or subtract from the applied field,  $\widetilde{\mathbb{H}}_0$ , resulting in a larger range of frequencies at which nuclei of the same type will absorb energy.

Rapid rotation and tumbling, as found in most liquids and gases, will average the local magnetic fields so that  $T_1$  and  $T_2$  become equivalent.

# NMR Lineshape Theory

To describe the time dependent variation of the components of the total nuclear magnetic moment per unit volume, Bloch used a set of phenomenological equations (62). Bloch considers a nucleus with  $|\widetilde{\widetilde{\mathbf{I}}}| = (h/2\pi)$ .  $|\widetilde{\mathbf{I}}| = (h/2\pi)$  and magnetic moment  $\widetilde{\mu} = \gamma \widetilde{\widetilde{\mathbf{I}}}$  as a tiny gyroscope. The forces it experiences in an external constant magnetic field in the z direction,  $\widetilde{\widetilde{\mathbf{H}}} = \{0,0,\mathbf{H}_0\}$ , cause it to move in such a way that the rate of change is given by the torque

$$\frac{d\widetilde{\mu}}{dt} = \gamma \left[ \widetilde{\mu} \times \widetilde{\widetilde{H}} \right] , \qquad (6)$$

with components

$$d\mu_{\mathbf{x}}/d\mathbf{t} = \gamma [\mu_{\mathbf{y}}^{\mathbf{H}}_{\mathbf{z}} - \mu_{\mathbf{z}}^{\mathbf{H}}_{\mathbf{y}}] = \gamma \mathbf{H}_{\mathbf{z}} \mu_{\mathbf{y}}$$
 (6a)

$$d\mu_{y}/dt = \gamma [\mu_{z}H_{x} - \mu_{x}H_{z}] = -\gamma H_{z}\mu_{x}$$
 (6b)

$$d\mu_z/dt = \gamma [\mu_x H_y - \mu_y H_x] = 0$$
 (6c)

These equations indicate that the nuclear moment  $\widetilde{\mu}$  precesses about the z-axis with an angular frequency  $\omega_0 = \gamma H_0$  in a clockwise fashion. In a sample containing a large number of identical dipoles, all will precess with angular frequency  $\omega_0$ , but their phases will be randomly distributed over a cone about the z-axis. The resultant macroscopic magnetization will therefore only have a component in the z direction,  $\widetilde{M}_0 = \{0,0,M_0\}$ .

If the system is disturbed by a second magnetic field,  $\widetilde{H}_1$ , rotating in the xy plane with an angular frequency  $\omega$ , in the neighborhood of  $\omega_0$ , and in the same sense as the precessional motion of the nuclei so that  $\widetilde{H}_1 = \{H_1 \cos \omega t, -H_1 \sin \omega t, 0\}$ , then the x and y components of  $\widetilde{M}$  will become different from zero. The quantitative description is

$$\frac{d\widetilde{\widetilde{M}}}{dt} = \gamma [\widetilde{\widetilde{M}} \times \widetilde{\widetilde{H}}] , \qquad (7)$$

with  $\widetilde{\mathbb{H}} = \{\mathbb{H}_1 \cos \omega t, -\mathbb{H}_1 \sin \omega t, 0\}$ . Instead of using the fixed laboratory coordinate system, it is useful to refer the components of the total magnetization to a set of axes rotating about  $\widetilde{\mathbb{H}}_0$  with angular frequency  $\omega$ . In this rotating frame  $\widetilde{\mathbb{H}}_1$  is stationary, causing the time dependence of the right-hand side of Equation (7) to vanish. With  $\widetilde{\mathbb{H}}_1$  coinciding with

the rotating x-axis, the components become

$$dM_{x}/dt = (\omega_{o} - \omega)M_{y}$$
 (7a)

$$dM_{v}/dt = -(\omega_{o}-\omega)M_{x} + \gamma H_{1}M_{z}$$
 (7b)

$$dM_z/dt = -\gamma H_1 M_v . (7c)$$

Equation (7c) shows that the M magnetization is responsible for a change in M and thus in the net nuclear Zeeman energy of the system. M corresponds to the absorption mode, and M describes the dispersion mode signal. Both effects can be expressed in a single equation if one defines the magnetization in the xy plane by the complex quantity

$$G = M_{x} + iM_{y} , \qquad (8)$$

so that Equations (7a) and (7b) can be combined to

$$\frac{dG}{dt} = -i(\omega_0 - \omega)G + i\gamma H_1 M_z \qquad (9)$$

The description of Equations (7) is still incomplete, since it only takes cognizance of  $\widetilde{\mathbb{H}}_0$  and  $\widetilde{\mathbb{H}}_1$ , and ignores all other factors that might influence  $\widetilde{\mathbb{M}}$ . The combined action of such factors is referred to as relaxation, which was discussed previously. The complete Bloch equations taking relaxation into account are

$$\frac{dG}{dt} = -i(\omega_0 - \omega)G + i\gamma H_1 M_z - G/T_2$$
 (10a)

$$\frac{dM_z}{dt} = -\gamma H_1 M_y - (M_z - M_o)/T_1 . \qquad (10b)$$

The Lineshape Equation with Exchange

The Bloch equation can be modified to include the effect of exchanging nuclei (63,64). Consider a proton that can reside in two different environments, A and B, with chemical shifts  $\nu_{\rm A}=(\omega_{\rm A}/2\pi)$  and  $\nu_{\rm B}=(\omega_{\rm B}/2\pi)$ , and that jumps back and forth between A and B. A jump from A to B results in a decrease of magnetization in site A and a jump from B to A results in an increase. A corresponding statement holds for the change of magnetization of B. McConnell (64) assumed that both the forward and reverse reactions can be described by first-order rate laws with rate constants  $k_{\rm A\to B}=1/\tau_{\rm A}$  and  $k_{\rm B\to A}=1/\tau_{\rm B}$ , where  $\tau_{\rm A}$  and  $\tau_{\rm B}$  are the mean lifetimes at sites A and B, respectively. The Bloch equations for the sites A and B may therefore be modified to read

$$\frac{dG_A}{dt} = -[i(\omega_A - \omega) + 1/T_{2A}]G_A + i\gamma H_1 M_z^A - G_A/\tau_A + G_B/\tau_B$$
 (11a)

$$\frac{dG_B}{dt} = -[i(\omega_B - \omega) + 1/T_{2B}]G_B + i\gamma H_1 M_z^B - G_B/\tau_B + G_A/\tau_A . \quad (11b)$$

Assuming that the system is in a state of equilibrium, the mean lifetimes in sites A and B must have the same ratio as the corresponding fractional populations p,

$$\tau_{A}/\tau_{B} = p_{A}/p_{B} . \qquad (12)$$

In addition it is convenient to introduce a new variable

$$\tau = \tau_A P_B = \tau_B P_A \quad . \tag{13}$$

If one sweeps slowly through the resonance ("slow passage") the magnetizations will manage to follow "isothermally", that is, they become stationary. It is also assumed that saturation is avoided by choosing a low H<sub>1</sub> field. These experimental conditions imply

$$\frac{dG_{A}}{dt} = \frac{dG_{B}}{dt} = 0; M_{z}^{A} = M_{o}^{A} = p_{A}M_{o}; M_{z}^{B} = M_{o}^{B} = p_{B}M_{o}.$$
 (14)

Combining Equations (14) with (11) the modified Bloch equations become linear equations in  $G_A$  and  $G_R$ :

$$-[i(\omega_{A}-\omega) + 1/T_{2A} + p_{B}/\tau]G_{A} + \frac{p_{A}}{\tau}G_{B} = -ip_{A}\gamma H_{1}M_{0}$$
 (15a)

$$\frac{P_B}{\tau} G_A - [i(\omega_B - \omega) + 1/T_{2B} + P_A/\tau] G_B = -iP_B \gamma H_1 M_0 . \qquad (15b)$$

These are easily solved if one defines

$$\alpha_{\Delta} = -[2\pi i(\nu_{\Delta} - \nu) + 1/T_{2\Delta} + p_{R}/\tau]$$
 (16a)

$$\alpha_{\rm B} = -[2\pi i(\nu_{\rm B} - \nu) + 1/T_{2_{\rm B}} + p_{\rm A}/\tau]$$
 (16b)

$$C = \gamma H_1 M_0 , \qquad (17)$$

where  $v_A$  and  $v_B$  are the chemical shifts in hertz relative to some standard and C may be taken as an arbitrary scaling factor; the total transverse magnetization,  $G = G_A + G_B$ , is given by

$$G = \frac{-iC\tau[2p_A^p_B - \tau(p_A^\alpha_B + p_B^\alpha_A)]}{p_A^p_B - \tau^2\alpha_A^\alpha_B}$$
 (18)

The real part of Equation (18) gives the dispersion u mode lineshape function and the imaginary part gives the absorption v mode lineshape function over the entire sweep range  $\nu$  as a function of the parameters  $\nu_A$ ,  $\nu_B$ ,  $T_{2_A}$ ,  $T_{2_B}$ ,  $P_A$ ,  $P_B$ , and  $\tau$ . These functions may be written as (11)

$$u = \frac{-C(QP - [1 + \tau(p_B/T_{2A} + p_A/T_{2B})]R)}{P^2 + R^2}$$
 (19a)

$$v = \frac{-C[P[1 + \tau(p_B/T_{2A} + p_A/T_{2B})] + QR]}{P^2 + R^2} .$$
 (19b)

The quantities P, Q, and R are defined for convenience as

$$P = \tau \left[ \frac{1}{T_{2}} T_{2} - (2\pi)^{2} \Delta v^{2} + (2\pi)^{2} (\delta v/2)^{2} \right] + p_{B}/T_{2} + p_{A}/T_{2}$$
 (20a)

$$Q = 2\pi\tau \left[\Delta \nu - \frac{\delta \nu}{2} \left( p_A - p_B \right) \right]$$
 (20b)

$$R = 2\pi\Delta\nu[1 + \tau(1/T_{2}_{A} + 1/T_{2}_{B})] + \pi\tau\delta\nu(1/T_{2}_{B} - 1/T_{2}_{A})$$
 (20c) 
$$+ \pi\delta\nu(p_{A} - p_{B}) ,$$

where  $\Delta v = v - v_0$ ,  $v_0$  is the average resonance frequency of  $v_A$  and  $v_B$ , and  $\delta v = v_A - v_B$ .

### Activation Parameters

The activation energy for the exchange process in N,N-disubstituted amides can be evaluated from the Arrhenius rate equation which is written as (65,66)

$$k = A \exp(-E_a/RT) , \qquad (21)$$

where k is the rate constant which is equal the inverse of twice the mean lifetime  $(\tau)$ , R is the molar gas constant, A is the frequency factor, and  $E_a$  is the activation energy for internal rotation or the energy barrier of the system. The quantities A and  $E_A$  can be evaluated by a linear least-squares analysis from the experimental data for each amide.

If one assumes that this exchange process obeys the absolute rate equation (66), the entropy and enthalpy of activation,  $\Delta S^{\ddagger}$  and  $\Delta H^{\ddagger}$ , for the internal rotation process can be written as

$$k = \kappa \frac{k_B T}{h} \exp(-\Delta H^{\dagger}/RT) \exp(\Delta S^{\dagger}/R) , \qquad (22)$$

where  $\kappa$  is the transmission coefficient, which is unity when every activated complex breaks up to give products,  $k_B$  is the Boltzmann constant, and h is Planck's constant. The free energy of activation at temperature  $T^{\circ}K$  can be found from the relationship

$$\triangle G_{\mathbf{T}}^{\ddagger} = \triangle \mathbf{H}^{\ddagger} - \mathbf{T} \triangle \mathbf{S}^{\ddagger} . \tag{23}$$

### Chemical Shifts

Chemical shifts, for molecules without unpaired electrons, have their origin in the magnetic screening of the nucleus which arises from the orbital electronic currents induced by an external magnetic field (67). These currents also give rise to diamagnetic polarization. When the external magnetic field is  $H_0$  the total magnetic moment of the induced current is  $\chi_M^{H_0}$  where  $\chi_M^{H_0}$  is the molecular diamagnetic susceptibility. The secondary magnetic field due to the induced currents at any given nucleus is  $-\sigma_1^{H_0}$  where  $\sigma_1^{H_0}$  is the magnetic screening constant. The total field experienced by a given nucleus, which determines its NMR frequency, is given by (68)

$$H_i = H_0(1 - \sigma_i) \quad . \tag{24}$$

The chemical shift may then be defined as

$$\delta \text{ (ppm)} = \frac{\text{H}_{i} - \text{H}_{ref}}{\text{H}_{ref}} \times 10^{6} , \qquad (25)$$

where H<sub>i</sub> is the resonant field of resonance being measured at a fixed frequency and H<sub>ref</sub> is the resonant field for a given reference. The chemical shift may also be defined in terms of frequency as

$$\delta \text{ (ppm)} = \frac{v_i - v_{ref}}{v_{ref}} \times 10^6 , \qquad (26)$$

where  $v_i$  is the resonant frequency of a signal being measured at a fixed field and  $v_{ref}$  is the resonant frequency for a given reference.

From Equation (24) it is seen that the differences in the shieldings of various nuclei are reflected by the differences in the screening constants. The theory of screening constants first proposed by Saika and Slichter (60) gives an atomic breakdown of diamagnetic currents. The total screening constant for any atom A may be broken down into the following four terms:

$$\sigma_{\mathbf{A}} = \sigma_{\mathbf{d}}^{\mathbf{A}\mathbf{A}} + \sigma_{\mathbf{p}}^{\mathbf{A}\mathbf{A}} + \sum_{\mathbf{B}(\neq \mathbf{A})} \sigma^{\mathbf{A}\mathbf{B}} + \sigma^{\mathbf{A}, \mathbf{ring}} . \tag{27}$$

The first term,  $\sigma_{\mathbf{d}}^{\mathrm{AA}}$ , is the contribution to the secondary magnetic field at nucleus A due to diamagnetic currents on atom A itself. For an isolated spherical atom, it is the only contribution and is given explicitly by the Lamb formula,

$$\sigma_{\rm d}^{\rm AA} = \frac{\rm e^2}{3{\rm mc}^2} \sum_{\rm i} \overline{r_{\rm i}^{-1}} , \qquad (28)$$

where e is the charge of the electron, m is the electron mass, c is the velocity of light, and  $r_i$  is the distance of the ith electron from the nucleus, the sum being over all the electrons.

The second term,  $\sigma_p^{AA}$ , is the contribution due to the paramagnetic currents on atom A, which gives the paramagnetic susceptibility. This term was first calculated by Saika and Slichter who showed that for fluorine atoms it was much more sensitive to chemical structure than  $\sigma_d^{AA}$ . For most other nuclei, variations in this term will give the main contribution to the chemical shift. The principal exception is hydrogen, where the absence of low-lying atomic p-orbitals will make the paramagnetic term negligibly small.

The third term,  $\int_{B(A)}^{AB}$ , is the contribution to the screening of atom B(A). A by the atomic circulations on atom B. When the magnetic effects of these neighboring currents are treated in a dipole approximation, this term involves only the local anisotropy of the local susceptibility on atom B. If atom A is on, or near, the axis of high diamagnetism of B, there will be an increase in the average screening. The effect falls off as the inverse cube of the AB distance.

Finally,  $\sigma^{A,ring}$  is the contribution of the screening due to ring currents which cannot be localized on any atom. The magnitude of this term is usually small, except it does play an important part in determining the proton spectra of aromatic compounds.

For carbon-13 chemical shifts the last two terms are relatively unimportant, and calculations of the diamagnetic term,  $\sigma_{\bf d}^{AA}$ , show that it is fairly constant for different types of carbon atoms. The paramagnetic term,  $\sigma_{\bf p}^{AA}$ , is therefore the dominant term in the expression for the calculation of the shielding for the carbon-13 nucleus (70). Considerable attention has been paid to the evaluation of this term using quantum mechanical treatments (71,72).

### Nuclear Spin-Spin Coupling

In 1951 Gutowsky, McCall, and Slichter observed that high resolution spectra frequently exhibited hyperfine structure which, in contrast to the linear dependence of chemical shifts, was independent of the applied magnetic field (73,74). Similar effects had been observed by Hahn and Maxwell in the modulation of the spin-echo envelope in the pulse experiments (75). It was concluded that the observed effects were caused by an indirect

interaction of the nuclear moments  $\mu_i$ , which is transmitted from nucleus to nucleus by the paired electrons comprising the valence bonds. The magnitude of this interaction is called the spin-spin coupling constant, J.

The interaction can be theoretically divided into three parts (76). In the first of these, one nuclear magnetic moment induces orbital electronic currents which consequently induce magnetic fields at the site of the second nucleus. In the second, the electron spin interacts with the magnetic moment of one nucleus producing an electron spin polarization which is then transferred to the adjoining nuclei. The third part, and the most significant contribution to the overall spin-spin coupling, is the Fermi contact interaction between nuclear spins and the spins of electrons in s-orbitals, which produces an electron spin polarization proportional to the density of the electrons at the nucleus.

In molecular orbital theory the spin-spin coupling constant,  $J_{AB}$ , may be written in terms of the wave functions of the ground and excited states,  $\psi_i$  and  $\psi_j$  (77). Summing over occupied and unoccupied levels for i and j, respectively,

$$J_{AB} \alpha - \sum_{i}^{\text{occ. unocc.}} \frac{(\psi_{i}\psi_{j})_{A} (\psi_{i}\psi_{j})_{B}}{(\epsilon_{j} - \epsilon_{i})} , \qquad (29)$$

where  $(\epsilon_j - \epsilon_i)$  is the energy difference between the occupied ground state  $\epsilon_i$  and unoccupied excited states  $\epsilon_j$ , and is always positive. From the above expression the sign of the coupling constant depends on whether the molecular orbital is symmetric or asymmetric. The symmetric molecular orbitals have the same sign at atom A and atom B, and the asymmetric molecular orbitals have different signs. For transitions from symmetric to symmetric or from asymmetric to asymmetric molecular orbitals, the

contribution to  $J_{AB}$  is negative. Transitions from symmetric to asymmetric molecular orbitals, or vice versa, gives a positive contribution to the coupling constant.

## Proton Decoupling

Spin decoupling, for the case where the coupled nuclei are of different species, involves the application of a second radiofrequency field oscillating at the resonance frequency of the nucleus to be decoupled.

This causes the nucleus to change spin states so rapidly that its spin vector no longer couples with the spin vectors of neighboring nuclei and multiplets due to this coupling collapse.

In a simple AX molecule, the elimination of proton-induced splittings can only be expected to collapse a doublet into a singlet, giving an enhancement of two-fold. Collapse of splittings in more complex molecules such as benzene can result in a signal-enhancement figure approaching an order of magnitude (78). The carbon-13 magnetic resonance spectrum of benzene (79) exhibits considerable proton splitting beyond the large doublet due to the directly bonded proton. These splittings are due to the long-range couplings between a carbon-13 and the remaining hydrogens in the molecule. The elimination of such complex splitting patterns leads to a dramatic improvement in the signal-to-noise ratio. As most organic molecules contain an even greater number of protons, benzene is by no means an exception to the rule, and multiplet collapse can be considered to give rise to about a 10-fold enhancement.

It should be pointed out that such techniques eliminate much useful information in the carbon-13 spectrum, such as the coupling constants

between carbon and hydrogen. However, it may also be argued that the chemical shift information obtained under proton decoupling conditions is more readily acquired and interpreted. Elimination of proton splittings leads to spectral singlets which are free from all second-order changes in line positions, and therefore shift data are obtained directly from the position of the spectral singlet. Also, the number of directly bonded, geminal, and vicinal protons in most organic molecules will produce splitting patterns of the carbon-13 resonance signal much more complicated than is found in the corresponding proton resonance bonds. Thus, it is concluded that the loss of spectral information may in many instances be more than offset by the benefits of spectral simplicity, which allows the chemical shift information to be obtained more readily and, in general, on a larger number of chemical systems.

In addition to the enhancement due to multiplet collapse, proton decoupling techniques give rise to a nuclear Overhauser enhancement.

## Nuclear Overhauser Enhancement

When the protons in a sample are decoupled by a strong irradiating field, the effect on the carbon-13 NMR spectrum is an enhancement of the carbon-13 signal due to a phenomenon known as the nuclear Overhauser effect (NOE). The NOE results from dynamic polarization of the carbon-13 nuclei when the proton resonances are saturated. This effect has been well studied in carbon-13 (80,81,82) and in nitrogen-15 (83) NMR.

The energy level diagram of a general two-spin system in a magnetic field is given in Figure 3 where the energy levels in the absence of a radiofrequency field have a Boltzmann distribution. When one nucleus is

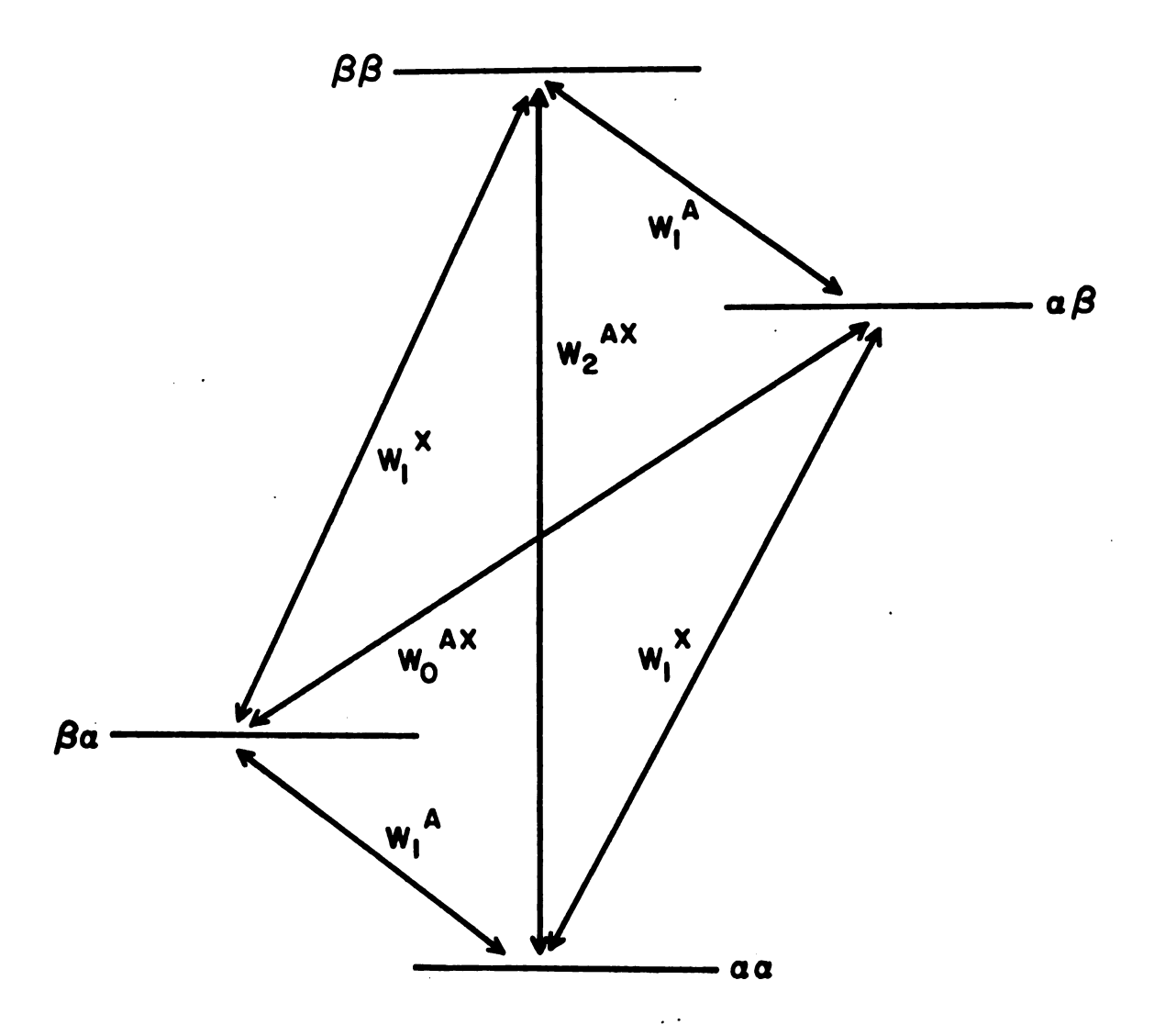


Figure 3. Energy-level diagram for an AX two-spin system in presence of a magnetic field.

irradiated by a radiofrequency field the other nucleus is enhanced by the nuclear Overhauser enhancement,  $\theta$ , of

$$\theta = 1 + \eta_{A-\{x\}} , \qquad (30)$$

where

$$\eta_{A-\{x\}} = (\gamma_{X}/\gamma_{A}) (W_{2}^{AX} - W_{0}^{AX}) / (W_{0}^{AX} + 2W_{1}^{A} + W_{2}^{AX}) .$$
 (31)

Equation (31) can be rewritten for proton and carbon-13 nuclei as

$$\eta_{C-\{H\}} = \frac{\gamma_H}{2\gamma_C} \left[ K^2 \sum_{i} J_{Di} / (K^2 \sum_{i} J_{Di} + 4W_{1C}^*) \right], \qquad (32)$$

where  $\gamma_{\rm H}$  and  $\gamma_{\rm C}$  are the magnetogyric ratios of <sup>1</sup>H and <sup>13</sup>C nuclei, respectively, K =  $h\gamma_{\rm H}\gamma_{\rm C}/2\pi$ ,  $J_{\rm Di}$  is the spectral density at the carbon-13 frequency arising from the fluctuating dipolar interaction between proton i and the carbon-13 nucleus, and  $W_{1C}^{*}$  represents all other relaxation contributions proportional to the carbon-13 z-magnetization,  $\langle I_{\rm Z} \rangle$ , other than dipolar.

If the dipole mechanism is dominant, i.e.,  $4W_{1C}^* \langle \langle K^2 \Sigma J_{Di}, Equation (32) \rangle$  reduces to

$$\eta_{C-\{H\}} = (\gamma_H/2\gamma_C) = 1.988$$
 (33)

and the Overhauser enhancement is  $\theta$  = 2.988. This is the maximum theoretical enhancement and other relaxation mechanisms will reduce this value. Kuhlmann and Grant (82) have measured the enhancement in formic acid and have found it to be 2.98.

When the dipole mechanism dominates, the number of nearest neighbor protons does not effect the enhancement since  $K^2\Sigma J_{Di}$  drops out of Equation (32). If other relaxation mechanisms are present the number of nearest neighbor protons can lead to variations in the value of  $\eta_{C-\{H\}}$ .

Kuhlmann, Grant, and Harris (80) have shown that

$$\frac{d\langle I_z \rangle}{dt} = (\frac{1}{2} K^2 \sum_i J_{Di} + 2W_{1C}^*) (\langle I_z \rangle - \theta \langle I_z \rangle_0) , \qquad (34)$$

where  $\langle I_z \rangle_0$  is the equilibrium magnetization in the absence of proton decoupling. The relaxation of enhanced carbon-13 nuclei is still governed by a single time constant,  $T_1$ , given by

$$\frac{1}{T_1} = \frac{1}{2} K^2 \sum_{i} J_{Di} + 2W_{1C}^* . \tag{35}$$

Equation (35) combined with (32) yields

$$K^{2} \Sigma J_{Di} = 4(\gamma_{C}/\gamma_{H}) (\eta_{C-\{H\}}/T_{1})$$
 (36)

and

$$W_{1C}^{*} = [1 - (2\gamma_{C}/\gamma_{H})\eta_{C-\{H\}}]/2T_{1} . \qquad (37)$$

Therefore,  $W_{1C}^{*}$  and  $K_{1Di}^{2}$  can be calculated from the measured values of the Overhauser enhancement and the spin-lattice relaxation time.

# Lanthanide Induced Chemical Shifts

Since the discovery by Hinckley (84) that large isotropic shifts are produced in the proton resonances of cholesterol when this molecule is placed in solutions of the dipyridinate of tris(dipivaloylmethanato) europium(III), Eu(dpm)3(py)2, considerable interest has been shown (85-101) in lanthanide "shift reagents". Some of the major discoveries are: (a) the finding that shift reagents cause isotropic shifts in a variety of functional organic molecules including alcohols (84,85-90,94,95), amines (85,91,96), ketones (85,92,94), aldehydes (85,96), and esters (93,94,96,97); (b) the observation (85) that  $Eu(dpm)_3$  is more efficient in effecting such shifts than is  $Eu(dpm)_3(py)_2$ ; (c) the discovery (86) that Pr(dpm) 3 causes upfield shifts of larger magnitude than the downfield displacements induced by Eu(dpm)3; also, the observation (94) of shifts for substrates in the presence of dpm complexes of Sm, Tb, Ho and Yb; (d) the observation that certain other lanthanide complexes (86), as well as β-diketonate chelates with less bulky substitutes than Ln(dpm) 3, are inadequate as shift reagents (96); (e) the finding (97) that partially fluorinated chelates of a similar variety are superior shift reagents because of greater solubility and greater Lewis acidities; and (f) the observation that shift reagents can be applied to study NMR spectra of nuclei other than protons (99-101).

The action of shift reagents is generally attributed to a through-space dipolar interaction (102,103). Dipolar shifts are proportional to the magnetic susceptibility anisotropy (102), and to the geometric factor  $\langle (3\cos^2\theta-1)r^{-3}\rangle_{AV}$ , where r is the length of a radius vector from the metal

atom to the resonating nucleus,  $\theta$  is the angle made by this vector with the principal axis, and the average is taken over motions rapid on the NMR time scale.

#### **EXPERIMENTAL**

## Preparation of Compounds

Methanol Enriched in Carbon-13 --- In order to locate carbon-13 resonances on our spectrometer it was necessary that a sample enriched in carbon-13 be prepared. The preparation of carbon-13 enriched methanol was performed by first converting enriched barium carbonate to carbon dioxide and then reducing the carbon dioxide to methanol (104,105).

Concentrated hydrochloric acid was added slowly to 0.05 moles of 57.2 percent carbon-13 enriched barium carbonate (Isomet Corp., Palisades Park, N.J.). The carbon dioxide generated was passed directly into a 0.5 M solution of lithium aluminum hydride in diethyl carbitol under a nitrogen atmosphere. The methanol was liberated by alcoholysis with the addition of one mole of n-butyl carbitol. Diethyl carbitol was selected as the solvent and n-butyl carbitol as the liberating agent because of their high boiling points which left methanol as the most volatile component of the system. The methanol was then obtained by simple distillation. The yield of methanol was approximately 75 percent, based on the amount of carbon dioxide generated.

N.N-Dimethyldichloroacetamide and N.N-Dimethyltrichloroacetamide --The preparation of N.N-dimethyldichloroacetamide and N.N-dimethyltrichloroacetamide was performed by following a general procedure for
tertiary amides (106,107). An aqueous solution of one mole of sodium
hydroxide was added slowly and with stirring to one mole of aqueous

dimethylamine. One mole of the appropriate acetyl chloride, in this case dichloroacetyl chloride or trichloroacetyl chloride, was then added to the basic amine solution, while maintaining the temperature between five and ten degrees Centigrade. After completion of the reaction, the mixture was neutralized and the aqueous solution was extracted with diethyl ether four times. The ether extracts were combined and dried overnight over anhydrous potassium carbonate. The ether was removed by distillation, and the product was purified by fractional distillation in vacuo.

# Physical Constants of Compounds Studied

All of the amides studied in this research are listed in Table 5 (N-monosubstituted amides), Tables 6 and 7 (symmetrically N,N-disubstituted amides), and Table 8 (unsymmetrically N,N-disubstituted amides). Boiling points or melting points are also given in these tables. The purity of each amide was determined by examination of its proton NMR spectrum. An amide was considered to be impure if there were unexplainable peaks in the proton NMR spectrum. If the amide was impure, it was purified by drying over anhydrous sodium sulfate and fractionally distilling in vacuo.

The chemical shift reagents tris(1,1,1,2,2,3,3-heptafluoro-7,7-dimethyl-4,6-octanedionato) europium(III), Eu(fod)<sub>3</sub>, and tris(1,1,1,2,2,-3,3-heptafluoro-7,7-dimethyl-4,6-octanedionato) praseodymium(III), Pr(fod)<sub>3</sub>, were purchased from the Norell Chemical Company, Landing, New Jersey. The shifts reagents were stored over phosphorous pentoxide in a vacuum desiccator.

Table 5. N-Monosubstituted amides studied.

Compound	<u>Source</u> <sup>a</sup>	Boiling Point <sup>b</sup>	
N-Methylformamide	A	56/6	
N-Methylacetamide	A	80.0-81.0/2	
N-Methylpropionamide	A	89.0-90.3/2	
N-Methylisobutyamide	В	78.0-78.5/2.5	
N-Methylpivalamide	В	M.P. 90.4-91.0	
N-Ethylformamide	A	63.2-64.0/1	
N-Ethylacetamide	A	80-83/1.5	
N-Ethylpropionamide	В	78.5-79.5/2.5	
N-Ethylisobutyramide	В	M.P. 69.0-71.0	
N-Isopropylformamide	В	70/1.5	
N-Isopropylacetamide	В	86.5-87.0/4	
N-Isopropylisobutyramide	В	M. P. 102	
N- <u>n</u> -Butylformamide	В	81/1	
N- <u>n</u> -Butylacetamide	В	111/6	
N- <u>t</u> -Butylformamide	В	67/1.5	

A - Eastman Organic Chemicals, Rochester, New York.
 B - Prepared by L. A. LaPlanche in this laboratory (107).

b<sub>Given as: °C/mm.</sub>

Table 6. N.N-Dimethylamides studied.

Compound	Sourcea	Boiling Point <sup>b</sup>
N, N-Dimethylformamide	A	31.5-34.0/25
N, N-Dimethylformamide-d <sub>1</sub> <sup>c</sup>	В	
N, N-Dimethylacetamide	С	44.0-45.0/3
N, N-Dimethylpropionamide	С	51.0-52.0/3
N, N-Dimethyl-n-butyramide	С	47.0-47.5/0.5
N, N-Dimethylisobutyramide	D	55/3
N, N-Dimethylpivalamide	D	73/2.5
N, N-Dimethylchloroacetamide	Е	72.5-73.0/2
N, N-Dimethyldichloroacetamide	F	96.5/11
N, N-Dimethyltrichloroacetamide	F	77/2
N, N-Dimethylcarbamylchloride	E	78/39
N, N-Dimethyltrifluoroacetamide	G	134.3/740
N, N-Dimethylacrylamide	Е	46/3
Ethyl-N, N-dimethylcarbamate	G	142/733

A - Matheson, Coleman and Bell, East Rutherford, New Jersey.
 B - Merck, Sharp and Dohme of Canada Limited, Quebec, Canada.

C - Eastman Organic Chemicals, Rochester, New York.

D - Received from L. A. Graham, Northern Illinois University.

E - Pfaltz and Bauer, Flushing, New York.

F - Prepared in this laboratory.

G - Prepared by J. C. Woodbrey in this laboratory (108).

bGiven as: °C/mm.

<sup>&</sup>lt;sup>c</sup>Studied without further purification.

Table 7. Other symmetrically N, N-disubstituted amides studied.

Compound	Source	Boiling Point <sup>b</sup>	
N, N-Diethylformamide	A	45.0/48.0/2	
N, N-Diethylacetamide	В	60.5-61.5/2	
N, N-Diethylpropionamide	В	53.0-54.0/1.5	
N, N-Diethyl- <u>n</u> -butyramide	В	61.0-63.0/1	
N, N-Diethylchloroacetamide	С	72.0-73.0/2	
N, N-Diethylacrylamide <sup>C</sup>	В		
N, N-Diisopropylformamide	D	69.0-71.0/7	
N, N-Diisopropylacetamide	В	56.0/1	
N, N-Diisopropylpropionamide	В	62.0-62.5/0.5	
N, N-Di-n-propylformamide	D	60.5-61.5/2.5	
N, N-Di- <u>n</u> -propylacetamide	В	68.0-68.3/5	

A - Matheson, Coleman and Bell, East Rutherford, New York.
B - Eastman Organic Chemicals, Rochester, New York.
C - K&K Laboratories, Inc., Jamaica, New York.
D - Prepared by L. A. LaPlanche in this laboratory (107).

bGiven as: °C/mm.

 $<sup>^{\</sup>mathbf{c}}$ Studied without further purification.

Table 8. Unsymmetrically N,N-disubstituted amides studied.

Compound	<u>Source</u> <sup>a</sup>	Boiling Pointb
N-Ethyl-N-methylformamide	A	82.0/44
N-Ethyl-N-methylacetamide	A	45.0/33
N-Ethyl-N-methylpivalamide	A	62.0-63.0/5
N-Isopropyl-N-methylformamide	A	58.5/7
N-Isopropyl-N-methylacetamide	A	60.0/17
N-n-Butyl-N-methylformamide	В	55.0-56.0/1
N-n-Butyl-N-methylacetamide	A	65.0/3
N-n-Butyl-N-methylisobutyramide	A	72.5-73.0/2.5
N-n-Butyl-N-methylpivalamide	A	75.0-76.0/2
N- <u>t</u> -Butyl-N-methylformamide	A	64.5/5
N- <u>t</u> -Butyl-N-methylacetamide	A	56.5/5
N-Cyclohexyl-N-methylacetamide	A	130/13
1-Methyl-2-pyrrolidinone	С	202/760

A - Prepared by L. A. LaPlanche in this laboratory (107).
 B - Eastman Organic Chemicals, Rochester, New York.
 C - Aldrich Chemicals, Milwaukee, Wisconsin.

bGiven as: °C/mm.

## Spectrometer

In this investigation, spectra were obtained on a Varian HA-100 high-resolution nuclear magnetic resonance spectrometer. The main magnetic field of 23,490 gauss was generated by a V-4014 twelve-inch high-impedence electromagnet equipped with a V-2100B regulated magnet power supply. Stability of this magnetic field was maintained to better than one part in 10<sup>8</sup> by a V-3506 flux stabilizer.

The system is capable of observing either proton resonances at 100 MHz or carbon-13 resonances at 25.1 MHz. In each case, the crystalcontrolled radiofrequency is produced by a separate V-4311 fixed frequency rf unit. The radiofrequency is transmitted to a V-4333 variable temperature probe where the resonance of the sample is detected by the crossedcoil method. The carbon-13 probe was double tuned so that the carbon resonances could be examined while irradiating the proton resonances to remove the coupling between the two nuclei. The pseudo-random noise at 100 MHz was generated by a V-3512 noise decoupler. A V-4354A internal reference NMR stabilization unit modulated the radiofrequency with two audio frequencies; one frequency, called the analytical channel, was used to detect the resonances in the sample and the other frequency, called the control channel, was used to lock the magnetic field to a reference frequency. The reference was one of the sample resonance frequencies or that of an added internal standard. Frequencies were counted with a Hewlett-Packard 5245L frequency counter.

In order to observe a carbon-13 spectrum it was necessary to work at the highest gain of the spectrometer. Working at this ultimate limit of the spectrometer produced an undesireable rolling baseline, as shown in Figure 4, as the result of a large modulation index. The modulation index (110) is a dimensionless quantity, the ratio between the frequency deviation, in hertz, and the modulation frequency, also in hertz. When the audio frequency is swept, the modulation index is large and the amplitude of the modulation signal varies greatly. The phase-sensitive detector used to detect the NMR signal is sensitive to changes in the modulation signal, which is normally small under the usual operating conditions of the spectrometer. However, under the conditions employed for the carbon-13 NMR experiment these changes are very large and are reflected in the spectrum.

In order to conduct the variable temperature studies it was necessary to stabilize the temperature of the probe and measure this temperature accurately. Temperature stability was maintained in the range of -60 to 200°C by a V-4343 variable temperature accessory connected to a heater sensor in the probe. Temperature calibration for the proton work was accomplished by using the chemical thermometers methanol and ethylene glycol. In the high temperature range, 30°C to 200°C, the temperature was found from the expression (109)

$$T^{\circ}K = -(\delta_{EG}) \ 1.017 + 464.9$$
 , (38)

where  $\delta_{EG}$  is the chemical shift difference between the two chemical shifts of the protons in ethylene glycol at 100 MHz. In the low temperature range, -100° to 30°C, the calibration equation is (109)

$$T^{\circ}K = -(\delta_{M}) \ 1.076 + 464.7$$
 , (39)

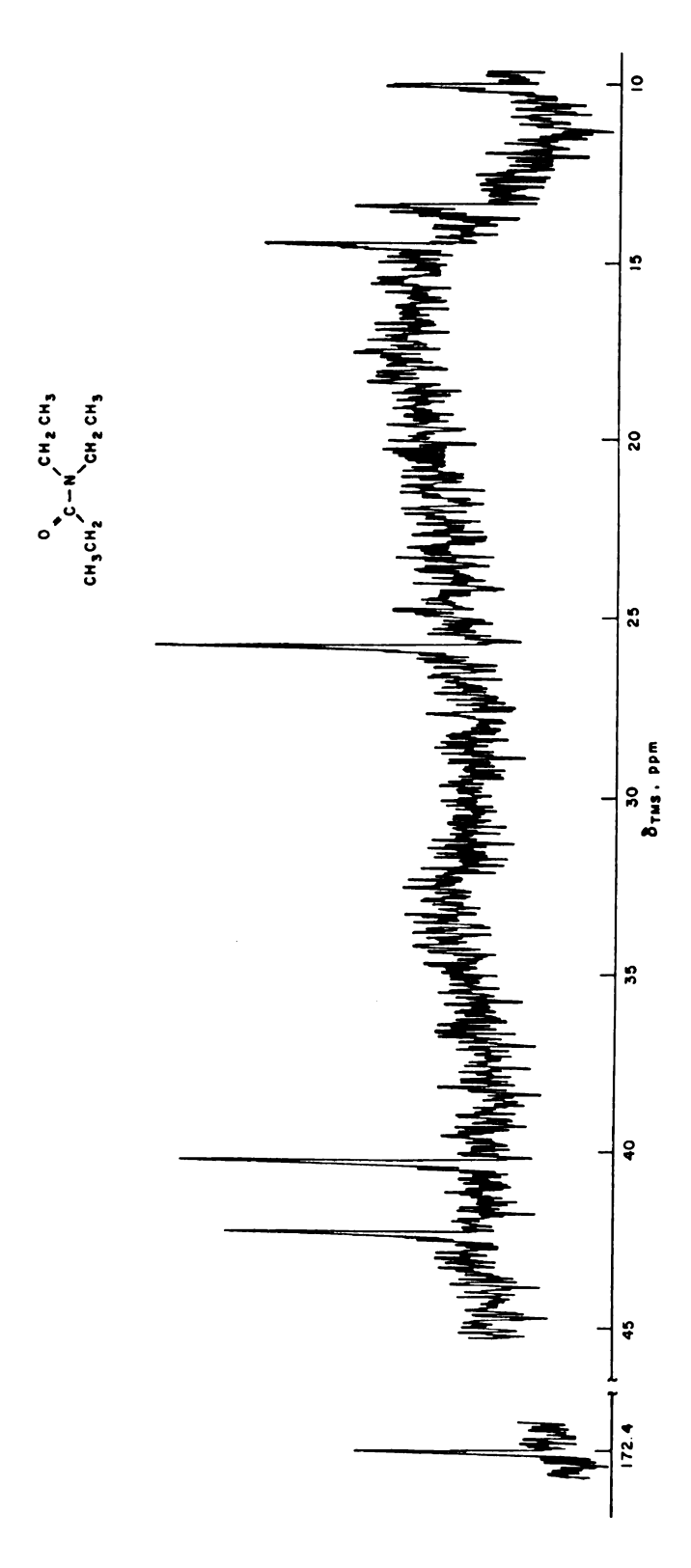


Figure 4. Carbon-13 NMR spectrum of N,N-diethylpropionamide.

where  $\delta_{\rm M}$  is the difference between the two chemical shifts of the protons in methanol at 100 MHz. The temperature calibration for the carbon-13 spectra was accomplished by using a copper-constantan thermocouple because no carbon-13 chemical thermometer has been found.

## Time Averaging and Digitization of Spectra

The Varian HA-100 was interfaced with a Varian C-1024 computer of averaged transients (CAT). When a spectrum of interest is swept repeatedly, signal information is added into memory channels of the C-1024 in direct proportion to the number of sweeps, while random noise is accumulated in proportion to the square root of the number of sweeps. The sensitivity of the NMR experiment, especially for carbon-13 spectra, is increased by accumulating repeated sweeps of the spectrum. Frequency calibration is accomplished by reading the information stored in memory out on to a recorder precalibrated to the spectral sweep width.

The C-1024 was also used to digitize a spectrum of interest for which purpose it was connected to a Varian C-1001 binary-to-octal coupler attached to a IBM 526 key punch. The punched cards containing the 1024 points in an octal format were read into a CDC 6500 computer for further processing. The C-1024 operated exclusively in this mode for the total lineshape analysis portion of this investigation.

# Sample Preparation

All proton and carbon-13 spectra were obtained by placing the samples in five millimeter, precision-ground, NMR tubes.

The tertiary amides for the hindered internal rotation studies were degassed and sealed by the freeze-pump-thaw method to remove any trace amounts of paramagnetic oxygen which broadens the NMR lines. The addition of five percent by volume of either tetramethylsilane (TMS) or hexamethyldisiloxane (HMDS) was required in each sample to provide a reference and lock signal. The substituted formamides, which have very high coalescence temperatures, were degassed and sealed in three millimeter tubes and placed in five millimeter NMR tubes containing tert-butyl benzene (TBB). The methyl resonance of TBB provided the reference and lock signal.

Solutions of the tertiary amides used in the resonance assignment study were initially 0.2 M in carbon tetrachloride and the shift reagent [Eu(fod)<sub>3</sub> or Pr(fod)<sub>3</sub>] was then added in increments up to a mole ratio of 0.4 (shift reagent to amide). Five percent by volume of TMS was added to each sample as an internal reference. The proton NMR spectrum was examined prior to and after each addition of the shift reagent. The series of spectra for each amide were acquired at a temperature well below the coalescence temperature.

The carbon-13 NMR spectra were obtained by placing the sample in a five millimeter NMR tube with a capillary containing 57% carbon-13 enriched methanol. The capillary was centered by means of a Teflon plug. The enriched methanol was used as a reference and lock signal. When necessary the spectra were run at temperatures low enough to slow the internal rotation and permit observation of both isomers.

# Bulk Diamagnetic Susceptibility Corrections

Where an external reference is used, a correction involving the difference between the bulk diamagnetic susceptibilities of the reference compound and the sample must be applied. This is necessitated by the fact that, in cylindrically shaped containers, the actual fields experienced by individual nuclei will depend on the magnetic polarization near the surface. The correction for a cylindrical sample is

$$\delta_{\text{CORR}} = \delta_{\text{OBS}} + \frac{2\pi}{3} \left( \chi_{\text{v,ref}} - \chi_{\text{v}} \right) , \qquad (40)$$

where  $\delta$  is the chemical shift in ppm and  $\chi_{_{\boldsymbol{V}}}$  is the volume diamagnetic susceptibility (68).

The volume diamagnetic susceptibilities of several compounds were measured by the Gouy method (111). The measurements were made on a magnetic susceptibility system manufactured by the Alpha Scientific Company. The measured values are given in Table 9. The chemical shift corrections

Table 9. Volume magnetic susceptibilities and bulk magnetic susceptibility corrections for several compounds

Compound	x <sub>v</sub>	$\frac{2\pi}{3} \left( \chi_{v, CH_3OH} - \chi_v \right)$
Methanol	O.525 ppm	_
N-Methylformamide	0.564 ppm	0.081 ppm
N-Methylpropionamide	0.619 ppm	0.197 ppm
N, N-Dimethylformamide	O.581 ppm	O.117 ppm
N, N-Diethylformamide	O.579 ppm	O.113 ppm
N, N-Diethylacetamide	O.615 ppm	O.188 ppm

for several amides (with methanol as the reference) are also given in this table. The correction factor for formamides is approximately 0.1 ppm and for other amides it is about 0.2 ppm. Since these corrections are within the experimental error of measurement of the chemical shifts in the carbon-13 spectrum, no bulk diamagnetic susceptibility corrections were made for the carbon-13 chemical shifts.

Determination of Energy Barriers for Hindered Internal Rotations

The rate of internal rotation about the C-N bond in several amides was obtained by an iterative computer fitting of the theoretical spectrum, calculated from the total lineshape equations as derived by Rogers and Woodbrey (11), to the experimental spectrum.

The curve fitting program was developed by Dye and Nicely (112).

The program minimizes the functional

$$\varphi = \sum_{i=1}^{n} W_{i} F_{i}^{2} , \qquad (41)$$

in which n is the number of data points, F<sub>i</sub> is the residual defined in such a way that it would approach zero for all i as the parameters approach their "best" values if the data were completely free from errors, and W<sub>i</sub> is a weight which was set to unity for all points; if desired W<sub>i</sub> can be calculated by the program. The general program will fit an arbitrary function of not more than 20 parameters (dependent plus independent) to a data set containing a maximum of 99 points.

The lineshape equation is a function of the spin-spin relaxation times at sites A and B ( $T_{2A}$ ,  $T_{2B}$ ), the chemical shift difference ( $\delta \nu$ ) in

the absence of exchange, the relative population at each site  $(p_A, p_B)$ , and the mean lifetime  $(\tau)$  at each site. These parameters were determined above and below the coalescence temperature for the N-methyl protons in each amide by the following techniques. The proton NMR spectrum of each amide was examined at a temperature well below the coalescence temperature to establish an estimated value of each parameter (except  $\tau$ ). In the temperature region below coalescence all of the parameters were determined by simultaneous iteration to obtain the best fit to the experimental lineshape. The final value of each parameter calculated was examined for experimental feasibility. For temperatures above coalescence, the experimental lineshape contains insufficient information to allow the simultaneous determination of all the parameters. In this case, all of the parameters except the mean lifetime  $(\tau)$  at each site were held constant at a value which was the average of those calculated from the experimental curves below the coalescence temperature.

#### RESULTS

### Hindered Internal Rotation in Tertiary Amides

The barrier to internal rotation about the central C-N bond for a series of tertiary amides, symmetrically and unsymmetrically substituted, was studied by total lineshape analysis. The proton NMR spectrum of the N-methyl protons was obtained at several temperatures above and below the coalescence temperature. The experimental curve at each temperature was then fitted to the theoretical lineshape equation in order to extract the parameters of interest. The proton NMR spectrum for each amide can be found elsewhere (107,108,109).

### Symmetrically Disubstituted Amides

N,N-Dimethylacetamide --- The barrier to internal rotation for neat N,N-dimethylacetamide was studied at various temperatures by fitting the experimental curve of the N-methyl resonances to the theoretical line-shape equation. The parameters in the theoretical equation were then adjusted by an iteration procedure to obtain the fit. Four of these plots are shown in Figures 5-8. In these figures, X's designate experimental points, O's designate calculated points, and ='s designate an experimental point and a calculated point which are in the same area element delta x by delta y. The experimental data obtained are given in Table 10. The logarithm of the rate constant is plotted against 103/ToK in Figure 9.

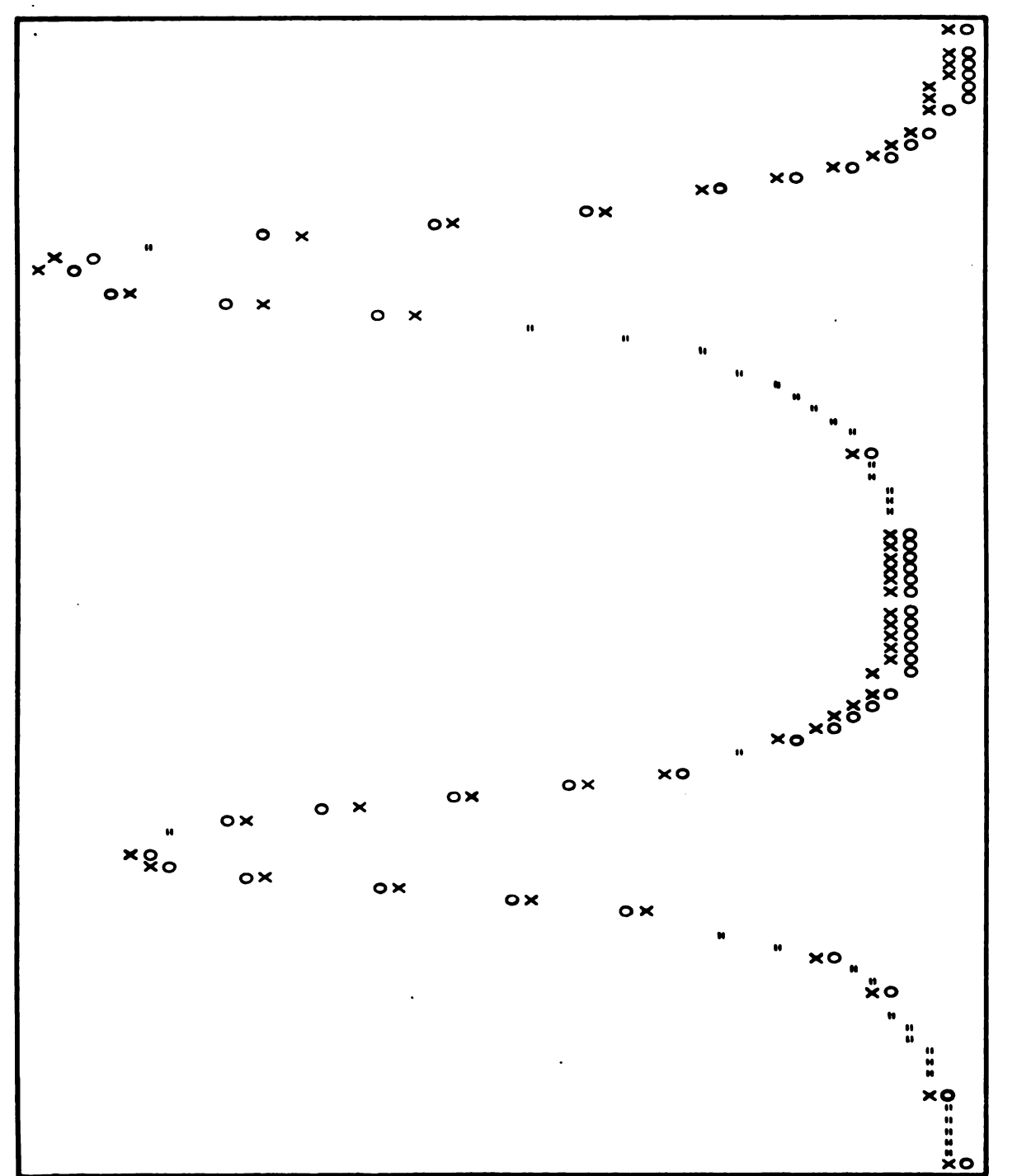


Figure 5. Observed (X) and calculated (O) signals of the N-methyl protons in neat N,N-dimethylacetamide at T = 325.7°K.

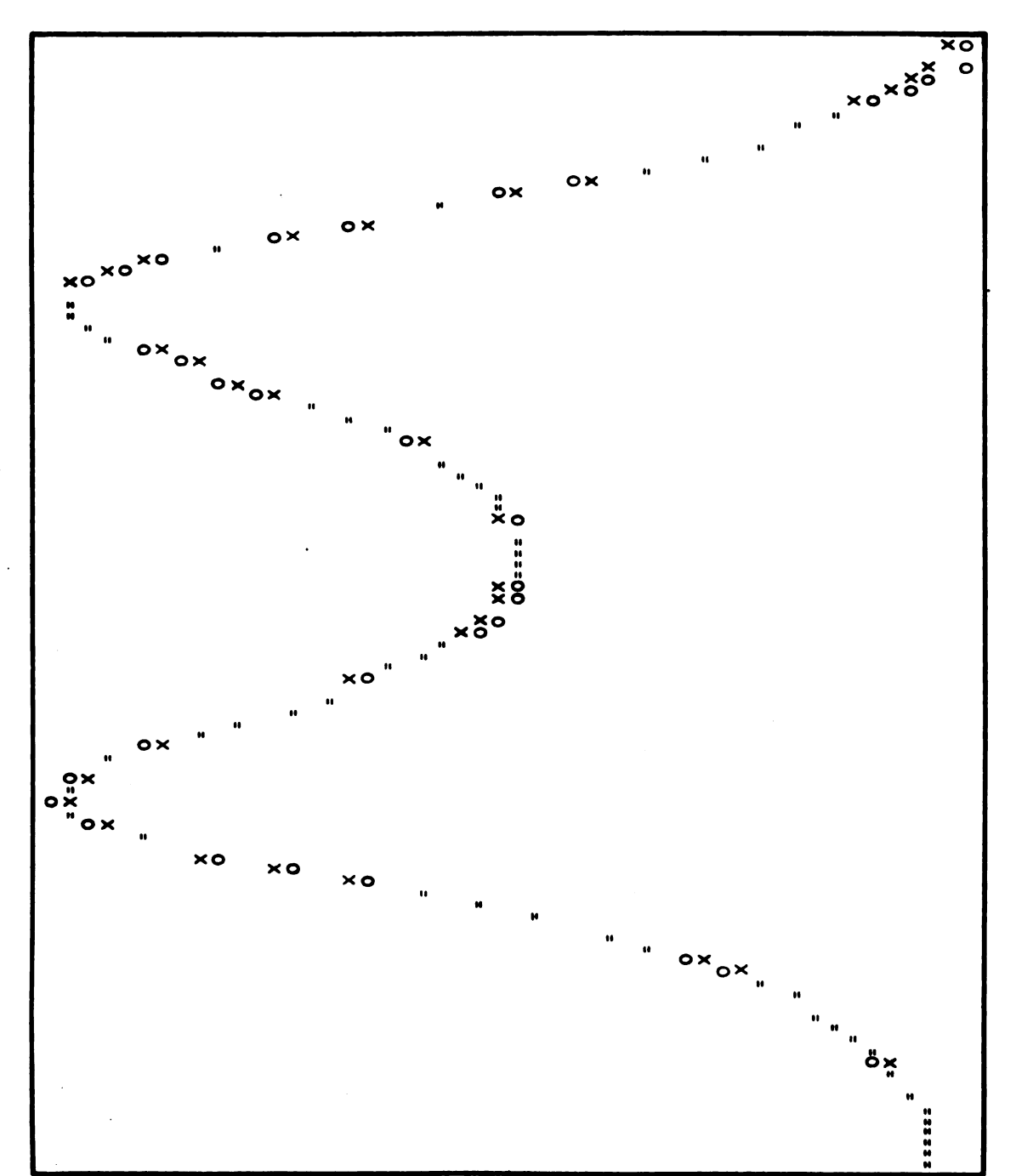


Figure 6. Observed (X) and calculated (O) signals of the N-methyl protons in neat N,N-dimethylacetamide at T =  $340.1^{\circ}$ K.

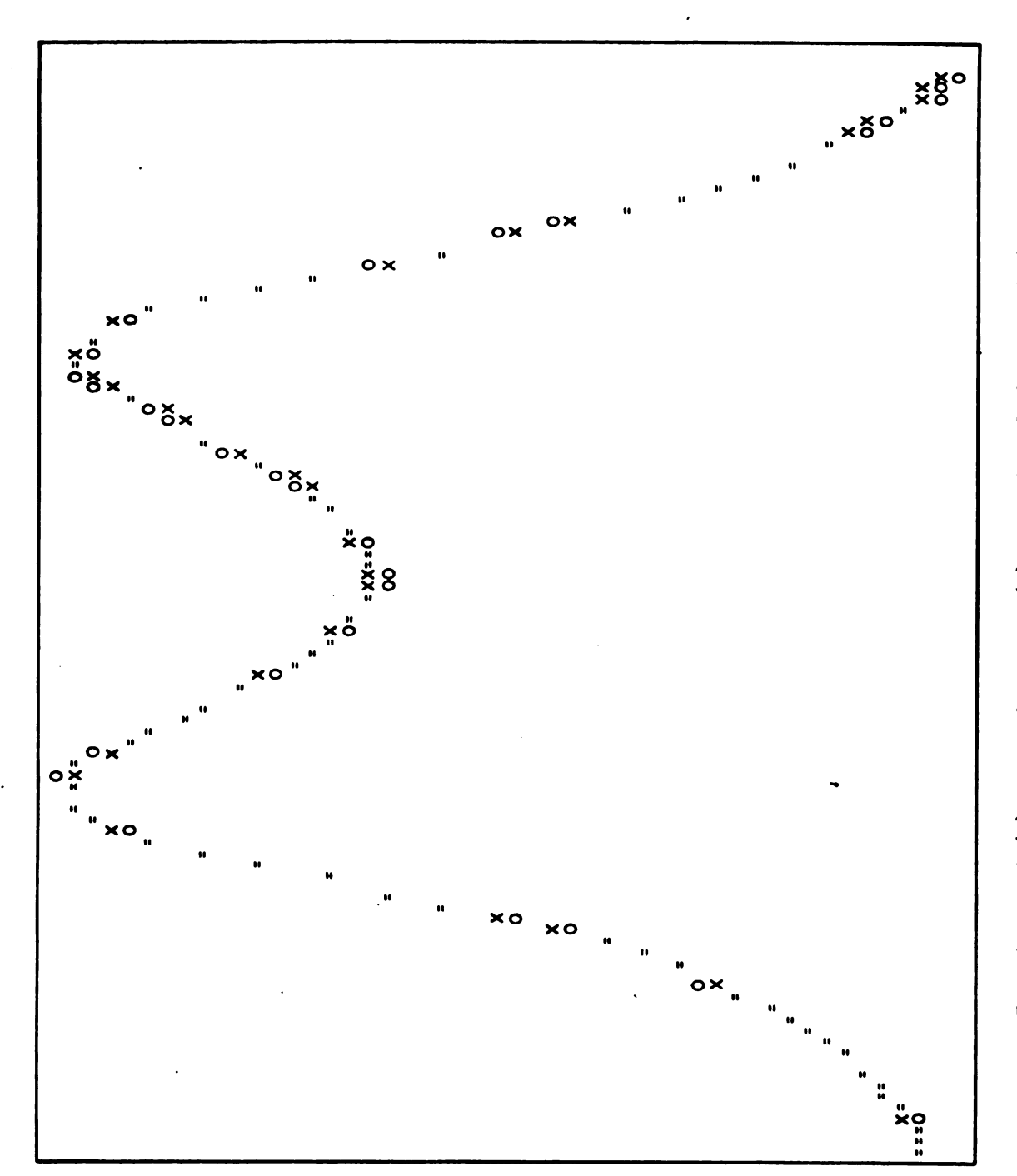


Figure 7. Observed (X) and calculated (0) signals of the N-methyl protons in neat N,N-dimethylacetamide at  $T=343.0^{\circ}K$ .

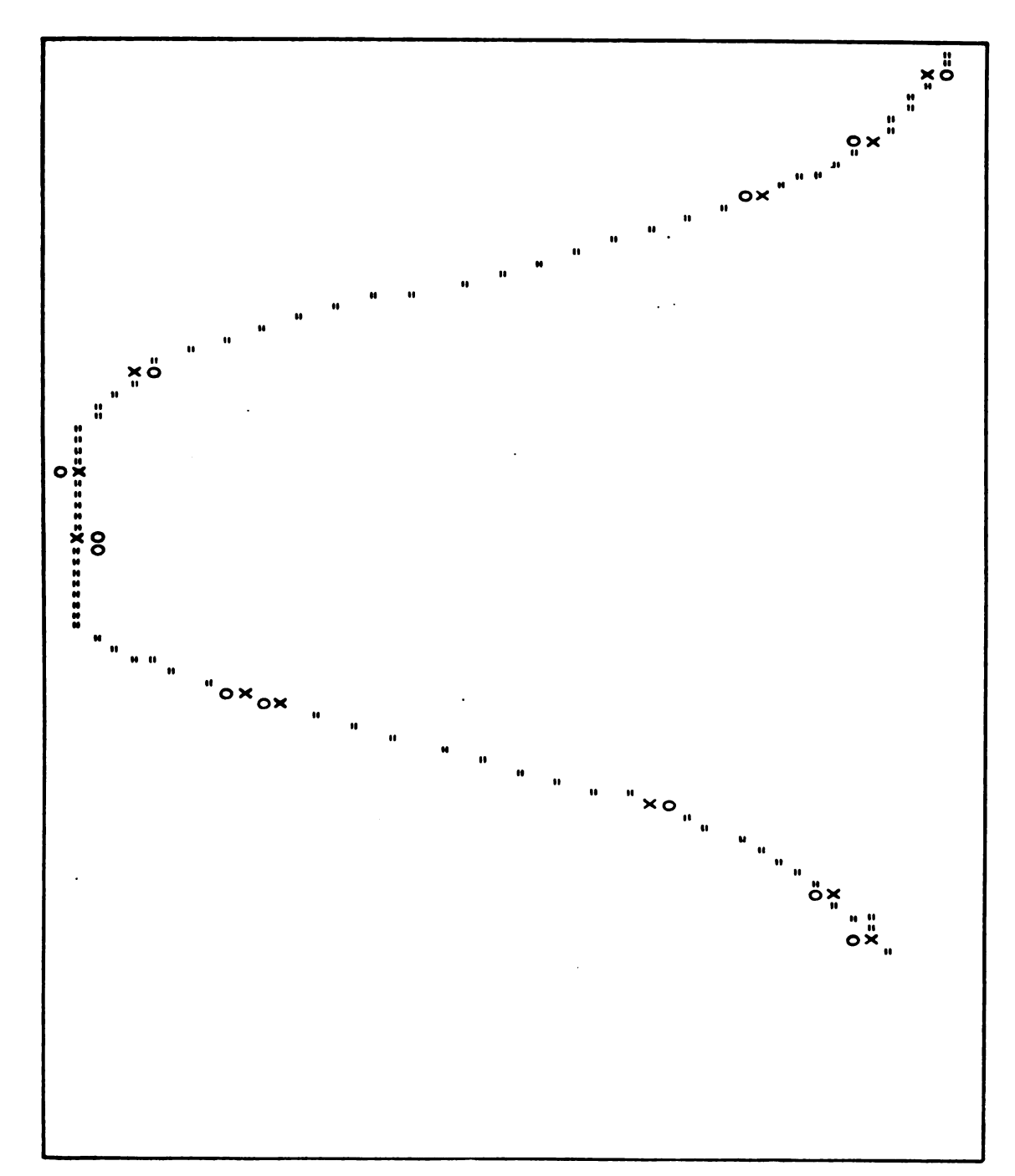


Figure 8. Observed (X) and calculated (0) signals of the N-methyl protons in neat N,N-dimethylacetamide at  $T=348.5^{\circ}K$ .

Table 10. Experimental data and calculated activation parameters for the internal rotation about the central C-N bond in neat N, N-dimethylacetamide.

T°K	10 <sup>3</sup> /T°K	τ <sup>*</sup> sec	ln(1/2τ)	δν* Hz	p <sub>A</sub> *
325.7	3.071	0.1181	1.443	17.7	0.498
331.8	3.014	0.0608	2.106	17.8	0.503
335.1	2.984	0.0419	2.480	17.6	0.505
335.1	2.984	0.0393	2.544	17.8	0.496
337.3	2.965	0.0331	2.716	17.2	0.489
340.1	2.940	0.0244	3.021	17.7	0.503
343.0	2.916	0.0213	3.157	17.5	0.501
346.2	2.888	0.0162	3.431	17.8	0.500
348.5	2.870	0.0138	3.586		
350.8	2.851	0.0113	3.788		
354.4	2.822	0.0084	4.082		
358.1	2.792	0.0067	4.317		
362.3	2.760	0.0051	4.594		

 $E_a = 19.7 \pm 0.5 \text{ kcal/mole}$ 

 $log_{10}A = 13.9 \pm 0.4$ 

Coalescence temperature = 348°K

 $<sup>\</sup>Delta G^{\dagger}_{298} = 18.1 \pm 0.5 \text{ kcal/mole}$   $\Delta H^{\dagger}_{} = 19.0 \pm 0.5 \text{ kcal/mole}$ 

 $<sup>\</sup>Delta S^{\ddagger} = 2.9 \pm 1.4 \text{ eu}$ 

<sup>\*</sup>Results from total lineshape analysis.

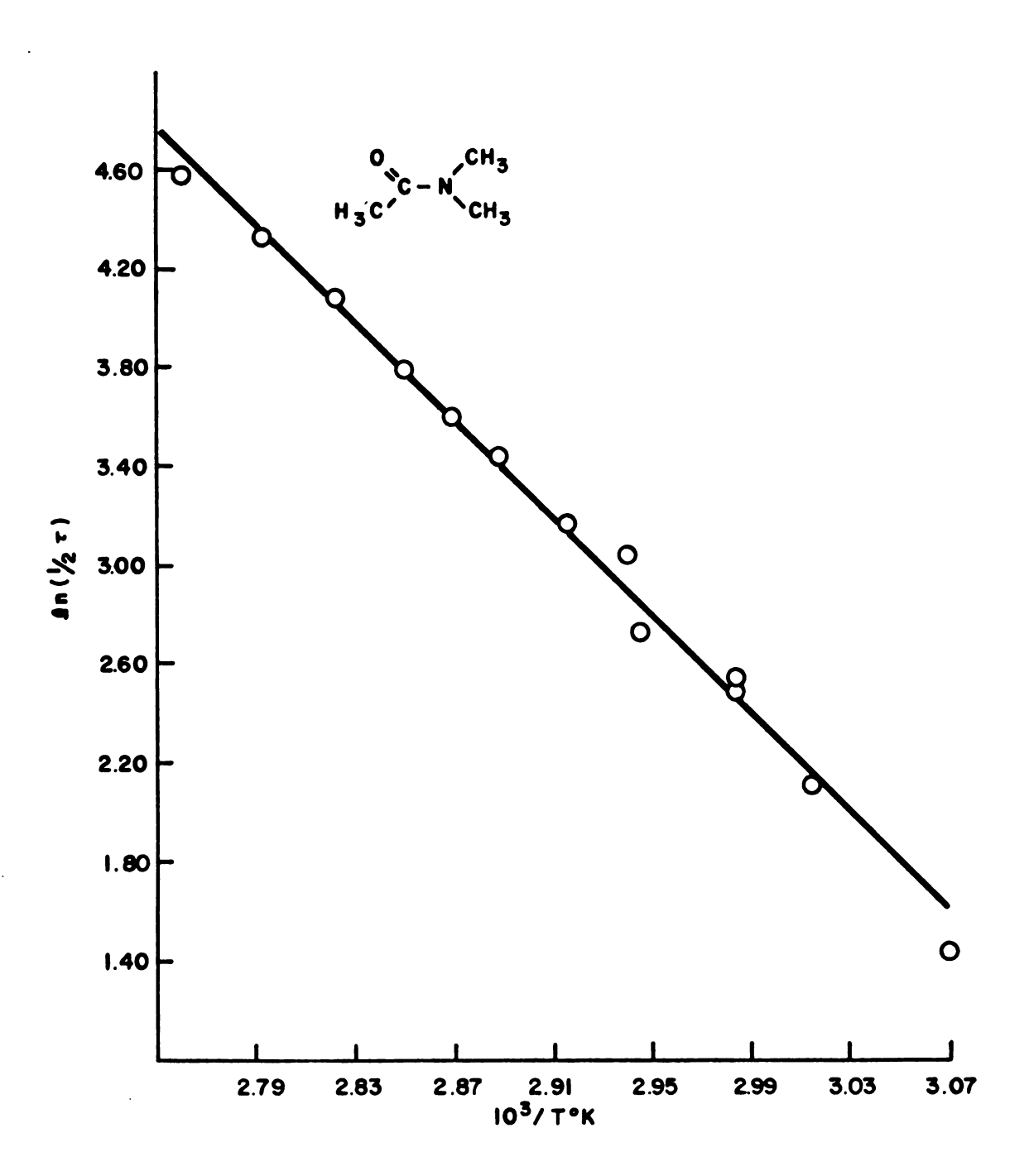


Figure 9. Plot of  $ln(1/2\tau)$  against  $10^3/T^\circ K$  for neat N,N-dimethylacetamide.

N,N-Dimethylcarbamylchloride --- Hindered internal rotation in neat N,N-dimethylcarbamylchloride was studied by total lineshape analysis.

The experimental data and calculated activation parameters are given in Table 11. The logarithm of the rate constant is plotted against 10<sup>3</sup>/T°K in Figure 10.

N.N-Dimethylformamide --- The proton resonances of the N-methyl protons in N,N-dimethylformamide are split into doublets due to coupling with the formyl proton. The <u>trans</u> coupling constant is 0.8 Hz and the <u>cis</u> coupling constant is 0.5 Hz. The barrier to internal rotation for this amide was studied by two methods.

Method I. The coupling to the formyl proton was neglected and the experimental curves were analyzed as a two-site case. The experimental activation parameters calculated by this method are given in Table 12. The logarithm of the rate constant is plotted against  $10^3/T^\circ K$  in Figure 11.

Method II. The coupling to the formyl proton was taken into consideration by assuming the pair of doublets to be a consequence of the superposition of two doublets (109) whose centers are separated by  $(J_{cis} + J_{trans})/2$ . The experimental spectrum was then fitted to the theoretical lineshape equation which had been modified to include the coupling constants. The experimental data and the activation parameters calculated are given in Table 13. The logarithm of the rate constant is plotted against  $10^3/T^{\circ}K$  in Figure 12.

N,N-Dimethylformamide-d<sub>1</sub> --- The effect of coupling by the formyl proton was removed by replacing this proton with a deuteron. The hindered internal rotation was studied by total lineshape analysis and the experimental data and the calculated activation parameters are tabulated in

Table 11. Experimental data and calculated activation parameters for the internal rotation about the central C-N bond in neat N, N-dimethylcarbamylchloride.

T°K	10 <sup>3</sup> /т°К	τ <sup>*</sup> _sec	ln(1/2τ)	δν <sup>*</sup> Hz	P <sub>A</sub> *
303.8	3.292	0.1623	1.125	10.8	0.498
308.7	3.239	0.0921	1.692	10.7	0.494
311.4	3.211	0.0746	1.903	10.8	0.502
316.0	3.165	0.0472	2.360	11.0	0.503
316.4	3.161	0.0481	2.341	10.7	0.492
319.3	3.132	0.0312	2.733	11.1	0.497
321.3	3.112	0.0240	3.036	11.5	0.506
323.5	3.091	0.0214	3.150		
325.6	3.071	0.0198	3.230		
328.8	3.041	0.0141	3.568		
330.7	3.024	0.0130	3.647		

 $E_a = 16.7 \pm 0.6 \text{ kcal/mole}$ 

 $log_{10}A = 13.9 \pm 0.4$ 

 $\Delta G^{\dagger}_{298} = 17.1 \pm 0.6 \text{ kcal/mole}$   $\Delta H^{\dagger}_{} = 18.0 \pm 0.6 \text{ kcal/mole}$ 

 $\triangle S^{\ddagger} = 3.0 \pm 1.8 \text{ eu}$ 

Coalescence temperature = 324°K

<sup>\*</sup>Results from total lineshape analysis.

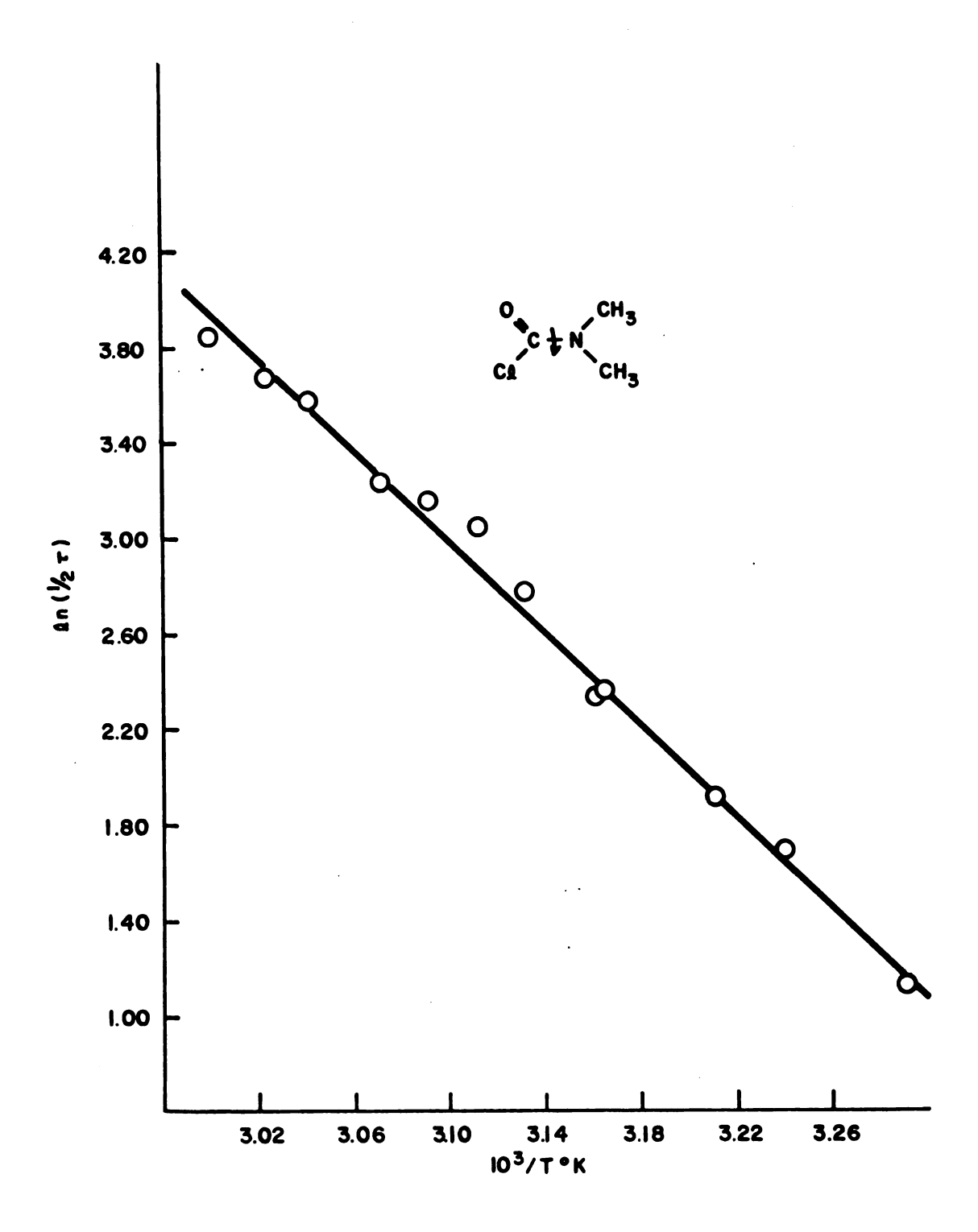


Figure 10. Plot of  $\ln(1/2\tau)$  against  $10^3/T^\circ K$  for neat N,N-dimethylcarbamylchloride.

Table 12. Experimental data and calculated activation parameters for the internal rotation about the central C-N bond in neat N,N-dimethylformamide - Method I.

т°к	10 <sup>3</sup> /T°K	τ* sec	ln(1/2τ)	* δν <u>Hz</u>	P <sub>A</sub> *
383.2	2.609	0.0499	2.304	15.0	0.500
386.3	2.589	0.0381	2.575	14.9	0.498
387.3	2.582	0.0357	2.639	15.1	0.505
389.3	2.568	0.0312	2.773	14.9	0.503
391.7	2.553	0.0276	2.897	15.3	0.509
392.7	2.546	0.0257	2.968	15.2	0.504
394.4	2.535	0.0240	3.036	15.1	0.496
394.8	2.533	0.0228	3.089	15.2	0.506
395.4	2.529	0.0218	3.134	15.4	0.510
395.7	2.527	0.0202	3.207	14.9	0.501
397.2	2.519	0.0196	3.241		
398.2	2.511	0.0174	3.359		
399.4	2.504	0.0171	3.378		
	•				

 $E_a = 19.8 \pm 0.5 \text{ kcal/mole}$ 

 $log_{10}A = 12.3 \pm 0.4$ 

 $\Delta H^{\ddagger} = 19.0 \pm 0.5 \text{ kca} 1/\text{mole}$ 

Coalescence temperature = 397°K

 $<sup>\</sup>Delta G^{\dagger} = 20.4 \pm 0.5 \text{ kcal/mole}$ 

 $<sup>\</sup>angle S^{\ddagger} = -4.7 \pm 1.5 \text{ eu}$ 

<sup>\*</sup>Results from total lineshape analysis.

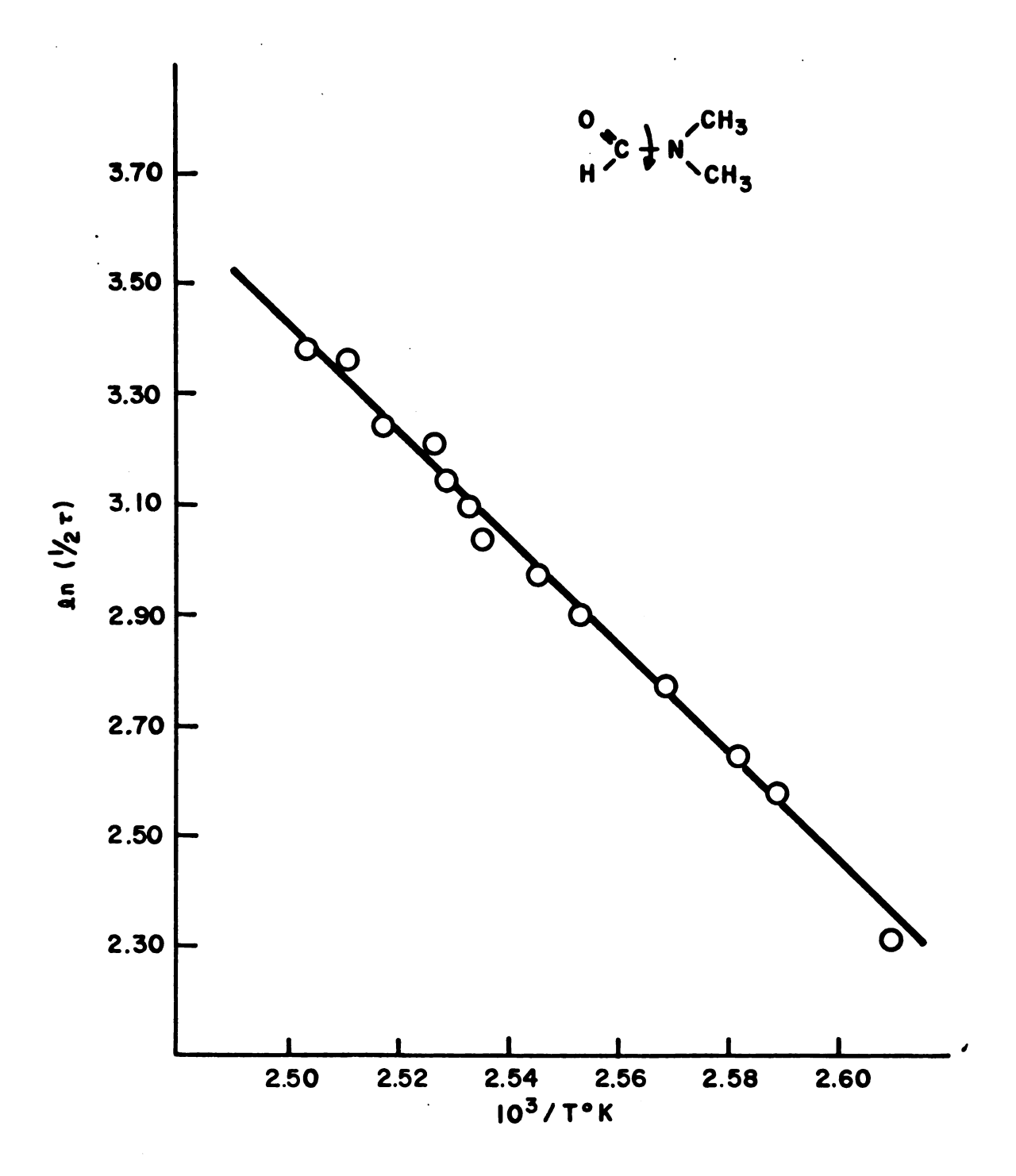


Figure 11. Plot of  $\ln(1/2\tau)$  against  $10^3/T^\circ K$  for neat N,N-dimethylformamide - Method I.

Table 13. Experimental data and calculated activation parameters for the internal rotation about the central C-N bond in neat N. N-dimethylformamide - Method II.

T°K	10 <sup>3</sup> /T°K	τ <sup>*</sup> sec	ln(1/2τ)	δν <sup>*</sup> Hz	PA*
386.3	2.589	0.0469	2.367	14.9	0.502
387.3	2.582	0.0433	2.450	14.9	0.505
389.3	2.568	0.0368	2.610	14.8 -	0.498
391.7	2.553	0.0285	2.866	15.2	0.509
392.7	2.546	0.0275	2.901	15.1	0.497
394.4	2.535	0.0240	3.037	15.2	0.507
394.8	2.533	0.0242	3.030	15.4	0.510
395.4	2.529	0.0222	3.115	14.8	0.498
395.7	2.527	0.0219	3.127		
397.2	2.518	0.0197	3.232		
398.2	2.511	0.0174	3.360		
399.4	2.504	0.0170	3.380		

 $E_a = 24.3 \pm 0.5 \text{ kcal/mole}$ 

 $log_{10}A = 14.8 \pm 0.4$ 

 $\Delta G^{\dagger}_{298} = 21.5 \pm 0.5 \text{ kcal/mole}$   $\Delta H^{\dagger}_{} = 23.5 \pm 0.5 \text{ kcal/mole}$ 

 $\Delta S^{\ddagger} = 6.5 \pm 2.0 \text{ eu}$ 

Coalescence temperature = 397°K

<sup>\*</sup>Results from total lineshape analysis.

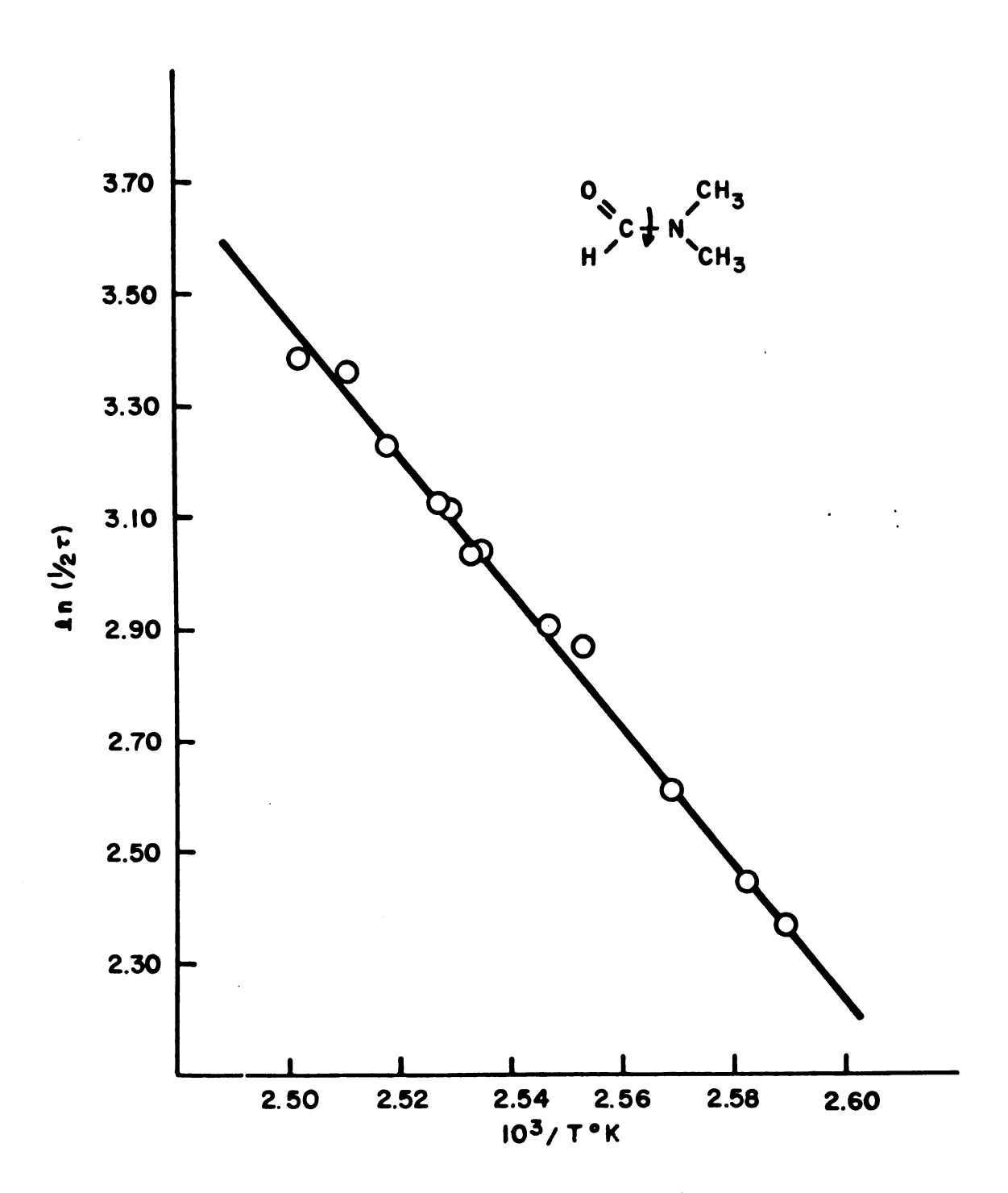


Figure 12. Plot of  $ln(1/2\tau)$  against  $10^3/T^\circ K$  for neat N,N-dimethylformamide - Method II.

Table 14. The logarithm of the rate constant is plotted against 10<sup>3</sup>/T°K in Figure 13.

N.N-Dimethylpropionamide --- Hindered internal rotation in N,N-dimethylpropionamide was studied in the neat liquid by total lineshape analysis and the experimental data and the calculated activation parameters are tabulated in Table 15. The logarithm of the rate constant is plotted against  $10^3/T^\circ K$  in Figure 14.

N.N-Dimethyltrichloroacetamide --- Hindered internal rotation in N,N-dimethyltrichloroacetamide in the neat liquid was studied by total lineshape analysis and the experimental data and the calculated activation parameters are tabulated in Table 16. The logarithm of the rate constant is plotted 10<sup>3</sup>/T°K in Figure 15.

## Unsymmetrically Disubstituted Amides

N-Ethyl-N-methylacetamide --- Hindered internal rotation in N-ethyl-N-methylacetamide in the neat liquid was studied by total lineshape analysis of the N-methyl proton resonances. The experimental data and the calculated activation parameters are tabulated in the Table 17. The logarithm of the rate constant is plotted against 10<sup>3</sup>/T°K in Figure 16.

N-n-Butyl-N-methylacetamide --- Hindered internal rotation in N-n-butyl-N-methylacetamide in the neat liquid was studied by total lineshape analysis of the N-methyl proton resonances. The experimental data and the calculated activation parameters are tabulated in Table 18. The logarithm of the rate constant is plotted against 10<sup>3</sup>/T°K in Figure 17.

N-Cyclohexyl-N-methylacetamide --- Hindered internal rotation in N-cyclohexyl-N-methylacetamide in the neat liquid was studied by total

Table 14. Experimental data and calculated activation parameters for the internal rotation about the central C-N bond in neat N,N-dimethylformamide-d<sub>1</sub>.

T°K	10 <sup>3</sup> /T°K	τ* sec	ln(1/2τ)	δν <sup>*</sup> Hz	P <sub>A</sub> *
370.3	2.700	0.279	0.583	15.0	0.506
373.9	2.675	0.217	0.835	15.2	0.502
379.0	2.639	0.118	1.446	15.0	0.499
383.5	2.607	0.0805	1.827	15.0	0.503
388.6	2.573	0.0651	2.038	14.9	0.496
397.8	2.514	0.0243	3.025	15.0	0.497
403.9	2.476	0.0169	3.390	15.1	0.501
407.5	2.454	0.0119	3.737		
412.5	2.424	0.0082	4.105		
417.1	2.397	0.0056	4.491		
422.2	2.369	0.0043	3.749		

 $E_a = 25.3 \pm 0.3 \text{ kcal/mole}$ 

 $log10A = 15.2 \pm 0.2$ 

 $\Delta H^{\ddagger} = 24.6 \pm 0.3 \text{ kcal/mole}$ 

Coalescence temperature = 404°K

 $<sup>\</sup>Delta G^{\dagger}_{298} = 22.1 \pm 0.3 \text{ kcal/mole}$ 

 $<sup>\</sup>Delta S^{\ddagger} = 8.5 \pm 1.2 \text{ eu}$ 

<sup>\*</sup>Results from total lineshape analysis.

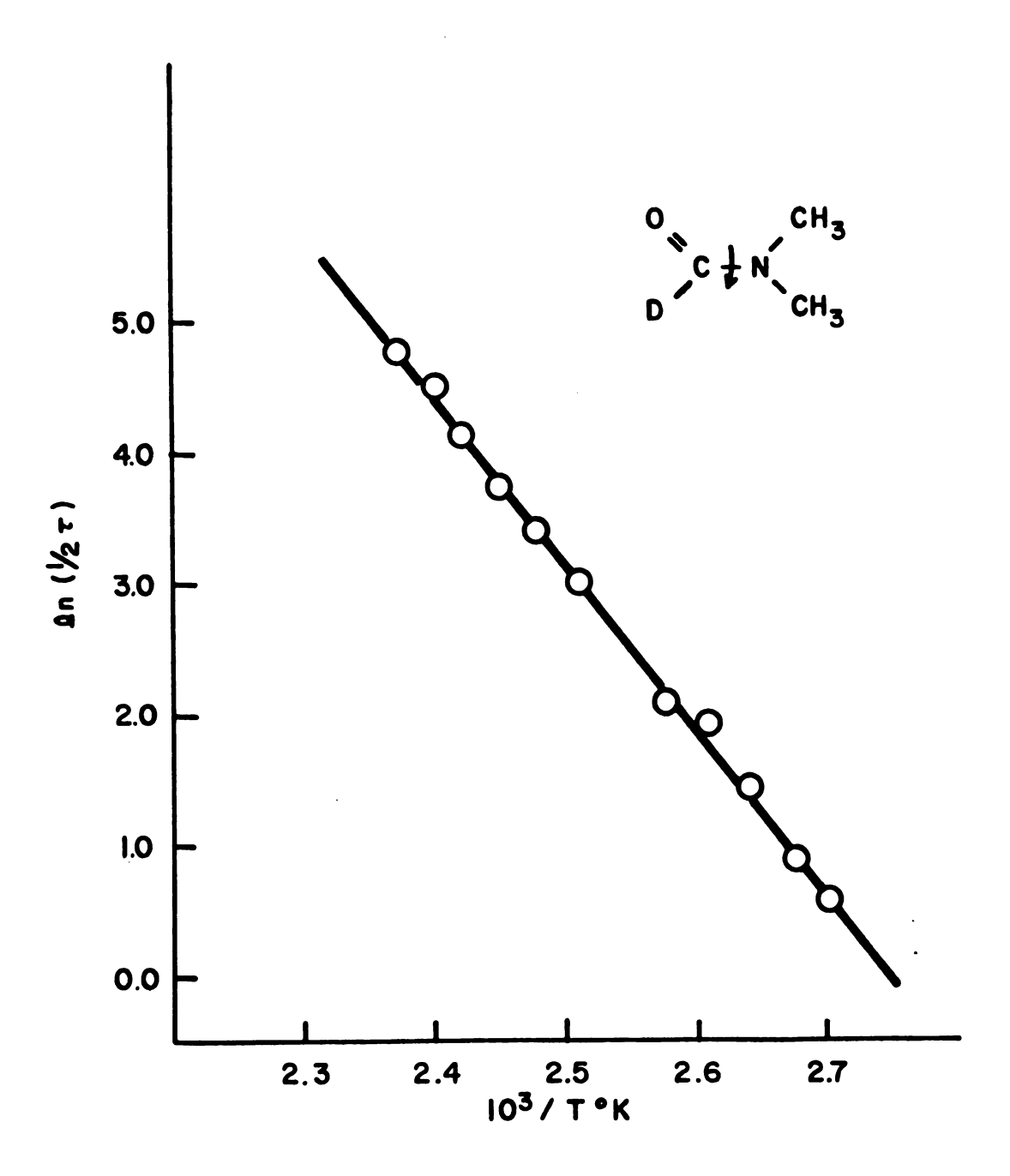


Figure 13. Plot of  $\ln(1/2\tau)$  against  $10^3/T^\circ K$  for neat N,N-dimethylformamide-d1.

Table 15. Experimental data and calculated activation parameters for the internal rotation about the central C-N bond in neat N,N-dimethylpropionamide.

T°K	10 <sup>3</sup> /T°K	* τ sec	ln(1/2τ)	δν Hz	P <sub>A</sub> *
314.2	3.183	0.0785	1.851	14.4	0.508
319.2	3.133	0.0455	2.396	14.5	0.504
321.0	3.115	0.0390	2.551	14.8	0.492
321.0	3.115	0.0393	2.545	14.5	0.504
322.2	3.103	0.0395	2.538	14.7	0.502
322.2	3.103	0.0358	2.640	14.8	0.507
323.5	3.091	0.0294	2.833	14.5	0.498
323.6	3.090	0.0289	2.851	15.0	0.495
325.9	3.069	0.0268	2.928	14.7	0.502
325.9	3.069	0.0268	2.925	14.9	0.496
326.2	3.066	0.0249	2.300		
327.5	3.053	0.0228	3.088		
327.9	3.050	0.0209	3.176		
329.3	3.036	0.0194	3.250		
330.5	3.026	0.0172	3.369		
332.9	3.004	0.0139	3.582		
334.8	2.987	0.0118	3.750		
337.2	2.966	0.0096	3.950		

 $E_a = 18.9 \pm 0.4 \text{ kcal/mole}$ 

 $\Delta H^{\ddagger} = 18.2 \pm 0.4 \text{ kcal/mole}$ 

 $\Delta S^{\ddagger} = 3.1 \pm 1.2 \text{ eu}$ 

Coalescence temperature = 331°K

 $log_{10}A = 13.9 \pm 0.3$ 

 $<sup>\</sup>Delta G^{\dagger}_{298} = 17.2 \pm 0.4 \text{ kcal/mole}$ 

<sup>\*</sup>Results from total lineshape analysis.

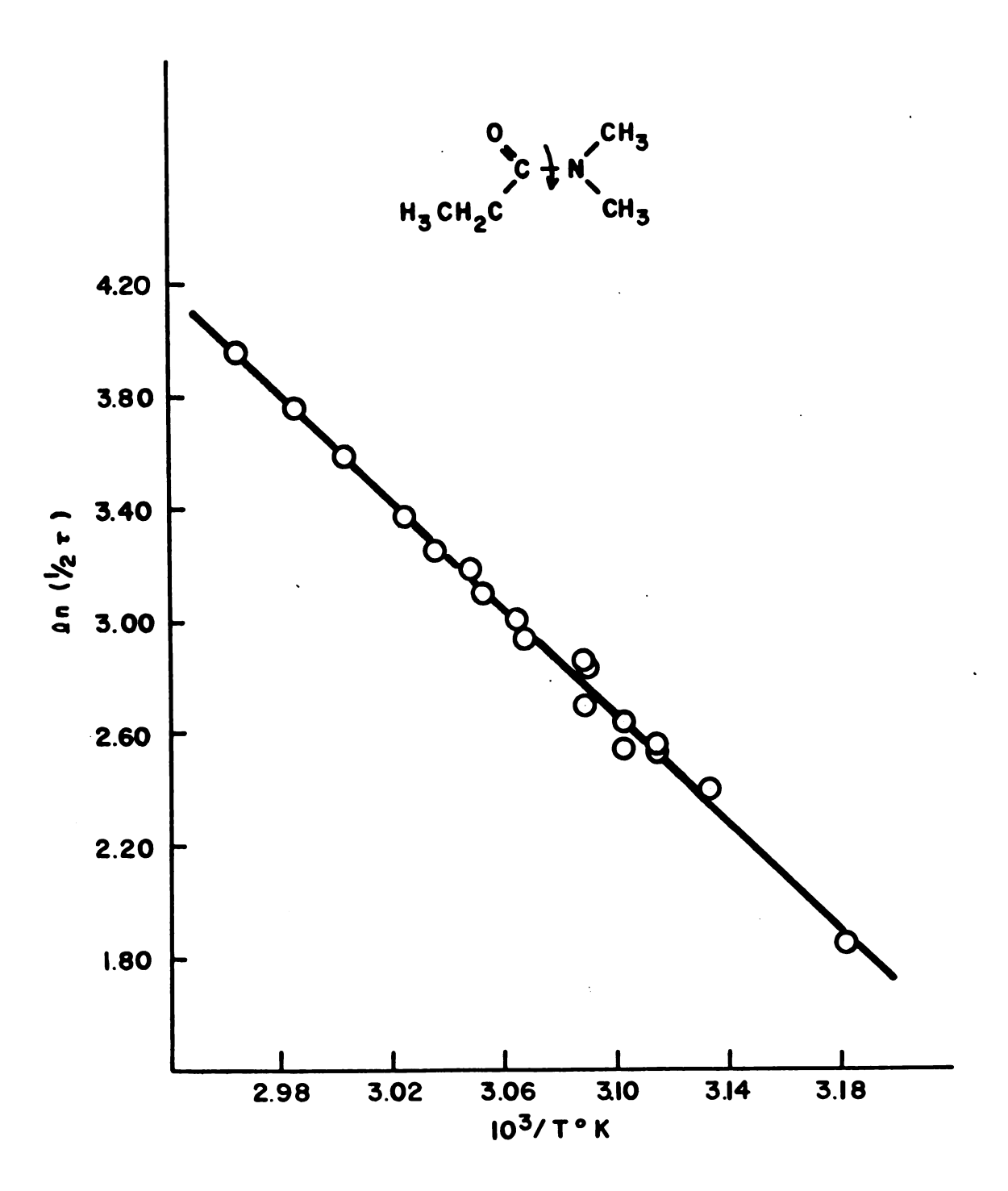


Figure 14. Plot of  $ln(1/2\tau)$  against  $10^3/T^\circ K$  for neat N,N-dimethylpropionamide.

Table 16. Experimental data and calculated activation parameters for the internal rotation about the central C-N bond in neat N,N-dimethyltrichloroacetamide.

T°K	10 <sup>3</sup> /T°K	* τ _sec	ln(1/2τ)	δν <sup>*</sup> Hz	P <sub>A</sub> *
283.2	3.531	0.0326	1.729	29.3	0.498
286.6	3.489	0.0233	3.067	29.2	0.496
288.0	3.472	0.0202	3.207	29.1	0.504
290.1	3.447	0.0171	3.378	29.2	0.512
292.1	3.423	0.0124	3.695	29.0	0.502
295.0	3.390	0.0106	. 3.851	29.2	0.495
296.8	3.369	0.0081	4.119	29.1	0.501
298.2	3.353	0.0074	4.212		
303.6	3.294	0.0047	4.666		
306.9	3.259	0.0033	5.030		

 $E_a = 16.7 \pm 0.3 \text{ kcal/mole}$ 

 $log_{10}A = 14.0 \pm 0.2$ 

 $\Delta H^{\ddagger} = 16.1 \pm 0.3 \text{ kcal/mole}$ 

Coalescence temperature = 299 °K

 $<sup>\</sup>Delta G^{\dagger}_{298} = 15.0 \pm 0.3 \text{ kcal/mole}$ 

 $<sup>\</sup>Delta S^{\dagger} = 3.7 \pm 1.1 \text{ eu}$ 

<sup>\*</sup>Results from total lineshape analysis.

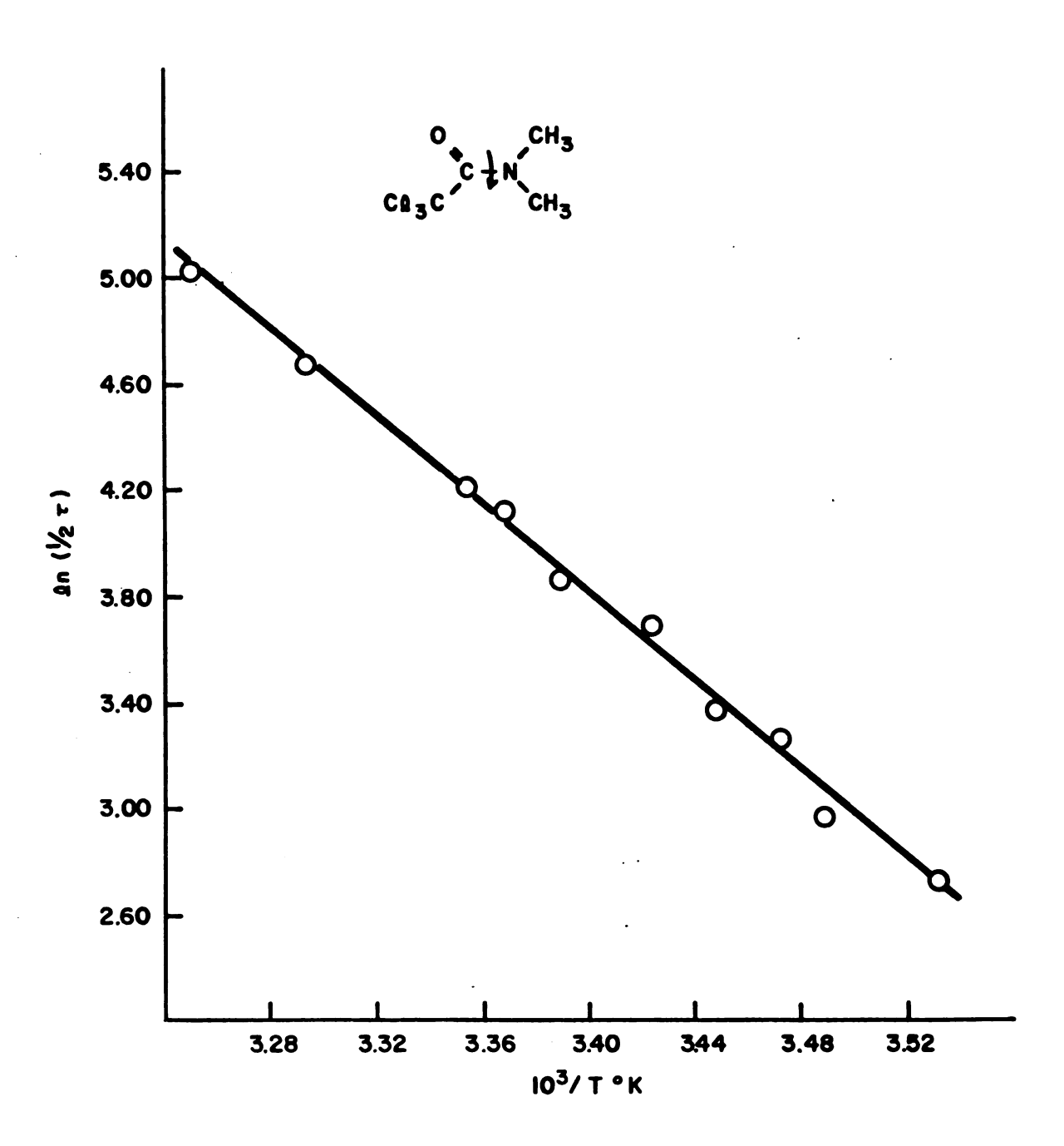


Figure 15. Plot of  $\ln(1/2\tau)$  against  $10^3/\text{T}^{\circ}\text{K}$  for neat N,N-dimethyltrichloroacetamide.

Table 17. Experimental data and calculated activation parameters for the internal rotation about the central C-N bond in neat N-ethyl-N-methylacetamide.

T°K	10 <sup>3</sup> /T°K	τ* sec	ln(1/2τ)	δν <sup>*</sup> Hz	P <sub>A</sub> *
325.7	3.070	0.0685	1.988	15.9	0.502
328.7	3.042	0.0543	2.220	15.9	0.493
331.8	3.014	0.0347	2.668	16.0	0.500
333.1	3.002	0.0314	2.766	15.8	0.464
334.8	2.987	0.0250	2.997	16.2	0.520
337.8	2.960	0.0206	3.191	15.9	0.470
338.2	2.957	0.0193	3.256	16.1	0.518
340.1	2.940	0.0173	3.362	15.6	0.475
340.8	2.934	0.0169	3.387	15.7	0.503
344.2	2.905	0.0122	3.714		
347.2	2.880	0.0092	3.994		
349.1	2.865	0.0077	4.176		

 $E_a = 20.8 \pm 0.5 \text{ kcal/mole}$ 

 $log_{10}A = 14.8 \pm 0.3$ 

 $\Delta G_{298}^{\dagger} = 18.0 \pm 0.5 \text{ kcal mole}$ 

 $\Delta H^{\ddagger} = 20.1 \pm 0.5 \text{ kcal/mole}$ 

 $\Delta S^{\ddagger} = 7.0 \pm 2.0 \text{ eu}$ 

Coalescence temperature = 344°K

<sup>\*</sup>Results from total lineshape analysis.

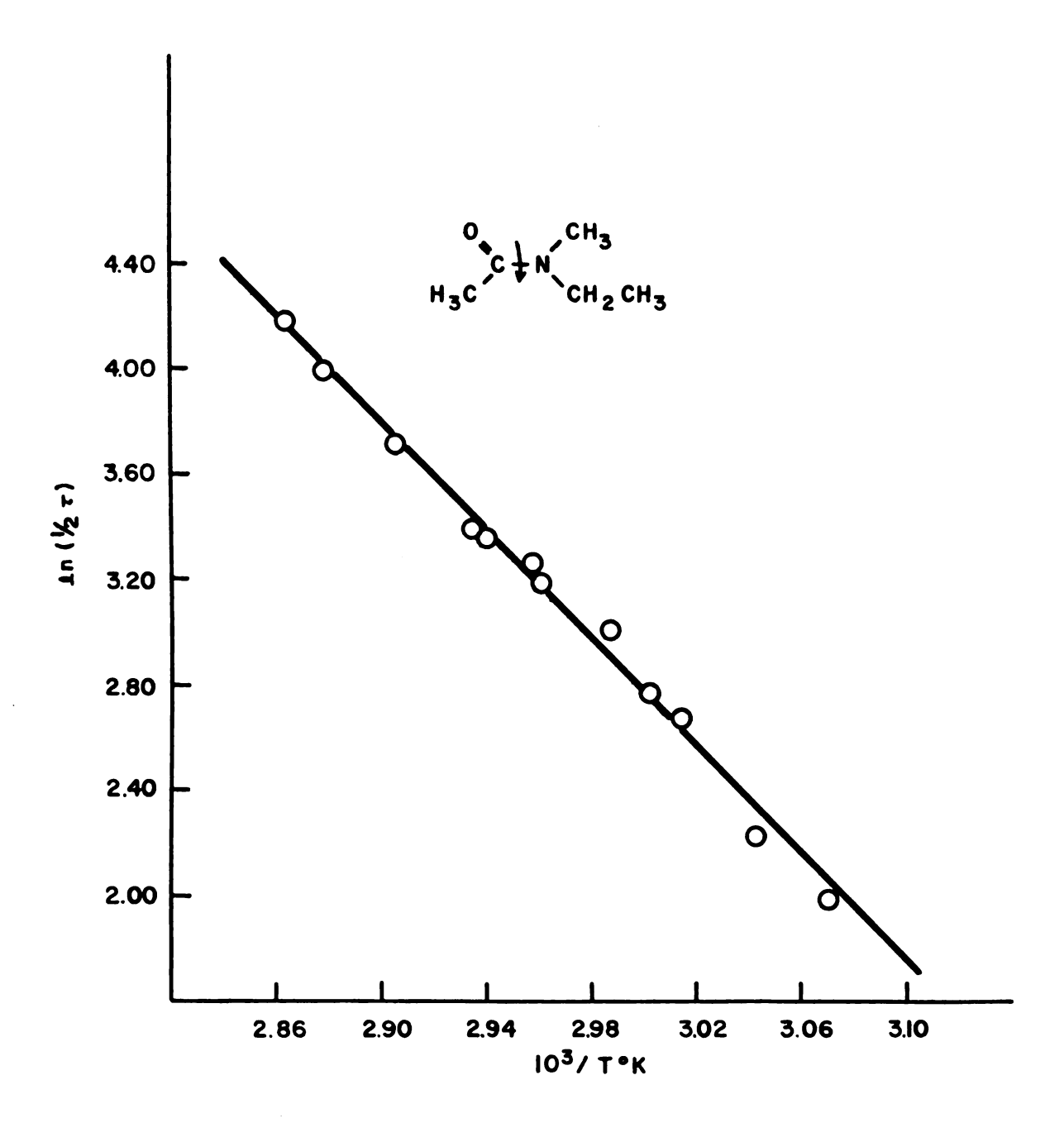


Figure 16. Plot of  $\ln(1/2\tau)$  against  $10^3/T^\circ K$  for neat N-ethyl-N-methylacetamide.

Table 18. Experimental data and calculated activation parameters for the internal rotation about the central C-N bond in neat N-n-butyl-N-methylacetamide.

333.8       2.996       0.0284       2.869       15.0       0         334.0       2.994       0.0295       2.832       14.8       0         337.8       2.961       0.0190       3.268       15.1       0	T°K	10 <sup>3</sup> /T°K	τ* sec	ln(1/2τ)	δν <sup>*</sup> Hz	P <sub>A</sub> *
334.0       2.994       0.0295       2.832       14.8       0         337.8       2.961       0.0190       3.268       15.1       0         338.2       2.957       0.0183       3.310       15.4       0         341.1       2.931       0.0154       3.478         342.6       2.919       0.0134       3.618         345.1       2.898       0.0112       3.798         347.2       2.880       0.0089       4.030	329.0	3.039	0.0432	2.449	14.7	0.476
337.8       2.961       0.0190       3.268       15.1       0         338.2       2.957       0.0183       3.310       15.4       0         341.1       2.931       0.0154       3.478         342.6       2.919       0.0134       3.618         345.1       2.898       0.0112       3.798         347.2       2.880       0.0089       4.030	333.8	2.996	0.0284	2.869	15.0	0.470
338.2       2.957       0.0183       3.310       15.4       0         341.1       2.931       0.0154       3.478         342.6       2.919       0.0134       3.618         345.1       2.898       0.0112       3.798         347.2       2.880       0.0089       4.030	334.0	2.994	0.0295	2.832	14.8	0.480
341.1       2.931       0.0154       3.478         342.6       2.919       0.0134       3.618         345.1       2.898       0.0112       3.798         347.2       2.880       0.0089       4.030	337.8	2.961	0.0190	3.268	15.1	0.474
342.6       2.919       0.0134       3.618         345.1       2.898       0.0112       3.798         347.2       2.880       0.0089       4.030	338.2	2.957	0.0183	3.310	15.4	0.494
345.1       2.898       0.0112       3.798         347.2       2.880       0.0089       4.030	341.1	2.931	0.0154	3.478		
347.2 2.880 0.0089 4.030	342.6	2.919	0.0134	3.618		
	345.1	2.898	0.0112	3.798		
347.8 2.875 0.0083 4.094	347.2	2.880	0.0089	4.030		
	347.8	2.875	0.0083	4.094		
352.1 2.840 0.0060 4.421	352.1	2.840	0.0060	4.421		

 $E_a = 19.7 \pm 0.5 \text{ kcal/mole}$ 

 $log_{10}A = 14.1 \pm 0.3$ 

 $\Delta G_{298}^{\dagger} = 17.9 \pm 0.5 \text{ kcal/mole}$ 

 $\Delta H^{\ddagger} = 19.1 \pm 0.5 \text{ kcal/mole}$ 

 $\Delta S^{\ddagger} = 4.1 \pm 2.0 \text{ eu}$ 

Coalescence temperature = 341°K

<sup>\*</sup>Results from total lineshape analysis.

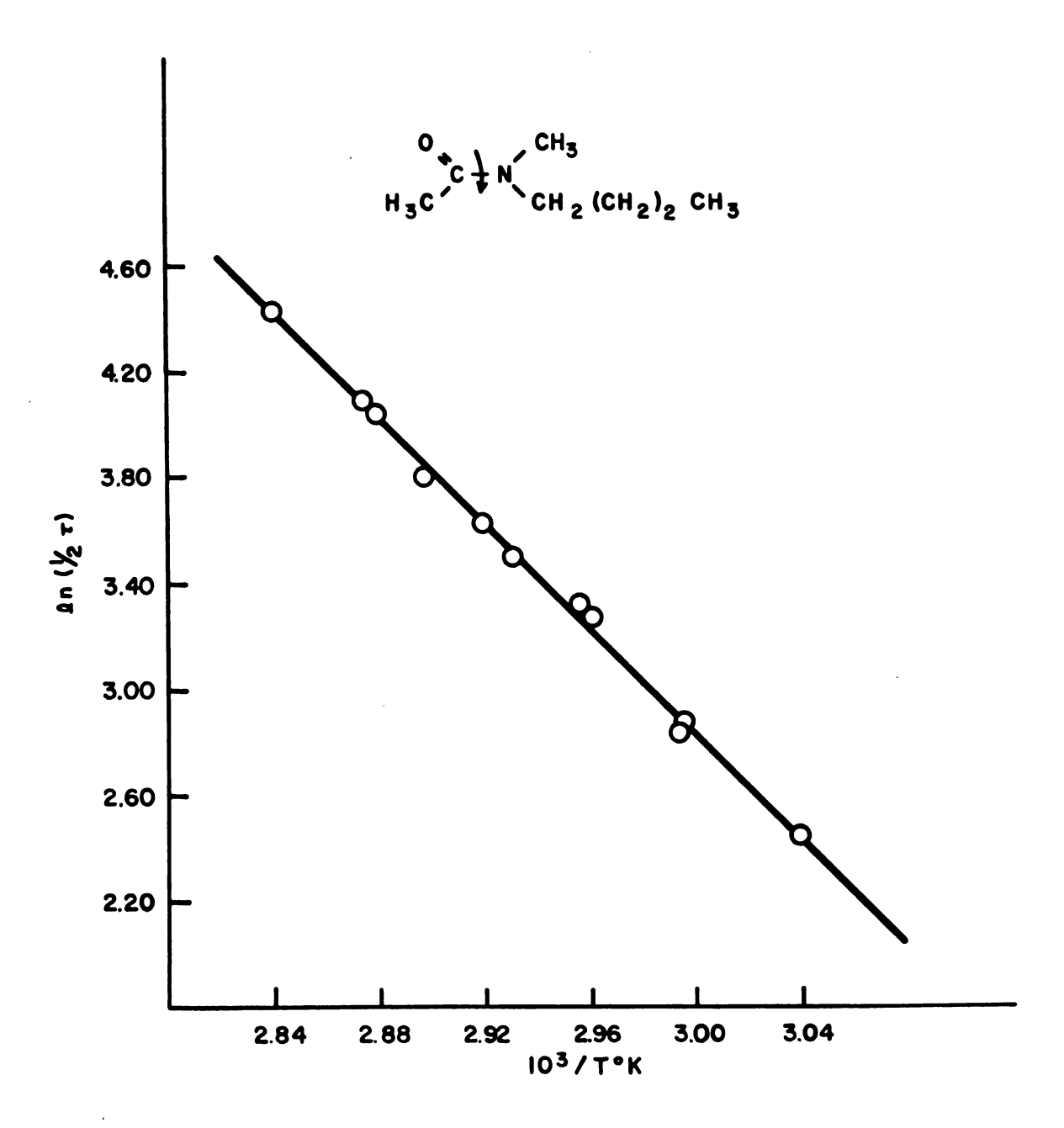


Figure 17. Plot of  $\ln(1/2\tau)$  against  $10^3/T^\circ K$  for neat N-n-butyl-N-methylacetamide.

lineshape analysis of the N-methyl proton resonance. The experimental data and the calculated activation parameters are tabulated in Table 19. The logarithm of the rate constant is plotted against  $10^3/\text{T}^{\circ}\text{K}$  in Figure 18.

N-Isopropyl-N-methylacetamide --- Hindered internal rotation in N-isopropyl-N-methylacetamide in the neat liquid was studied by total line-shape analysis of the N-methyl proton resonance. The experimental data and calculated activation parameters are tabulated in Table 20. The logarithm of the rate constant is plotted against 10<sup>3</sup>/T°K in Figure 19.

Resonance Assignments in the Proton NMR Spectra of Several Tertiary Amides

In this study, Eu(fod)<sub>3</sub>, tris(1,1,1,2,2,3,3-heptafluoro-7,7-dimethyl-4,6-octanedionato) europium (III), a paramagnetic shift reagent, was used to assign the proton resonances in substituted amides. Spectra were obtained at 100 MHz at a temperature chosen for each amide to be well below the coalescence temperature so that the rotational isomers are distinguishable. Samples were 0.2 M amide in CCl<sub>4</sub> and increasing amounts of Eu(fod)<sub>3</sub> were added. The chemical shifts relative to TMS were plotted versus the mole ratio of shift reagent to amide. A linear correlation was found for each group of protons. A linear least-squares analysis was applied to each data set to ascertain the chemical shift in the absence of shift reagent and the  $\triangle$ Eu ( $\triangle$ Eu =  $\delta$ CCl<sub>4</sub> -  $\delta$ CCl<sub>4</sub> ) value for each group of protons. The chemical shift in the absence of shift reagent was used to assign the resonance to the corresponding group of protons.

1-Methyl-2-pyrrolidinone --- To establish the validity of the method, 1-methyl-2-pyrrolidinone was chosen as a model system since the N-methyl

Table 19. Experimental data and calculated activation parameters for the internal rotation about the central C-N bond in neat N-cyclohexyl-N-methylacetamide.

T°K	10 <sup>3</sup> /T°K	* r 	ln(1/2τ)	* δν Hz	P <sub>A</sub> *
305.1	3.277	0.1439	1.245	11.1	0.457
314.1	3.184	0.0506	2.290	11.2	0.447
318.5	3.140	0.0364	2.621	11.1	0.470
320.7	3.118	0.0347	2.667	10.7	0.487
321.8	3.107	0.0304	2.801	10.7	0.485
322.3	3.102	0.0292	2.840	11.1	0.450
324.7	3.080	0.0212	3.159		
326.8	3.060	0.0171	3.376		
330.1	3.029	0.0124	3.699		

$$E_a = 18.9 \pm 0.5 \text{ kcal/mole}$$

 $log_{10}A = 14.1 \pm 0.3$ 

$$\Delta G^{\dagger}_{298} = 17.1 \pm 0.5 \text{ kcal/mole}$$

 $\triangle H^{\ddagger} = 18.3 \pm 0.5 \text{ kcal/mole}$ 

$$\Delta S^{\ddagger} = 3.9 \pm 2.0 \text{ eu}$$

Coalescence temperature = 325°K

<sup>\*</sup>Results from total lineshape analysis.

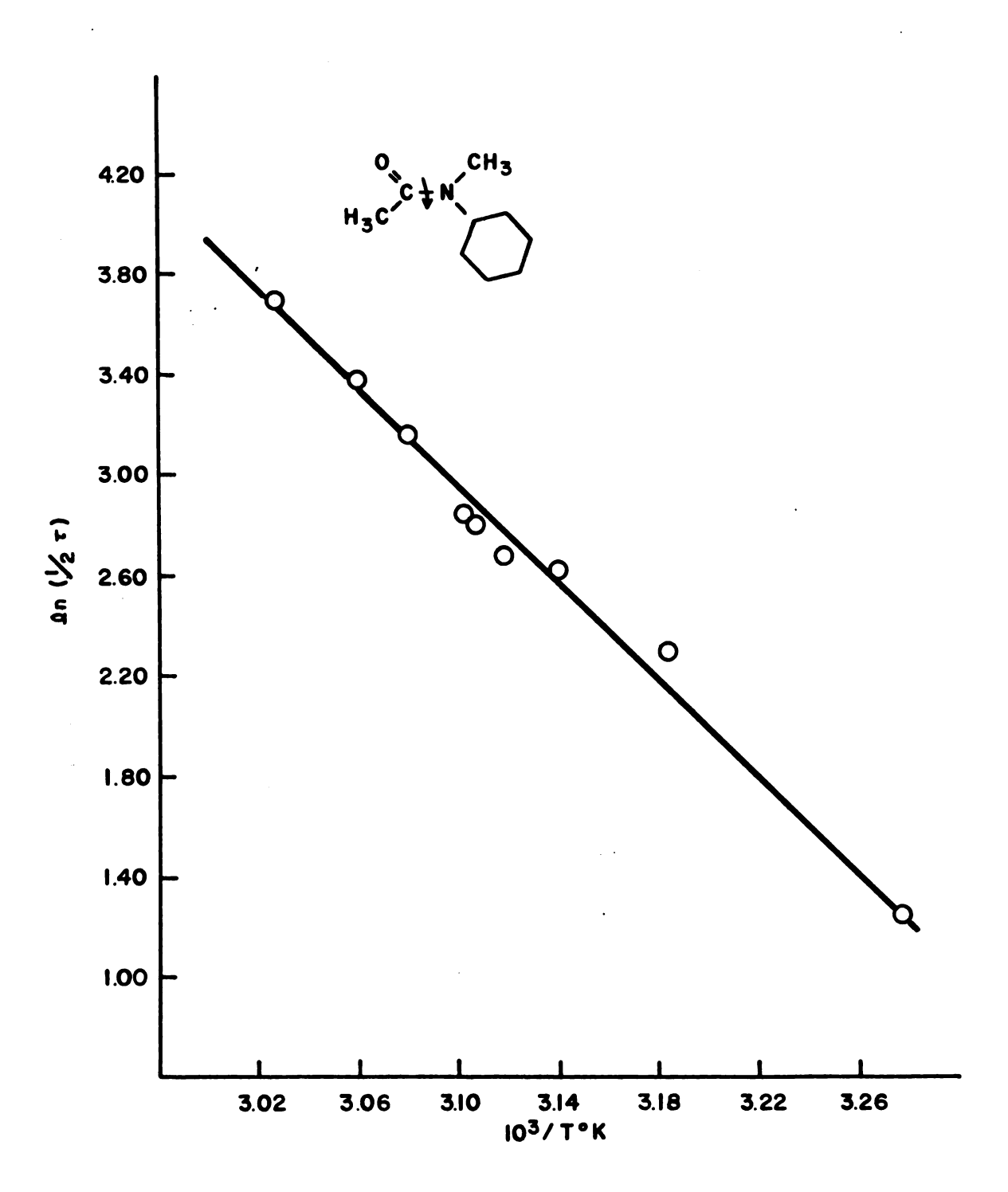


Figure 18. Plot of  $ln(1/2\tau)$  against  $10^3/T^\circ K$  for neat N-cyclohexyl-N-methylacetamide.

Table 20. Experimental data and calculated activation parameters for the internal rotation about the central C-N bond in neat N-isopropyl-N-methylacetamide.

T°K	10 <sup>3</sup> /т°К	* τ sec	1n(1/2τ)	δν* Hz	P <sub>A</sub> *
305.6	3.272	0.1028	1.581	11.4	0.444
314.8	3.177	0.0453	2.402	11.5	0.459
316.7	3.157	0.0414	2.492	11.2	0.441
318.9	3.136	0.0335	2.704	11.2	0.457
320.8	3.117	0.0278	2.888	11.3	0.440
322.3	3.102	0.0233	3.066	11.2	0.448
325.4	3.073	0.0181	3.319		
326.6	3.062	0.0156	3.467		
330.8	3.023	0.0104	3.873		

 $E_a = 18.1 \pm 0.5 \text{ kcal/mole}$ 

 $log_{10}A = 13.6 \pm 0.3$ 

 $\Delta G_{298}^{\dagger} = 17.0 \pm 0.5 \text{ kcal/mole}$ 

 $\Delta H^{\ddagger} = 17.5 \pm 0.5 \text{ kcal/mole}$ 

 $\Delta S^{\ddagger} = 1.6 \pm 2.0 \text{ eu}$ 

Coalescence temperature = 322°K

<sup>\*</sup>Results from total lineshape analysis.

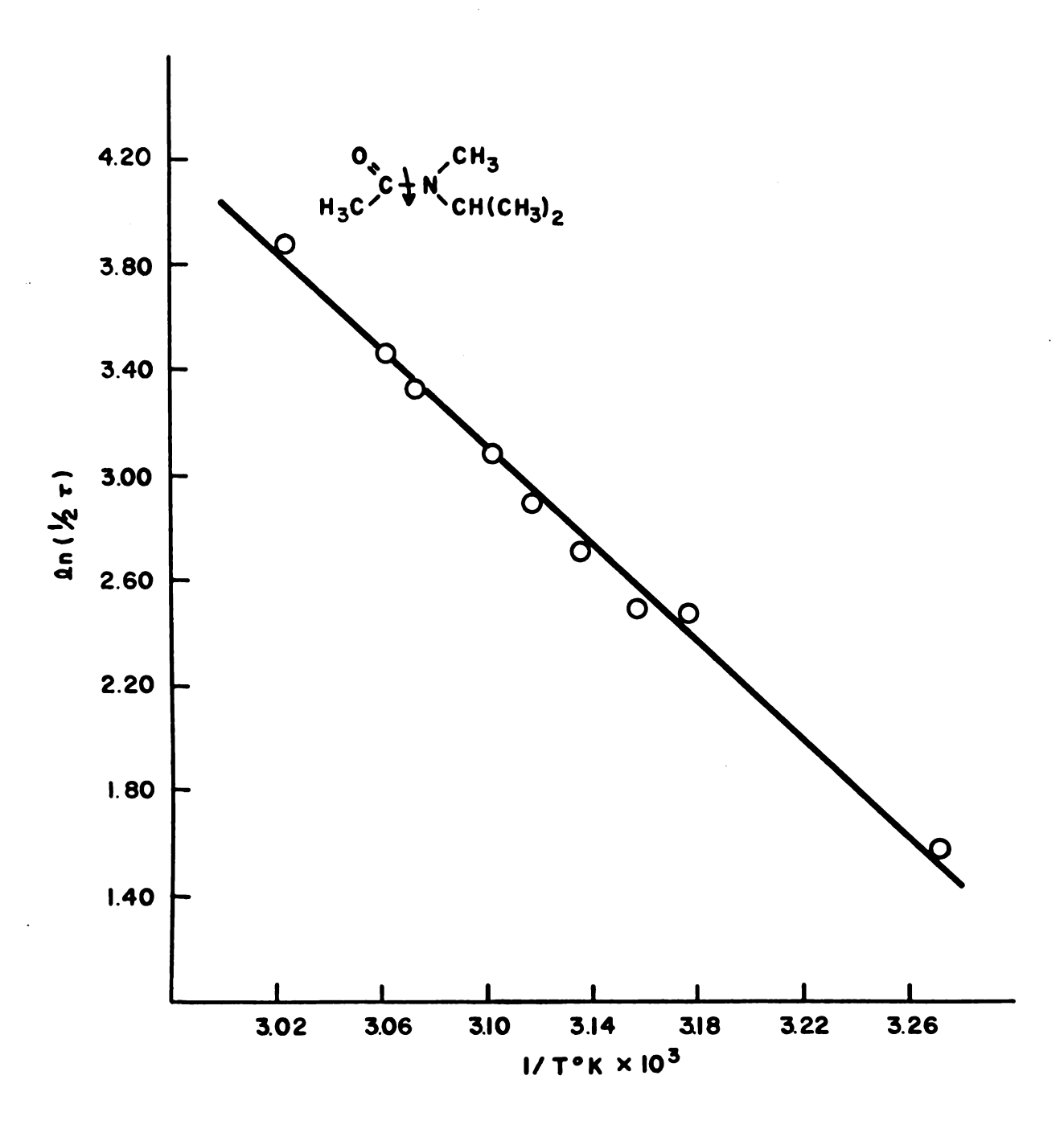


Figure 19. Plot of  $ln(1/2\tau)$  against  $10^3/T^\circ K$  for neat N-isopropyl-N-methylacetamide.

group is fixed in the <u>cis</u> (to oxygen) position. The proton resonance of the N-methyl group can be identified even without the addition of the shift reagent because the resonance appears as a singlet, the only singlet in the spectrum. The chemical shifts from the addition of Eu(fod)<sub>3</sub>, and the results of the least-squares analysis, are given in Table 21.

As expected the <u>cis</u>-methyl protons were shifted to a greater extent than the <u>trans</u>-methylene protons in solutions containing the amide complexed with the shift reagent. The AEu value for the <u>cis</u>-methyl protons is 10.12 ppm and for the <u>trans</u>-methylene protons is 5.49 ppm. For the remaining amides the resonances of the <u>cis</u>-trans pair which are shifted the greater amount are assigned to the cis group.

N,N-Dimethylformamide --- The proton spectrum of N,N-dimethylformamide shows three resonances. The formyl proton resonance appears at 7.86 ppm and the two N-methyl protons resonate at 2.93 and 2.81 ppm. The results from the addition of Eu(fod)<sub>3</sub>, and the least-squares analysis, are tabulated in Table 22. For the uncomplexed amide the chemical shift at 2.81 ppm was assigned to the <u>cis</u>-methyl protons ( $\triangle$ Eu = 9.39 ppm) and the chemical shift at 2.93 ppm to the trans-methyl protons ( $\triangle$ Eu = 4.04 ppm).

N.N-Diethylformamide --- The proton NMR spectrum of N,N-diethylformamide shows five resonances: a singlet at 7.90 ppm from the formyl proton, two quartets at 3.30 and 3.26 ppm from the N-methylene protons, and two triplets at 1.19 and 1.10 ppm from the methyl protons. The data from the addition of Eu(fod)<sub>3</sub> are tabulated in the Table 23 along with the results of the least-squares analysis. The quartet at 3.30 ppm was assigned to the <u>cis</u> (to oxygen)-methylene proton ( $\triangle$ Eu = 9.86 ppm) and the quartet at 3.26 ppm to the <u>trans</u>-methylene protons ( $\triangle$ Eu = 3.87 ppm). The triplet at 1.19 ppm was assigned to the <u>trans</u>-methyl protons ( $\triangle$ Eu = 2.48

Table 21. Proton chemical shifts a, observed and calculated, in 1-methyl-2-pyrrolidinone, with increasing amounts of Eu(fod)3.

$$\begin{array}{c|c}
C & CH_3(1) \\
CH_2(2) & CH_2(3)
\end{array}$$

	Mole Ratio of Shift Reagent/Amide				gent/Amide	
	0.00	0.097	0.194	0.291	0.00	
Proton Resonance		δο	b bs		δcalc	∆Eu
(1)	2.76	3.78	4.78	5.75	2.80 ± 0.02	10.12 ± .08
(2)	3.32	3.87	4.41	4.93	3.34 ± 0.01	5.49 ± 0.05
(3)	1.98	2.49	2.99	3.48	2.00 ± 0.01	5.09 ± 0.05
(4)	2.19	3.54	4.85	6.12	2.25 ± 0.03	13.33 ± 0.12

<sup>&</sup>lt;sup>a</sup>Spectra were obtained at 32°C.

bAll chemical shifts are in ppm from TMS.

Table 22. Proton chemical shifts a, observed and calculated, in N,N-dimethylformamide with increasing amounts of Eu(fod)<sub>3</sub>.

	Mole Ratio of Shift Reagent/Amide						
	0.00	0.084	0.166	0.248	0.330	0.00	
Proton Resonance			δ <sub>obs</sub>			<sup>δ</sup> calc	∆Eu
(1)	2.81	3.65	4.37	5.18	5.97	2.85 ± 0.03	9.32 ± 0.16
(2)	2.93	3.30	3.60	3.96	430.1	2.95 ± 0.02	4.04 ± 0.10
(3)	7.86	9.09	10.12	11.29	12.43	7.94 ± 0.06	13.42 ± 0.20

<sup>&</sup>lt;sup>a</sup>Spectra were obtained at 32°C.

bAll chemical shifts are in ppm from TMS.

Table 23. Proton chemical shifts a, observed and calculated, in N,N-diethylformamide with increasing amounts of Eu(fod)<sub>3</sub>.

$$\begin{array}{c|c}
C & CH_{2}(1) - CH_{3}(2) \\
C & CH_{2}(3) - CH_{3}(4)
\end{array}$$

		Mole R	Ratio of	Shift	Reagent	/Amide	
	0.00	0.100	0.200	0.300	0.400	0.0	
Proton Resonance	<u> </u>		δ <sub>obs</sub>			<sup>δ</sup> calc	∆Eu
(1)	3.30	4.33	5.40	6.34	7.24	3.35 ± 0.07	9.68 ± 0.27
(2)	1.10	1.72	2.35	2.92	3.46	1.12 ± 0.04	5.79 ± 0.15
(3)	3.26	3.68	4.11	4.49	4.84	3.26 ± 0.03	3.87 ± 0.12
(4)	1.19	1.46	1.74	1.98	2.21	1.18 ± 0.02	2.48 ± 0.08
(5)	7.90	9.29	10.23	12.01	13.23	7.99 ± 0.10	13.10 ± 0.36

<sup>&</sup>lt;sup>a</sup>Spectra were obtained at 32°C.

 $<sup>^{\</sup>rm b}$ All chemical shifts are in ppm from TMS.

ppm) and the triplet at 1.10 ppm to the <u>cis</u>-methyl protons ( $\triangle Eu = 5.79$  ppm).

N.N-Diisopropylformamide --- The proton NMR spectrum of N,N-diisopropylformamide shows five resonances: the formyl proton resonates at 8.03 ppm, the N-methine protons resonate at 3.87 and 3.55 ppm, and the methyl protons resonate at 1.27 and 1.26 ppm. The data from the addition of Eu(fod)<sub>3</sub> in Table 24 along with the results of the least-squares analysis. The chemical shift at 3.87 ppm was assigned to the <u>cis</u> (to oxygen) methine proton ( $\triangle$ Eu = 8.24 ppm) and the chemical shift at 3.55 ppm was assigned to the <u>trans</u>-methine proton ( $\triangle$ Eu = 3.07 ppm). The assignment for the methyl protons is very uncertain because of the proximity of the resonances. Tentatively, the resonance at 1.27 ppm was assigned to the <u>trans</u>-methyl protons ( $\triangle$ Eu = 2.14 ppm) and the resonance at 1.26 ppm to the cis-methyl proton ( $\triangle$ Eu = 6.03 ppm).

N.N-Dimethylacetamide --- The proton NMR spectrum of N,N-dimethylacetamide shows three resonances. The N-methyl protons resonate at 2.99 and 2.85 ppm and the acetyl protons resonate at 1.96 ppm. This amide was studied by use of two different shift reagents,  $Eu(fod)_3$  and tris(1,1,1,-2,2,3,3-heptafluoro-7,7-dimethyl-4,6-octanedionato) praseodymium (III),  $Pr(fod)_3$ . The shift reagent  $Pr(fod)_3$  produces upfield shifts, however the resultant effect is identical to  $Eu(fod)_3$ . The results from the least-squares analysis and the addition of  $Eu(fod)_3$  are given in Table 25 and the results from  $Pr(fod)_3$  in Table 26. The resonance at 2.99 ppm was assigned to the trans-methyl protons ( $\Delta Eu = 5.24$  ppm,  $\Delta Pr = -9.04$  ppm) and the resonance at 2.86 ppm to the trans-methyl protons ( $\Delta Eu = 10.18$  ppm,  $\Delta Pr = -16.16$  ppm).

Table 24. Proton chemical shifts<sup>a</sup>, observed and calculated, in N,N-disopropylformamide with increasing amounts of Eu(fod)<sub>3</sub>.

$$\begin{array}{c|c}
CH(1)-(CH_3)_2(2) \\
CH(3)-(CH_3)_2(4)
\end{array}$$

		Mole Ra					
	0.00	0.100	0.200	0.300	0.400	0.00	
Proton Resonance			δ <sub>obs</sub>			<sup>δ</sup> calc	∆Eu
(1)	3.87	4.80	5.60	7.27	8.28	3.96 ± 0.02	8.24 ± 0.10
(2)	1.26	1.90	2.46	3.07	3.70	1.27 ± 0.03	6.03 ± 0.10
(3)	3.55	3.95	4.24	4.55	4.87	3.62 ± 0.01	3.07 ± 0.05
(4)	1.27	1.50	1.70	1.93	2.14	1.28 ± 0.01	2.14 ± 0.03
(5)	8.03	9.18	10.21	11.29	12.42	8.07 ± 0.04	10.81 ± 0.16

<sup>&</sup>lt;sup>a</sup>Spectra were obtained at 32°C.

<sup>&</sup>lt;sup>b</sup>All chemical shifts are in ppm from TMS.

Table 25. Proton chemical shifts a, observed and calculated, in N,N-dimethylacetamide with increasing amounts of Eu(fod)<sub>3</sub>.

$$C - N$$
 $CH_3(1)$ 
 $CH_3(2)$ 

Mole Ratio of Shift Reagent/Amide

	0.00	<u>0.100</u>	0.200	0.300	0.00	
Proton Resonance		δ <sub>ob</sub>	s S		<sup>δ</sup> calc	∆Eu
(1)	2.85	3.92	4.94	5.96	2.90 ± 0.03	10.18 ± 0.02
(2)	2.99	3.50	4.02	4.54	2.97 ± 0.005	5.24 ± 0.01
(3)	1.96	3.17	4.30	5.45	2.03 ± 0.01	11.39 ± 0.06

<sup>&</sup>lt;sup>a</sup>Spectra were obtained at 32°C.

 $<sup>^{\</sup>mathbf{b}}\mathbf{All}$  chemical shifts are in ppm from TMS.

Table 26. Proton chemical shifts<sup>a</sup>, observed and calculated, in N,N-dimethylacetamide with increasing amounts of Pr(fod)<sub>3</sub>.

$$C - N$$
 $CH_3(1)$ 
 $CH_3(2)$ 

	M	ole Rat				
	0.00	0.095	0.190	0.285	0.00	
Proton Resonance		δο	bs		<sup>δ</sup> calc	ΔPr
(1)	2.85	1.32	-0.16	-1.74	2.87 ± 0.03	$-16.16 \pm 0.10$
(2)	2.99	2.09	1.29	0.38	2.97 ± 0.02	- 9.03 ± 0.09
(3)	1.96	0.34	-1.17	-2.92	2.02 ± .05	-17.22 ± 0.16

<sup>&</sup>lt;sup>a</sup>Spectra were obtained at 32°C.

 $<sup>^{\</sup>mathbf{b}}\mathbf{All}$  chemical shifts are in ppm from TMS.

N.N-Dimethylcarbamylchloride --- The proton spectrum of N,N-dimethylcarbamylchloride shows two resonances, at 3.17 and 3.06 ppm, for the N-methyl protons. The results from the addition of Eu(fod)<sub>3</sub> and the least-squares analysis are given in Table 27. The chemical shift at 3.17 ppm was assigned to the <u>trans</u>-methyl protons ( $\triangle Eu = 6.18$  ppm) and the chemical shift at 3.06 ppm to the <u>cis</u>-methyl protons ( $\triangle Eu = 11.65$  ppm).

N.N-Dimethyltrichloroacetamide --- The proton spectrum of N.N-dimethyltrichloroacetamide shows two resonances, at 3.38 and 3.10 ppm, from the N-methyl protons. The results from the addition of Eu(fod)<sub>3</sub> and the least-squares analysis are tabulated in Table 28. The resonance at 3.38 was assigned to the <u>trans</u>-methyl protons ( $\triangle Eu = 7.99$  ppm) and the resonance at 3.10 ppm to the cis-methyl protons ( $\triangle Eu = 16.63$  ppm).

N.N-Dimethyltrifluoroacetamide --- The proton NMR spectrum of N,N-dimethyltrifluoroacetamide shows two resonances, at 3.13 and 3.02 ppm, from the N-methyl protons. Each of these resonances is split into quartets due to the long-range coupling with fluorine (I = 1/2). The results from the addition of Eu(fod)<sub>3</sub> and the least-squares analysis are given in Table 29. The chemical shift at 3.13 ppm was assigned to the transmethyl protons ( $\triangle Eu = 5.12$  ppm) and the chemical shift at 3.02 ppm to the cis-methyl protons ( $\triangle Eu = 9.38$  ppm).

Ethyl-N,N-dimethylcarbamate --- The proton NMR spectrum of ethyl-N,N-dimethylcarbamate shows four resonances. The methylene and methyl protons of the ethoxy group resonate at 4.18 and 1.32 ppm, respectively. The N-methyl protons resonate at 2.94 and 2.92 ppm. The results from the addition of Eu(fod)<sub>3</sub> are given in Table 30. The resonances assignments for the N-methyl protons could not be made with certainty because the chemical shift (2.0 Hz) between the cis and trans resonances is smaller

Table 27. Proton chemical shifts a, observed and calculated, in N,N-dimethylcarbamylchloride, with increasing amounts of Eu(fod)<sub>3</sub>.

$$\begin{array}{c}
C & CH_3(1) \\
C & CH_3(2)
\end{array}$$

	Mo	le Rati	ent/Amide			
	0.00	0.099	0.198	0.297	0.00	
Proton Resonance		δ <sub>ob</sub>	b <u>s</u>		δcalc	∆Eu
(1)	3.06	4.10	5.37	6.43	2.97 ± 0.08	11.65 ± 0.30
(2)	3.17	3.71	4.38	4.94	3.11 ± 0.04	6.18 ± 0.10

 $<sup>^{\</sup>mathrm{a}}$ Spectra were obtained at -22°C.

 $<sup>^{\</sup>rm b}$ All chemical shifts are in ppm from TMS.

Table 28. Proton chemical shifts<sup>a</sup>, observed and calculated, in N,N-dimethyltrichloroacetamide with increasing amounts of Eu(fod)<sub>3</sub>.

$$CH_{3}(1)$$
 $CH_{3}(2)$ 

	M	ole Rat				
	0.00	0.097	0.194	0.291	0.00	
Proton Resonance		δ <sub>ob</sub>	b s		δcalc	ΔEu
(1)	3.10	4.75	6.40	7.92	3.18 ± 0.07	16.63 ± 0.30
(2)	3.38	4.16	4.92	5.68	3.40 ± 0.002	7.99 ± 0.02

<sup>&</sup>lt;sup>a</sup>Spectra were obtained at -22°C.

<sup>&</sup>lt;sup>b</sup>All chemical shifts are in ppm from TMS.

Table 29. Proton chemical shifts  $^{\rm a}$ , observed and calculated, in N,N-dimethyltrifluoroacetamide with increasing amounts of Eu(fod)<sub>3</sub>.

$$C - N = CH_3(1)$$
 $F_3C - N = CH_3(2)$ 

	M	ole Rat				
	0.00	0.100	0.200	0.300	0.00	
Proton Resonance		δ <sub>ob</sub>	b s		<sup>δ</sup> calc	∆Eu
(1)	3.02	3.97	4.92	5.94	2.97 ± 0.04	9.38 ± 0.14
(2)	3.13	3.58	4.09	4.60	3.07 ± 0.005	5.12 ± 0.02

<sup>&</sup>lt;sup>a</sup>Spectra were obtained at 32°C.

<sup>&</sup>lt;sup>b</sup>All chemical shifts are in ppm from TMS.

Table 30. Proton chemical shifts<sup>a</sup>, observed and calculated, in ethyl-N,N-dimethylcarbamate with increasing amounts of Eu(fod)<sub>3</sub>.

$$0$$
  $C - N$   $CH_3(1)$   $CH_3(2)$   $CH_3(2)$ 

Mole Ratio of Shift Reagent/Amide 0.00 0.100 0.200 0.300 0.00  $\delta_{\underline{obs}}$  $\delta_{calc}$ Proton Resonance Œu 4.88  $2.97 \pm 0.06$  $9.80 \pm 0.21$ (1) 2.92 3.89 5.75 (2) 2.94 3.48 4.11 4.66  $2.90 \pm 0.05$  $6.24 \pm 0.16$ 4.18 5.65 (3) 7.12 8.44  $4.28 \pm 0.09$  $14.55 \pm 0.30$ (4)  $1.28 \pm 0.01$  $4.18 \pm 0.05$ 1.32 1.68 2.07 2.48

<sup>&</sup>lt;sup>a</sup>Spectra were run at -22°C.

bAll chemical shifts are in ppm from TMS.

than the error of the analysis. The △Eu value for the <u>cis</u> (to carbonyl oxygen) methyl protons is 9.80 ppm and for the <u>trans</u>-methyl protons is 6.24 ppm.

N-Isopropyl-N-methylformamide --- The proton NMR resonance of N-Isopropyl-N-methylformamide shows eight resonances, four from each rotational isomer. The formyl proton chemical shift is different for each isomer being 7.97 and 7.84 ppm. The N-methyl protons resonate at 2.78 and 2.67 ppm. The N-methine protons resonate at 4.53 and 3.78 ppm. protons of the isopropyl groups resonate at 1.23 and 1.13 ppm. sults from the addition of Eu(fod) and the least-squares analysis are given in Table 31. The resonance at 2.78 ppm was assigned to the trans (to oxygen) N-methyl protons ( $\triangle Eu = 4.20$  ppm) and the resonance at 2.67 ppm to the <u>cis</u> N-methyl protons ( $\Delta Eu = 9.81$  ppm). The resonance at 4.53 ppm was assigned to the cis (to oxygen) N-methine proton (△Eu = 14.14 ppm) and the resonance at 3.78 ppm to the trans N-methine proton ( $\Delta Eu = 4.14 \text{ ppm}$ ). The resonance at 1.23 ppm was assigned to the transmethyl proton ( $\triangle Eu = 2.62$  ppm) of the isopropyl group and the resonance at 1.13 ppm, to the cis-methyl protons ( $\Delta Eu = 4.86$  ppm) of the isopropyl group.

## Carbon-13 Chemical Shifts of Aliphatic Amides

The carbon-13 chemical shifts given in this section were obtained at a radiofrequency of 25.1 MHz on a Varian HA-100 NMR spectrometer with noise-modulated proton decoupling. The chemical shifts were initially referenced to an external sample of 57% enriched carbon-13 methanol and converted to the TMS standard by the following relationship:

Table 31. Proton chemical shifts a, observed and calculated, in N-isopropyl-N-methylformamide with increasing amounts of Eu(fod)<sub>3</sub>.

	M	ole Rat				
	0.00	0.096		0.289	0.00	
Proton Resonance		δ <sub>ο</sub>	b bs	<del></del>	δcalc	∆Eu
(1)	2.67	3.60	4.57	5.46	2.68 ± 0.05	9.81 ± 0.21
(2)	3.78	4.16	4.57	4.95	3.77 ± 0.02	4.14 ± 0.09
(3)	1.23	1.49	1.74	1.99	1.24 ± 0.003	2.62 ± 0.01
(4)	7.97	9.26	10.64	11.89	7.96 ± 0.08	13.82 ± 0.35
(5)	4.53	5.76	7.15	8.45	$4.43 \pm 0.06$	14.14 ± 0.25
(6)	1.13	1.56	2.02	2.49	1.10 ± 0.001	4.86 ± 0.01
(7)	2.78	3.14	3.56	3.94	$2.74 \pm 0.03$	4.20 ± 0.15
(8)	7.84	9.06	10.41	11.68	7.76 ± 0.05	13.77 ± 0.25

<sup>&</sup>lt;sup>a</sup>Spectra were run at 32°C.

 $<sup>^{\</sup>mathbf{b}}$ All chemical shifts are in ppm from TMS.

$$\delta_{\text{TMS}} = \delta_{\text{CH}_3\text{OH}} + 49.4 \tag{42}$$

In order to comply with the accepted convention for proton NMR spectra, carbon-13 chemical shifts downfield from TMS are positive and upfield shifts from TMS are negative. The uncertainty in the carbon-13 chemical shift measurements is  $\pm$  0.1 ppm.

Time-averaging with a Varian C-1024 computer was employed in some cases to increase the signal-to-noise ratio; however, as a result of the rolling baseline discussed in the Experimental Section, the number of scans possible was limited. Fortunately, most of the resonances were detected after a single scan. Some of the carbon-13 spectra were obtained below the ambient temperature so that both rotational isomers could be distinguished.

Chemical shift assignments for the first several amides in each series were rather simple to make. Using these systems as a base, along with chemical shift data available in the literature, assignments were then made for the rest of the amides.

## Monosubstituted Amides

The carbon-13 chemical shifts for fifteen monosubstituted amides are given in Table 32. The proton NMR spectra of monosubstituted formamides exhibit two sets of resonances, one from the conformer for which the N-alkyl substituent is <u>cis</u> (to carbonyl oxygen) and one from the corresponding <u>trans</u> conformer (114). However, one configuration was dominant; its fraction decreased from 0.92 for N-methylformamide to 0.88 for N-ethylformamide and N-isopropylformamide, and to 0.82 for N-t-butylformamide.

Carbon-13 chemical shifts a,b in some N-monosubstituted amides. Table 32.

			Nitrogen Substituent	gen tuent		Carbonyl Substituent	ny1 .uent
Amide	0=0	α-C <sub>c</sub>	B-C	2-C	υ- <sub>Θ</sub>	ς σ	B-C
N-Methylformamide N-Methylacetamide	163.8	24.7				20 5	
N-Methylpropionamide	175.9	26.1					10.3
N-Methylisobutyramide	178.9	26.2				35.4	20.0
N-Methylpivalamide <sup>d</sup>	179.7	27.4				39.4	28.7
N-Ethylformamide	162.8	33.4	14.8				
N-Ethylacetamide	171.4	34.7	14.8			22.8	
N-Ethylpropionamide	175.1	34.7	15.0			29.8	10.4
N-Ethylisobutyramide <sup>d</sup>	177.4	34.8	15.5			35.5	20.5
N-Isopropylformamide	161.5	40.5	22.8				
N-Isopropylacetamide	170.2	41.7	23.3			22.9	
N-Isopropylisobutyramide <sup>d</sup>	176.9	41.5	23.5			35.6	20.7
N-n-Butylformamide	162.6	38.2	32.1	20.6	14.0		
N-n-Butylacetamide	170.9	39.6	32.3	20.8	14.1	22.9	
N- <u>t</u> -Butylformamide	161.7	51.1	29.4				

 $<sup>^{</sup>m a}$ All spectra were obtained at 35°C.

bChemical shifts are in ppm from TMS.

<sup>&</sup>lt;sup>C</sup>Carbon position relative to nitrogen or carbonyl carbon is denoted lpha, eta,  $\gamma$  ... .

 $<sup>^{\</sup>rm d}_{\rm 50\%}$  solution in  ${\rm CCl}_{4}$ .

In all other monosubstituted amides, only one resonance was observed in the proton NMR spectrum for each group of protons of the N-alkyl substituent.

The carbon-13 NMR spectrum of each monosubstituted amide exhibits only one set of resonances for the N-alkyl substituent. The spectrometer was not able to detect the less abundant configuration in the formamides.

In N-monosubstituted amides, the preferred configuration has been shown to be the one in which the N-alkyl substituent is <u>cis</u> to carbonyl oxygen by a variety of methods including dipole-moment measurements and infrared, Raman, ultraviolet spectroscopy (for a detailed bibliography see reference 114). Thus, the carbon-13 resonances of the N-alkyl substituents in Table 32 are for the configuration in which the substituent on nitrogen is <u>cis</u> to carbonyl oxygen.

# Symmetrically Disubstituted Amides

The carbon-13 chemical shifts for twenty-four symmetrically N,N-disubstituted amides are given in Table 33 (N,N-dimethylamides) and Table 34 (N,N-diethylamides, N,N-diisopropylamides, and N,N-di-n-propylamides). In some cases, the spectrum of a particular amide was recorded at temperature of 0°C so that both rotational isomers could be distinguished.

The chemical shift assignment of the N-methyl substituents in dimethylamides was based on an expected upfield steric shift for the methyl group <u>cis</u> to the carbonyl oxygen. This expectation was confirmed experimentally for N,N-dimethylformamide, N,N-dimethylacetamide, and N,N-dimethylcarbamylchloride by McFarlane (55), who found that the upfield

Table 33. Carbon-13 chemical shifts an some N,N-dimethylamides.

	S	Nitrogen Substituent		Su	Carbonyl Substituent	
Ami de	C=0	<b>۵</b>	α-υ			
		trans	cds	α-c	B-C	7-C
N,N-Dimethylformamide	162.8	36.2	31.2			
N,N-Dimethylacetamide	170.2	38.0	34.9	21.9		
N,N-Dimethylpropionamide	173.8	37.3	35.4	26.8	9.8	
N,N-Dimethyl-n-butyramide	172.6	37.3	35.5	35.2	19.2	14.6
N,N-Dimethylisobutyramide	173.8	37.4	35.5	30.5	20.1	
N,N-Dimethylpivalamide	176.5	38.6	38.6	39.1	30.0	
N,N-Dimethyltrifluoroamide	174.5	42.0	36.8			
N,N-Dimethylcarbamylchloride	149.2	40.8	39.0			
N,N-Dimethylchloroacetamide	167.2	38.2	36.5	43.1		
N,N-Dimethyldichloroacetamide	164.6	38.7	37.9	6.99		
N,N-Dimethyltrichoroacetamide	160.6	41.3	40.5	64.7		
N,N-Dimethylacrylamide	166.2	37.5	35.7	129.2	127.6	
Ethyl-N,N-dimethylcarbamate	156.6	36.3	35.8	61.4	15.2	
6						

aChemical shifts are in ppm from TMS.

 $^{\mathrm{b}}\mathrm{Spectra}$  were obtained at 35°C, all other spectra were obtained at 0°C.

<sup>c</sup>Carbon position relative to nitrogen or carbonyl carbon is denoted  $\alpha$ ,  $\beta$ ,  $\gamma$  ...

Carbon-13 chemical shifts a,b of some other symmetrically N,N-disubstituted amides. Table 34.

				Nitrogen Substituent	gen tuent			S C	Carbonyl Substituent	ļt.
Amide	0=0	α-C trans	α-c cis	β-C trans	β-C c1s	γ-C cis	γ-C trans	α-ς	в-с 	λ-C
N,N-Diethylformamide N,N-Diethylacetamide	162.6	42.3	36.9	15.4	13.4			21.6		
N, N-Diethylpropionamide		45.4	9.04	15.0	13.8			26.6	10.2	
N, N-Diethyl-n-butyramide		42.4	40.4	15.1	13.8			35.2	19.5	14.6
N,N-Diethylchloroacetamide	169.4	45.9	41.4	15.1	13.4			43.3		
N,N-Diethylacrylamide	165.2	45.6	41.3	15.9	13.9			129.4	127.5	
N,N-Diisopropylformamide	162.0	47.8	44.0	23.4	20.7					
N, N-Diisopropylacetamide	169.0	50.1	45.8	21.4	21.4			24.2		
N,N-Diisopropylpropionamide	171.8	48.7	45.8	21.4	21.4			28.6	10.2	
N,N-Di- $\overline{\mathbf{n}}$ -propylformamide	163.0	49.3	44.1	22.6	21.2	11.7	11.2			
N,N-Di-n-propylacetamide	169.7	50.7	47.7	23.0	21.8	12.0	11.7	21.9		

<sup>&</sup>lt;sup>a</sup>Chemical shifts are in ppm from TMS.

<sup>&</sup>lt;sup>b</sup>All spectra were obtained at 0°C.

<sup>&</sup>lt;sup>c</sup>Carbon position relative to nitrogen or carbonyl carbon is  $\beta$  denoted  $\alpha$ ,  $\beta$ ,  $\gamma$  ....

carbon-13 shift of the N-methyl substituents in each of these amides was cis to the carbonyl oxygen.

The carbon assignments in N-alkyl substituents larger than methyl were made with the aid of the two lanthanide shift reagents, Eu(fod)3 and Pr(fod)3. The effect of the shift reagent on an amide will be the same in the carbon-13 spectrum as in the proton spectrum; that is, the resonance of a cis-trans pair which is shifted the greater amount can be assigned to the group cis to carbonyl oxygen. The results of the addition of 0.2 grams of Eu(fod)<sub>3</sub> to a five percent by volume solution of N,N-di- $\underline{n}$ -propylformamide in carbon tetrachloride and 0.2 grams of Pr(fod)  $_3$ to a five percent by volume solution of N, N-di-n-propylformamide in carbon tetrachloride are given in Table 35. Eu(fod) 3 shifts the resonances downfield and Pr(fod) 3 shifts the resonances upfield. For the cis-trans pair  $\alpha$  to nitrogen, the carbon resonance upfield was shifted to greater amount and was assigned to the carbon cis to carbonyl oxygen. result was found for the cis-trans pair  $\beta$  to nitrogen; however, for the cis-trans pair  $\gamma$  to nitrogen, the downfield resonance was shifted the greater amount and was assigned to the carbon in the substituent cis to carbonyl oxygen. The assignments of carbon resonances for the N-alkyl substituents in the carbon-13 spectra of the rest of the amides are based on this experiment.

The carbon-13 spectrum of N,N-dimethylpivalamide shows a single resonance for the N-methyl carbons. The reason for this is that the coalescence temperature is below the freezing point of this amide.

Assignment of carbon-13 chemical shifts a for the N-alkyl substituents of N,N-di- $\overline{n}$ -propylformamide in carbon tetrachloride. Table 35.

	N(CH2CH2CH3)2	CH <sub>3</sub> ) 2	N(CH <sub>2</sub> CH <sub>2</sub> CH <sub>3</sub> ) <sub>2</sub>	<sub>2</sub> (£H3 <sub>2</sub>	N(CH2CH2CH3)2	2 <mark>C</mark> H3) 2
	trans	cis	trans	cis	cis	trans
$\delta_{ m TMS}$ (No Shift Reagent)	48.5	43.5	21.8	20.4	11.2	10.8
$\delta_{ m TMS}({ m Eu(fod)_3})$	49.2	45.2	22.6	21.7	12.0	11.0
$\delta_{ extsf{TMS}}( ext{Pr(fod)}_3)$	48.2	42.5	21.2	18.8	10.6	10.6

aChemical shifts are in ppm from TMS.

# Unsymmetrically Disubstituted Amides

The carbon-13 chemical shifts for eleven unsymmetrically N,N-disubstituted amides are given in Table 36. All of the spectra were obtained at O°C so that both rotational isomers could be distinguished. The assignment of the N-alkyl substituents are based on the results of the effect of the lanthanide shift reagent on N,N-di-n-propylformamide.

The carbon-13 NMR spectra of N-ethyl-N-methylpivalamide and N-n-butyl-N-methylpivalamide exhibit only one set of resonances for each set of N-alkyl substituents. The reason for this observation is that the coalescence temperature is below the freezing point of each of these amides. The carbon-13 spectra of N-t-butyl-N-methylformamide and N-t-butyl-N-methylacetamide also exhibit only one set of resonances for each N-alkyl substituent. This may be a result of the coalescence temperature being below the freezing point in these amides or one of the rotational isomers may be strongly preferred over the other (49).

Table 36. Carbon-13 chemical shifts a, b of some unsymmetrically N,N-disubstituted amides.

				Nitr	Nitrogen Substituents	stituen	ıts			
	N-methy1	hy1				N-alkyl	ky1			
Ami de			υ-υ		B-C		- 1	7-C	S−C	
	trans	cis	trans	cis	trans	cis	cis	trans	trans	cis
N-Ethyl-N-methylformamide	34.0	28.9	44.5	39.1	14.5	12.5				
N-Ethyl-N-methylacetamide	35.6	32.4	45.5	42.3	14.0	12.9				
N-Ethyl-N-methylpivalamide	36.0	36.0	45.2	45.2	13.5	13.5				
N-Isopropyl-N-methylformamide	28.9	24.4	49.7	42.7	21.2	19.5				
N-Isopropyl-N-methylacetamide	29.2	25.6	49.2	43.8	20.8	19.9				
N-n-Butyl-N-methylformamide	34.4	29.5	48.9	43.8	30.8	29.1	20.6	20.2	14.4	14.4
N-n-Butyl-N-methylacetamide	36.1	32.9	50.7	47.2	31.4	30.3	21.7	20.8	14.6	14.6
N-n-Butyl-N-methylisobutyramide	35.4	33.6	6.64	47.7	32.1	30.7	20.8	20.5	14.6	14.6
N-n-Butyl-N-methylpivalamide	36.7	36.7	50.4	50.4	30.5	30.5	20.8	20.8	14.6	14.6
N-t-Butyl-N-methylformamide	31.9	31.9	55.1	55.1	29.2	29.2				
N-t-Butyl-N-methylacetamide	33.3	33.3	56.5	56.5	28.9	28.9				

 $<sup>^{\</sup>mathbf{a}}$ Chemical shifts are in ppm from TMS.

<sup>&</sup>lt;sup>b</sup>All spectra were obtained at 0°C.

<sup>&</sup>lt;sup>C</sup>Carbon position relative to nitrogen or carbonyl carbon is denoted lpha, eta,  $\gamma$  ... .

Table 36. (Cont'd.)

	25.9	170.7	N-t-Butyl-N-methylacetamide
		161.2	N-t-Butyl-N-methylformamide
29.1	39.3	175.9	$N-\underline{n}-Butyl-N-methylpivalamide$
20.0	30.2	175.8	N-n-Butyl-N-methylisobutyramide
	22.3	169.5	N-n-Butyl-N-methylacetamide
		163.3	N-n-Butyl-N-methylformamide
	22.9	169.5	N-Isopropyl-N-methylacetamide
		162.6	N-Isopropyl-N-methylformamide
29.0	39.3	176.3	N-Ethyl-N-methylpivalamide
٠	22.3	170.0	N-Ethyl-N-methylacetamide
		163.7	N-Ethyl-N-methylformamide
B-C	<b>υ-</b> δ	000	Amide
Carbonyl Substituents	Su		

## DISCUSSION

#### Hindered Internal Rotation

# Total Lineshape Analysis

The only reliable method for extracting kinetic results from NMR data is by direct comparison of the experimental lineshape with the spectrum calculated using the theoretical lineshape equation. To obtain the best values of the NMR parameters a curve fitting procedure is required and this can best be achieved by means of the digital computer. For exchange between two sites, the parameters required are: (a) the chemical shift in the absence of exchange,  $\delta v$ ; (b) the relative populations at sites A and B,  $P_A$  and  $P_B$ ; (c) the spin-spin relaxation times in the absence of exchange,  $1/T_{2A}$  and  $1/T_{2B}$ , as measured from the individual linewidths; and (d) the rate constant for the exchange process  $1/2\tau$ .

The chemical shift in the absence of exchange was initially determined at a temperature where the exchange process is slow. It was then introduced into the lineshape analysis as an adjustable parameter to be determined at each temperature below the coalescence temperature. For the amides studied in this research the calculated chemical shift in the absence of exchange varied unsystematically about the value initially measured. However, it has been shown (24) that the chemical shifts of each resonance do change individually with temperature relative to some

standard, but the chemical shift difference between the two resonances remains fairly constant over a large temperature range.

The relative populations,  $p_A$  and  $p_B$ , should be exactly 0.5 for symmetrically disubstituted amides. For the unsymmetrical amides  $p_A$  may vary between zero and unity, but should approach 0.5 with increase in temperature. In practice, this factor changes only slightly with temperature from the value measured in the absence of exchange. Gutowsky et al. (29) were able to use the constant value  $p_A = 0.54$  over the entire temperature range covered in the investigation of the barrier of N-methyl-N-benzylformamide without introducing appreciable error into the rate constants. In the research described in this thesis, the curve fitting program calculated values of  $p_A$  and  $p_B$  at each temperature up to the coalescence temperature.

The spin-spin relaxation times as measured from the linewidths in the absence of exchange become relatively unimportant as the temperature increases and exchange broadens the linewidths. These values have no particular significance since they include inhomogeneity broadening, and the rate constants are not appreciably altered if these values are held constant throughout the entire temperature range studied.

The Frequency Factor in the Arrhenius Equation

The question of what frequency factors might reasonably be expected in unimolecular reactions is discussed at length in Glasstone, Laidler and Eyring (115). According to absolute reaction rate theory the normal expectation is for the frequency factor to lie in the range  $10^{13}$  to  $10^{14}$  sec<sup>-1</sup> for the gas phase; Kondrat'ev (116) has reached the same conclusion.

Drastic exceptions can be expected only for rather unusual molecules such as those whose activated state may be a triplet electronic state with the transition back to the singlet ground state highly forbidden. Smaller departures in the liquid phase could result if the molecular ground and excited states were quite dissimilar in some important aspect such as interaction with solvent molecules. However, with amides, even if there is preferential solvation of one state or the other, it seems unlikely that the preference should change greatly from amide to amide (16). Thus, it seems reasonable that amide frequency factors should lie in the range  $10^{13}$  to  $10^{14}$  sec<sup>-1</sup>.

# Rotational Barriers in N, N-Disubstituted Amides

The energy barriers for hindered internal rotation about the C-N bond in N,N-disubstituted amides is believed to result largely from the partial double-bond character of this bond. There is a variety of evidence that the resonance structures of Figure 1 contribute nearly equally to the resonance hybrid (117,118). However, there is an insufficient amount of reliable data available to evaluate the substituent effects of  $R_1$ ,  $R_2$ ,  $R_3$  on the rotational barrier, despite the many articles that have appeared on the subject. Thus, an attempt has been made in this research to obtain more precise values for a series of N,N-dimethylamides and to extend the method of analysis to four unsymmetrically N,N-disubstituted amides. The results are summarized in Tables 37 and 38.

The barrier heights in amides are indicative of the degree of stabilization of the approximately planar ground state relative to the non-planar activated state. The factors that tend to stabilize the planar

Activation parameters for hindered internal rotation in some symmetrically N,N-disubstituted amides. Table 37.

Amide	Ea kcal/mole	$log_{1o}A$ $(A=sec^{-1})$	$\Delta G^{\dagger}$ kcal/mole	∆H <sup>†</sup> kcal/mole	eu eu	Ref.
N, N-Dimethylformamide (DMF)	19.8±0.5	12.3±0.4	20.4±0.5	19.0±0.5	4.7±1.5	This work
DMF	24.3±0.5	14.8±0.4	21.5±0.5	23.5±0.5	6.5±2.0	This work
$ exttt{N,N-Dimethylformamide-d}_1$	25.3±0.3	15.2±0.2	22.1±0.3	24.6±0.3	8.5±1.2	This work
N,N-Dimethylacetamide (DMA)	19,6±0,3	13.8±0.2	18.2±0.6		2.7	20
DMA	19,0±0,1	1	18,1±0,1	18,3±0,1	0.7±1	113
DMA	19,7±0.5	13.9±0.3	18.1±0.5	19.0±0.5	2.9±1.4	This work 90
N,N-Dimethylcarbamylchloride (DMCC)	16.9±0.5	$12.9\pm0.4$	16.8		-1.6±2.0	70
DMCC	16.7±0.3	13.9±0.4	17.1±0.6	18.0±0.6	3.0±1.8	This work
N,N-Dimethyltrichloroacetamide (DMTCA)	15.7±0.3		15.0±0.1	15.1±0.6	0.3±0.6	26
DMTCA	16.7±0.3	14.0±0.2	15.0±0.3	16, 1±0, 3	3,7±1,1	This work
N,N-Dimethylpropionamide (DMP)	21.0	15	16.6	20.4	12.7	11
DMP	16.6±0.1	ı	17.2±0.1	16.0±0.1	-4.1±1	113
DMP	18.9±0.4	13.9±0.3	17.2±0.4	18.2±0.4	3.1±1.2	This work
DMP	16.6±0.1 18.9±0.4	13.9±0.3	17.2±0.1 17.2±0.4		16.0±0.1 18.2±0.4	ı

<sup>b</sup>Long-range coupling to formyl proton was considered in total lineshape analysis. <sup>a</sup>Long-range coupling to formyl proton was neglected in total lineshape analysis.

Table 38. Activation parameters for hindered internal rotation in some unsymmetrically N,N-disubstituted amides.

	(전 · (전 ·	log A	*57	*H7	*S7	;	ES CE
Amide	kcal/mole	$(A=sec^{-1})$	kcal/mole	kcal/mole	eu,	*6	8
N-Ethyl-N-methylacetamide	20.8 ± 0.5	$14.8 \pm 0.3$	$18.0 \pm 0.5$	$20.1 \pm 0.5$	$7.0 \pm 2$	-0.10	-0.07
N-n-Butyl-N-methylacetamide	19.7	14.1	17.9	19.1	4.1	-0.13	-0.39
N-Cyclohexyl-N-methylacetamide	18.9	14.1	17.1	18.3	3.9	-0.15	-0.79
N-Isopropyl-N-methylacetamide	18.1	13.6	17.0	17.5	1.6	-0.19	-0.47

<sup>a</sup>The parameters  $\sigma^*$ , E<sub>s</sub> are the polar and steric substituent constants appropriate for non-aromatic systems and are from Ref. 120.

ground state are: (1) The degree of double-bond character in the C-N bond. The double-bond character and the bond energy should be maxima when the oxygen, carbon, and nitrogen atoms of the amide framework are coplanar. Alternatively, if the carbon and nitrogen sigma bonds have sp<sup>2</sup> hydridization the framework would be coplanar. This tends to stabilize the coplanar state. Inductive effects may alter the double-bond character by withdrawing or supplying electrons. Conjugation of the C-N bond with substituents will also have an effect. (2) Steric effects. Large, rigid substituents tend to force the trigonally hybridized atoms of the amide framework out of the plane. Repulsive forces increase as the substituent size increases, but may be relieved somewhat if the substituents can be distorted or can rotate internally themselves to reduce their effective size. Westheimer and Mayer (119) have pointed out the importance of the bending or distortion of bonds in relieving steric strain. (3) Intermolecular interactions. A substituent group may interact with another molecule, for example, intermolecular hydrogen bonding. This could cause a variety of effects. The result might be to increase the effective size of the substituent group and thereby tend to force the trigonal atoms of the amide framework out of the plane. Alternatively, the association might cause the double-bond character to increase and thereby stabilize the planar ground state.

The NMR spectra of N,N-dimethylformamide were analyzed by two different methods: (1) complete neglect of the coupling between the N-methyl protons and the formyl proton; and (2) the introduction of the coupling constants into the theoretical lineshape equation. The results from the second method agree favorably with the results for N,N-dimethylformamide-d<sub>1</sub> in which the effect of this coupling is largely removed. The barrier in N,N-dimethylformamide is considerably higher than in the remainder of the dimethylamides. The increased height of the barrier may be due to the effect of intermolecular hydrogen bonding which will stabilize the ground state (11,25,35) by formation of dimers or polymers.

For N,N-dimethylacetamide, N,N-dimethylcarbamylchloride, N,N-dimethyltrichloroacetamide, and N,N-dimethylpropionamide (Table 37) the values of  $\Delta G^{\dagger}$  agree with the best recent values within  $\pm$  0.2 kcal/mole while  $E_a$  and  $\Delta H^{\dagger}$  differ by as much as 1.0 kcal/mole, and  $\Delta S^{\dagger}$  by as much as 4.6 eu, even though all were obtained by total lineshape analysis. These differences are not far from being within the sums of the random errors and probably give a reasonable idea of the accuracy of the activation parameters determined in this study.

The effect of substituents appears to be, in nearly all cases studied, a lowering of the barrier to internal rotation. The effects are not large and separating out the steric, polar and resonance contributions is difficult (24). Both polar and resonance contributions should be small and similar for a series of saturated hydrocarbons substituents (120) and steric factors might therefore be expected to dominate. Larger substituents, whether on nitrogen or on carbonyl carbon, should tend to make the ground state more nonplanar and so reduce the barrier. In the solid state it has been shown that larger groups produce increasing nonplanar distortions in substituted amides by a twisting about the C-N bond (121). Solvent effects on  $\Delta G^{\ddagger}$  have been shown to be small so one may be justified in comparing  $\Delta G^{\ddagger}$  for neat liquids (37).

It has been pointed out (27) that  $\triangle G^{\dagger}$  decreases with the size of the aliphatic group R in the series RCON(CH<sub>3</sub>)<sub>2</sub>. The new values for N,N-dimethylacetamide and N,N-dimethylpropionamide fit neatly into this group,

for which  $\triangle G^{\dagger}$  has the values 21.0 kcal/mole (R = H) (25), 18.1 kcal/mole (R = CH<sub>3</sub>), 17.2 kcal/mole (R = -C<sub>2</sub>H<sub>5</sub>), 16.2 kcal/mole (R = -CH(CH<sub>3</sub>)<sub>2</sub>) (122) and 12.2 kcal/mole (R = -C(CH<sub>3</sub>)<sub>3</sub> (27). It was similarly shown in a study of the series CH<sub>3</sub>CONR'<sub>2</sub> that the barrier decreases with increasing size of R' (28), with  $\triangle G^{\dagger}$  = 17.7 kcal/mole (R' = - C<sub>2</sub>H<sub>5</sub>), 17.6 kcal/mole (R' = isobutyl), and 16.2 kcal/mole (R' = isopropyl) reported.

In the series of unsymmetrically N,N-disubstituted amides  $CH_3CON(CH_3)R'$  studied (Table 38) it is found that  $\Delta G^{\dagger}$  decreases in the sequence 18.1 kcal/mole (R' = methyl), 18.0 kcal/mole (R' = ethyl), 17.9 kcal/mole (R' = n-butyl), 17.1 kcal/mole (R' = cyclohexyl), and 17.0 kcal/mole (R' = isopropyl);  $\Delta H^{\dagger}$  and  $E_a$  decrease in the same order. Values of the steric and inductive substituent constants,  $E_a$  and  $\sigma^*$  (120), are given in Table 38 and it is seen that  $\Delta G^{\dagger}$  decreases with increasing ability to withdraw electrons inductively and with increasing size (except for cyclohexyl). Both factors (more negative  $\sigma^*$  and more negative  $E_a$  values) would be expected to lead to a decrease in  $\Delta G^{\dagger}$  for substituents on nitrogen so the results are reasonable; however, one cannot judge their relative importance. Since values of  $E_a$  may contain a hyperconjugative component, and since the parameters are being used here in a somewhat different situation than that for which they were derived (120), any more detailed analysis of the correlations would not be justified.

The values of K and of  $-\Delta G_{300}$ ° for the conformational equilibria in unsymmetrically N,N-disubstituted amides (Table 39) are somewhat lower than those obtained earlier from peak areas (49), but the errors in each case are rather large. Substituents decrease  $\Delta G_{300}$ ° in the same order that they lead to decreases in the rotational barrier, but the energy changes are much larger for  $\Delta G^{\ddagger}$ . There must then be important substituent

Table 39. Conformer equilibria in unsymmetrically N.N-disubstituted amides.

Compound	K=p <sub>A</sub> /p <sub>B</sub>	ΔG <sub>300°</sub> (cal/mole)	K(peak areas) <sup>a</sup>
N-Ethyl-N-methylacetamide	1.04 <sup>b</sup>	-21	1.04
N-n-Butyl-N-methylacetamide	1.09	-50	1.13
N-Cyclohexyl-N-methylacetamide	1.15	-81	1.22
N-Isopropyl-N-methylacetamide	1.25	-131	1.38

The preferred configuration (A) has the larger alkyl group <u>cis</u> to carbonyl oxygen (49).

effects on the energy of the transition state. These would be expected to be quite different from those for the ground state since the configuration at nitrogen can be nonplanar as a result of the decreased delocalization of the lone pair.

# Resonance Assignments in Tertiary Amides by Lanthanide-induced Shifts

The use of lanthanide complexes as reagents to induce paramagnetic shifts in the NMR spectra of polar organic molecules is now well established (84-101). The paramagnetic shift arises from the association of the lanthanide complex with the polar organic substrate and is largely dominated by dipolar (pseudo-contact) interactions (102,103). The magnitude of the paramagnetic shift is largely determined by the distance of the given nuclei from the lanthanide ion. Amides are known to protonate preferentially on the carbonyl oxygen (123), since the nitrogen lone pair

The error in K is a few percent for each method.

is extensively delocalized; one would, therefore, expect that the chemical shift reagent would be complexed through the lone pairs of electrons on oxygen and that the induced shifts in the <u>cis</u> (to carbonyl oxygen) and <u>trans</u> N-alkyl substituents would differ.

A linear correlation was found for the chemical shift for each group of protons in several amides and the mole ratio of shift reagent to amide. Chemical shifts relative to TMS were plotted against the mole ratio of added shift reagent and values of the chemical shift for an equimolar ratio of shift reagent  $(\delta_{\text{CCl}_4}^{n=1})$  and pure amide  $(\delta_{\text{CCl}_4}^{n=0})$  were obtained by extrapolation. From these, values of  $\Delta \text{Eu}(\Delta \text{Eu} = \delta_{\text{CCl}_4}^{n=1} - \delta_{\text{CCl}_4}^{n=0})$  were calculated for each group of protons (Table 40). Extrapolation of the lines to a molar ratio of zero allows assignments to be made for the amide resonances in the uncomplexed amide (Table 41).

The validity of the method was established by the choice of 1-methyl-2-pyrrolidinone as a model system since the N-methyl group is fixed in the <u>cis</u> position. As expected, the <u>cis</u> methyl protons were shifted to a greater extent than the <u>trans</u>-methylene protons in the solutions containing the complexed amide. For the remaining amides, the resonances of the <u>cis-trans</u> pair shifted the greater amount were assigned to the <u>cis</u> group.

The assignments of Table 41 for the uncomplexed amides confirm those previously made by other methods for N,N-dimethylformamide (47,48,50,51, 124), N,N-dimethylacetamide (47,48,50,51,124), N,N-dimethyltrifluoroacetamide (11), N,N-diethylformamide (51), N,N-diisopropylformamide (51), and N-methyl-N-isopropylformamide (49). The method is rapid, readily applicable to a wide variety of amides and, to the extent of this investigation, appears to be generally valid. When a single resonance is observed

Table 40. AEu values for several N,N-disubstituted amides.

<sup>&</sup>lt;sup>a</sup>Both isomers of CHON( $CH_3$ )(i- $C_3H_7$ ) are present in the same solution.

Table 41. Proton resonance assignments in some N,N-disubstituted amides in CCl<sub>4</sub> solution.

	Assign		ofield Resonand cans Pair <sup>a</sup>	ce of
Compound	<u>-СН</u> 3	-С <u>Н</u> 2	<u>-сн</u>	T°Cb
N,N-Dimethylformamide	cis			32
N,N-Dimethylacetamide <sup>C</sup>	cis			32
${\tt N,N-Dimethyltrifluoroacetamide}^{ extbf{d}}$	cis			32
N,N-Dimethyltrichloroacetamide	cis			-22
N,N-Dimethylcarbamylchloride	cis			-22
N,N-Diethylformamide	cis	trans		32
N,N-Diisopropylformamide <sup>e</sup>	cis		trans	32
	-С <u>Н</u> 3	-С <u>н</u>	-CH(C <u>H</u> <sub>3</sub> ) <sub>2</sub>	
N-Methyl-N-isopropylformamide <sup>f</sup>	cis	trans	cis	32

The designation "cis" in this table indicates that the upfield resonance of the cis-trans pair for the indicated group is cis to oxygen in the CCl, solution containing no shift reagent.

The temperature was chosen, in each case, to be well below the coalescence temperature so that the isomers are distinguishable by NMR.

<sup>&</sup>lt;sup>C</sup>Use of Pr(fod)<sub>3</sub> gave upfield induced shifts but the assignment of the proton resonances was the same.

In this amide the spin-spin couplings  $J_{H-F}$  are anomalous in that  $J_{H-F}(\underline{cis}) > J_{H-F}(\underline{trans})$  (11).

<sup>&</sup>lt;sup>e</sup>This result is less certain than the others since the chemical shift between the methyl protons in the uncomplexed amide ( $\simeq 1 \text{ Hz}$ ) is the same order of magnitude as the error in carrying out the extrapolation.

f The major isomer (67%) has the N-methyl substituent cis to oxygen (49).

for the <u>cis</u> and <u>trans</u> protons this method can be used to determine whether the chemical shifts are accidentally equal or whether the amide is above the coalescence temperature.

#### Carbon-13 Chemical Shifts of Amides

The major advantage of carbon-13 over proton NMR for structure studies is in the increased separation of the chemically shifted peaks. Under normal operating conditions the linewidths in the spectra of the two nuclei are not very different whereas the shift range for carbon-13 nuclei is about twenty times larger than for protons. Since chemical shifts are sensitive to structural changes, the increased separation of chemical shifts for carbon provides a more powerful way of differentiating proposed structures. The theory relating chemical shifts to structure is complex and, at present, does not allow quantitative interpretation of the experimental data. The most useful approach for structural determination has proved to be a semi-empirical one based on the considerable body of experimental evidence, and supported in specific applications by the use of model compounds. The carbon-13 chemical shifts in fifty monosubstituted and symmetrically and unsymmetrically disubstituted amides are given in Tables 32, 33, 34, and 36.

The carbon-13 chemical shifts in amides are to a substantial degree influenced by inductive, resonance, and steric effects in a manner which is familiar for a variety of phenomena involving organic compounds. The inductive effect of the nitrogen or carbonyl oxygen in amides on the chemical shifts of the carbons in substituents may be assumed to be independent of conformation but dependent on the degree to which each carbon

is substituted. The resonance effect relates to the kinds and stereochemical relationships between pairs of atoms on vicinal carbons and is assumed to affect only the shifts of the carbons directly involved. This effect, which has been considered by Grant et al. (57), is expected to be sensitive to the conformation. Steric effects have been shown to be very important in various kinds of hydrocarbons and are expected to be especially sensitive to conformational changes (57). The problem in sorting out these influences is that with many substitutions a composite of effects can be expected.

Nevertheless, comparison of the chemical shifts in amides allows certain generalizations to be drawn. The carbon directly bonded to nitrogen is shifted downfield by approximately 1.5 ppm whenever the formyl proton is replaced by an alkyl group, probably as a result of an inductive effect which is transmitted by the electrons delocalized in the central C-N bond. A carbon directly bonded to nitrogen is also shifted downfield by about 9.0 ppm when the hydrogen bonded to nitrogen, as in a monosubstituted amide, is replaced by a carbon atom. This shift is almost identical to the negative inductive effect (+9.4 ppm) which is observed for hydrocarbons. The chemical shift difference between the carbons directly bonded to nitrogen which are cis and trans to the carbonyl oxygen is consistently about 5 ppm for disubstituted formamides and decreases with the degree or kind of substitution on the carbonyl carbon. The large chemical shift difference arises from intramolecular electric and magnetic fields which are produced by the anisotropies of the C=O and OC-R (R = H,CH3...) bonds (55). The chemical shift differences between cis and trans aliphatic carbons get smaller for carbons farther away from the carbonyl group. This is to be expected, since the anisotropy effect

falls off as the cube of the inverse of the distance from the center of the anisotropic group.

The monosubstituted amides exhibit only one set of carbon resonances for the N-alkyl substituent. Proton NMR studies, and a variety of other methods (114), have shown that the preferred configuration or isomer in monosubstituted amides is the one in which the N-alkyl substituent is cis to the carbonyl oxygen. In most of the disubstituted amides studied the internal rotation about the central C-N bond can be slowed down on the NMR time scale by decreasing the temperature so that both rotational isomers could be observed. However, when the carbonyl carbon is bonded to a t-butyl group, decreasing the temperature to the freezing point of the particular pivalamide did not sufficiently slow down the rotation about the C-N bond so that both isomers could be distinguished.

Assignment of the carbon-13 chemical shifts for nitrogen substituents were made with the aid of lanthanide shift reagents. The effect of the shift reagent in the carbon-13 spectrum of an amide was assumed to be the same as in the proton NMR spectrum, that is, the carbon is a cistrans pair shifted the greater amount can be assigned to the nitrogen substituent cis to the carbonyl oxygen. For the  $\alpha$  and  $\beta$  carbons on nitrogen in N,N-di-n-propylformamide the up-field carbon resonance for each cis-trans pair was shifted the greater amount and was assigned to the carbon in the nitrogen substituent cis to the carbonyl oxygen. However, the  $\gamma$  carbons are reversed, the down-field carbon resonance for this cis-trans pair being shifted the larger amount.

One of the purposes in obtaining the carbon-13 chemical shifts for a large number of amides was to use the data to derive a set of parameters by which the chemical shifts in any amide could be predicted,

analogous to the method developed by Grant et al. (57) for hydrocarbons. However, because of the inductive effects of both the nitrogen atom and the carbonyl group, and the large steric interactions between substituents, a set of parameters could not be found with any reasonable certainty for the amides studied.

## SUMMARY

Nuclear magnetic resonance methods have been employed in a series of studies of the molecular structure and internal motions of amides in the liquid phase.

- (1) It has been shown that lanthanide shift reagents provide a reliable method of assigning the NMR resonances to the <u>cis</u> and <u>trans</u> isomers in disubstituted amides. Assignments have been made for a representative series of compounds.
- (2) The carbon-13 chemical shifts in fifty monosubstituted and disubstituted amides have been measured and empirically correlated with structural effects.
- (3) The barriers hindering internal rotation about the central C-N bond of a series of dimethylamides have been measured. The NMR method for carrying out these studies has been improved by the digitization of spectra followed by computer curve fitting of the lineshapes to the NMR parameters.
- (4) Internal rotation about the central C-N bond of a series of unsymmetrically N,N-disubstituted amides has been studied by the NMR technique developed in this thesis. The energies of activation have been related to properties of the substituents.

LIST OF REFERENCES

## LIST OF REFERENCES

- 1. L. Pauling, "The Nature of the Chemical Bond," 3rd ed., Cornell University Press, Ithaca, N. Y., 1960, p. 281.
- J. Zabicky, Ed., "The Chemistry of Amides," Interscience, New York, N. Y., 1970.
- 3. J. Ladell and B. Post, Acta. Cryst., 7, 559 (1954).
- 4. J. L. Katz, Dissertation Abstr., 17, 2039 (1957).
- 5. C. Pedone, E. Benedetti, A. Immirzi, and G. Allegra, J. Amer. Chem. Soc., 92, 3549 (1970).
- 6. C. C. Costain and J. M. Dowling, J. Chem. Phys., 32, 158 (1960).
- 7. R. H. Schwendeman, private communication.
- 8. W. D. Phillips, J. Chem. Phys., 23, 1363 (1955).
- 9. H. S. Gutowsky and C. H. Holm, J. Chem. Phys., 25, 1228 (1956).
- 10. J. C. Woodbrey and M. T. Rogers, J. Amer. Chem. Soc., 84, 13 (1962).
- 11. M. T. Rogers and J. C. Woodbrey, J. Phys. Chem., 66, 540 (1962).
- 12. A. Allerhand, H. S. Gutowsky, J. Jonas, and R. A. Meinzer, J. Amer. Chem. Soc., 88, 3185 (1966).
- 13. C. S. Johnson, Jr., in "Advances in Magnetic Resonance," Vol. I, J. S. Waugh, Ed., Academic Press, New York, N. Y., 1965, pp. 33-102.
- 14. G. Binsch in "Topics in Stereochemistry," Vol. III, E. L. Eliel and N. L. Allinger, Eds., Interscience, New York, N. Y., 1968, pp. 97-192.
- 15. W. E. Stewart and T. H. Siddall, III, Chem. Rev., 70, 517 (1970).
- 16. W. E. Stewart and T. H. Siddall, III, in "Progress in NMR Spectroscopy," Vol. VI, J. W. Emsley, J. Feeney, and L. H. Sutcliffe, Eds., Pergamon Press, London, 1969, pp. 33-147.
- 17. H. Kessler, Agnew. Chem. Int. Ed., 9, 219 (1970).

- 18. J. P. Lowe in "Progress in Physical Organic Chemistry," Vol. VI, A. Streitweiser and R. W. Taft, Eds., Interscience, New York, N. Y., 1968, pp. 1-80.
- 19. T. Drakenberg and S. Forsen, Chem. Commun., 1404 (1970).
- 20. R. C. Neuman, Jr., and V. Jonas, J. Amer. Chem. Soc., 90, 1970 (1968).
- 21. L. W. Reeves, R. C. Shaddick, and K. N. Shaw, J. Phys. Chem., 75, 3372 (1971).
- 22. L. W. Reeves and K. N. Shaw, Can. J. Chem., 49, 3683 (1971).
- 23. L. W. Reeves and K. N. Shaw, Can. J. Chem., 49, 3671 (1971).
- 24. R. F. Hobson, Ph.D. thesis, University of Waterloo, Waterloo, Canada, 1972.
- 25. M. Rabinovitz and A. Pines, J. Amer. Chem. Soc., 91, 1585 (1969).
- 26. T. Drakenberg, K. Dahlqvist, and S. Forsen, Acta Chem. Scand., 24, 694 (1970).
- 27. L. L. Graham and R. E. Diel, J. Phys. Chem., 73, 2696 (1969).
- 28. T. H. Siddall, III, W. E. Stewart, and F. D. Knight, J. Phys. Chem., 74, 3580 (1970).
- 29. H. S. Gutowsky, J. Jonas, and T. H. Siddall, III, J. Amer. Chem. Soc., 89, 4300 (1967).
- 30. R. C. Neuman, Jr., and V. Jonas, J. Phys. Chem., 75, 3532 (1971).
- 31. O. A. Gansow, J. Killough, and A. R. Burke, J. Amer. Chem. Soc., 93, 4297 (1971).
- 32. E. S. Gore, D. J. Blears, and S. S. Danyluk, Can. J. Chem., <u>43</u>, 2135 (1965).
- 33. A. G. Whittaker and S. Siegel, J. Chem. Phys., 42, 3320 (1965).
- 34. G. Fraenkel and C. Franconi, J. Amer. Chem. Soc., 82, 4478 (1960).
- 35. R. C. Neuman, Jr., and L. B. Young, J. Phys. Chem., 69, 2570 (1965).
- 36. F. Conti and W. von Philipsborn, Helv. Chim. Acta., 50, 603 (1967).
- 37. C. W. Fryer, F. Conti, and C. Franconi, Ric. Sci., 35 [2A], 788 (1965).
- 38. D. G. Gehring, W. A. Mosher, and G. S. Reddy, J. Org. Chem., <u>31</u>, 3436 (1966).
- 39. A. Allerhand and H. S. Gutowsky, J. Chem. Phys., <u>41</u>, 2115 (1964).

- 40. R. C. Neuman, Jr., D. N. Roark, and V. Jonas, J. Amer. Chem. Soc., 89, 3412 (1967).
- 41. C. Franconi, Scienza e Tecnica, N. S., 4, 183 (1960); Z. Elektrochem., 65, 645 (1961).
- 42. J. A. Weil, A. Blum, A. H. Heiss, and J. K. Kinnaird, J. Chem. Phys., 46, 3132 (1966).
- 43. A. Mannschreck, Tetrahedron Lett., 1341 (1965).
- 44. A. Mannschreck, H. A. Staab, and D. Wurmb-Gerlich, Tetrahedron Lett., 2003 (1963).
- 45. A. Calzolari, F. Conti, and C. Franconi, J. Chem. Soc. (B), 555 (1970).
- 46. P. T. Narasimhan and M. T. Rogers, J. Phys. Chem., 63, 1388 (1959).
- 47. V. J. Kowalewski and D. G. Kowalewski, J. Chem. Phys., <u>32</u>, 1272 (1960).
- 48. J. V. Hatton and R. E. Richards, Mol. Phys., 3, 253 (1960); 5, 139 (1962).
- 49. L. A. LaPlanche and M. T. Rogers, J. Amer. Chem. Soc., <u>85</u>, 3728 (1963).
- 50. F. A. L. Anet and A. J. R. Bourn, J. Amer. Chem. Soc., <u>87</u>, 5251 (1965).
- 51. M. Frucht, A. H. Lewin, and F. A. Bovey, Tetrahedron Lett., 1083, 3707 (1970).
- 52. J. B. Stothers, Appl. Spectrosc., 26, 1 (1972).
- 53. E. W. Randall, Chem. Brit., 7, 371 (1971).
- 54. P. C. Lauterbur, J. Chem. Phys., 26, 217 (1957).
- 55. W. McFarlane, Chem. Commun., 418 (1970).
- 56. G. C. Levy and G. L. Nelson, J. Amer. Chem. Soc., 94, 4897 (1972).
- 57. D. M. Grant and E. G. Paul, J. Amer. Chem. Soc., 86, 2984 (1964).
- 58. T. D. Brown, Ph.D. thesis, University of Utah, Salt Lake City, Utah, 1965.
- J. D. Roberts, F. J. Weigert, J. I. Kroschwitz, and H. J. Reich,
   J. Amer. Chem. Soc., <u>92</u>, 1338 (1970).
- 60. R. Hagen and J. D. Roberts, J. Amer. Chem. Soc., 91, 4504 (1969).

- B. V. Cheney, Ph.D. thesis, University of Utah, Salt Lake City, Utah, 1966.
- 62. F. Bloch, W. W. Hansen, and M. Packard, Phys. Rev., 70, 460 (1946).
- 63. H. S. Gutowsky, D. W. McCall, and C. P. Slichter, J. Chem. Phys., 21, 279 (1953).
- 64. H. M. McConnell, J. Chem. Phys., 28, 430 (1958).
- 65. K. J. Laidler, "Chemical Kinetics," McGraw-Hill, New York, N. Y., 1962.
- 66. S. W. Benson, "The Fundamentals of Chemical Kinetics," McGraw-Hill, New York, N. Y., 1960.
- 67. J. A. Pople, Disc. Faraday Soc., 34, 7 (1962).
- 68. J. A. Pople, W. G. Schneider, and H. J. Bernstein, "High-Resolution Nuclear Magnetic Resonances," McGraw-Hill, New York, N. Y., 1959.
- 69. A. Saika and C. P. Slichter, J. Chem. Phys., 22, 26 (1954).
- 70. M. Karplus and J. A. Pople, J. Chem. Phys., 38, 2803 (1963).
- 71. J. W. Emsley, J. Chem. Soc. (A), 1387 (1968).
- 72. J. E. Bloor and D. L. Green, J. Amer. Chem. Soc., 89, 6835 (1967).
- 73. H. S. Gutowsky and D. W. McCall, Phys. Rev., <u>82</u>, 748 (1951).
- 74. H. S. Gutowsky, D. W. McCall, and C. P. Slichter, Phys. Rev., 84, 589 (1951).
- 75. E. L. Hahn and D. E. Maxwell, Phys. Rev., <u>84</u>, 1246 (1951); <u>88</u>, 1070 (1952).
- 76. N. F. Ramsey, Phys. Rev., <u>91</u>, 303 (1953).
- 77. J. A. Pople and D. P. Santry, Mol. Phys., 8, 1 (1964).
- 78. E. G. Paul and D. M. Grant, J. Amer. Chem. Soc., <u>86</u>, 2977 (1964).
- 79. F. J. Weigert and J. D. Roberts, J. Amer. Chem. Soc., 89, 2967 (1967).
- 80. K. F. Kuhlmann, D. M. Grant, and R. K. Harris, J. Chem. Phys., <u>52</u>, 3439 (1970).
- 81. D. Doddrell, V. Glushko, and A. Allerhand, J. Chem. Phys., <u>56</u>, 3683 (1972).
- 82. K. F. Kuhlmann and D. M. Grant, J. Amer. Chem. Soc., 90, 755 (1968).

- 83. R. L. Lichter and J. D. Roberts, J. Amer. Chem. Soc., 93, 3200 (1971).
- 84. C. C. Hinckley, J. Amer. Chem. Soc., 91, 5160 (1969).
- 85. J. K. M. Sanders and D. H. Williams, Chem. Commun., 422 (1970).
- 86. J. Briggs, G. H. Frost, F. A. Hart, G. P. Moss, and M. L. Staniforth, Chem. Commun., 749 (1970).
- 87. G. H. Wahl, Jr. and M. R. Peterson, Jr., Chem. Commun., 1167 (1970).
- 88. J. Briggs, F. A. Hart, and G. P. Moss, Chem. Commun., 1506 (1970).
- 89. P. V. Demarco, T. K. Elzey, R. B. Lewis, and E. Wenkert, J. Amer. Chem. Soc., 92, 5734 (1970).
- 90. P. V. Demarco, T. K. Elzey, R. B. Lewis, and E. Wenkert, J. Amer. Chem. Soc., <u>92</u>, 5737 (1970).
- 91. G. M. Whitesides and D. W. Lewis, J. Amer. Chem. Soc., <u>92</u>, 6979 (1970).
- 92. C. C. Hinckley, J. Org. Chem., 35, 2834 (1970).
- 93. F. I. Carroll and J. T. Blackwell, Tetrahedron Lett., 4173 (1970).
- 94. D. R. Crump, J. K. M. Sanders, and D. H. Williams, Tetrahedron Lett., 4419 (1970).
- 95. K. L. Liska, A. F. Fentiman, Jr., and R. L. Foltz, Tetrahedron Lett., 4650 (1970).
- 96. J. K. M. Sanders and D. H. Williams, J. Amer. Chem. Soc., <u>93</u>, 641 (1971).
- 97. R. E. Rondeau and R. E. Sievers, J. Amer. Chem. Soc., <u>93</u>, 1525 (1971).
- 98. W. Horrocks, Jr., and J. P. Sipe, III, J. Amer. Chem. Soc., <u>93</u>, 6800 (1971).
- 99. J. Briggs, F. A. Hart, G. P. Moss, and E. W. Randall, Chem. Commun., 364 (1971).
- E. Wenkert, D. W. Cochran, E. D. Hagaman, R. B. Lewis, and F. M. Schell, J. Amer. Chem. Soc., 93, 6271 (1971).
- 101. M. Witanowski, L. Stefaniak, H. Januszewski, and Z. W. Wolkowski, Tetrahedron Lett., 1653 (1971).
- 102. R. J. Kurland and B. R. McGarvey, J. Magn. Res., 2, 286 (1970).
- 103. B. R. McGarvey, J. Chem. Phys., 53, 86 (1970).
- 104. R. F. Nystrom, W. H. Yanko, and W. G. Brown, J. Amer. Chem. Soc., <u>70</u>, 441 (1948).

- 105. J. D. Cox and R. J. Warne, Nature, 165, 563 (1950).
- 106. S. M. McElvain and C. L. Stevens, J. Amer. Chem. Soc., <u>69</u>, 2667 (1947).
- 107. L. A. LaPlanche, Ph.D. thesis, Michigan State University, East Lansing, Michigan, 1963.
- 108. J. C. Woodbrey, Ph.D. thesis, Michigan State University, East Lansing, Michigan, 1960.
- 109. W. C-T. Tung, Ph.D. thesis, Michigan State University, East Lansing, Michigan, 1968.
- 110. D. DeMaw, Ed., "The Radio Amateur's Handbook," 47th Ed., 1970, p. 244.
- 111. L. N. Mulay in "Treatise on Analytical Chemistry," Pt. I, Vol. IV, I. M. Kolthoff and P. J. Elving, Eds., Interscience, New York, N. Y., 1963, p. 1827.
- 112. J. L. Dye and V. A. Nicely, J. Chem. Ed., 48, 443 (1971).
- 113. T. Drakenberg, K-I. Dahlqvist, and S. Forsen, J. Phys. Chem., <u>76</u>, 2178 (1972).
- 114. L. A. LaPlanche and M. T. Rogers, J. Amer. Chem. Soc., <u>86</u>, 337 (1964).
- 115. S. Glasstone, K. J. Laidler, and H. Eyring, "The Theory of Rate Processes," McGraw-Hill, New York, N. Y., 1941, p. 296.
- 116. V. N. Kondrat'ev, "Kinetics of Chemical Gas Reactions," Book 1, Academy of Sciences of U.S.S.R., Moscow, 1958. Translated by U.S. Joint Publications Research Service, New York, N. Y., 1962.
- 117. R. J. Kurland and E. B. Wilson, Jr., J. Chem. Phys., 27, 585 (1957).
- 118. R. J. Kurland, J. Chem. Phys., 23, 2202 (1955).
- 119. F. H. Westheimer and J. E. Mayer, J. Chem. Phys., 14, 733 (1946).
- 120. J. Shorter, Quart. Rev. (London), 24, 433 (1970).
- 121. P. Ganis, G. Avitabile, S. Migdal, and M. Goodman, J. Amer. Chem. Soc., 93, 3328 (1971).
- 122. G. Isaksson and J. Sandstrom, Acta Chem. Scand., 21, 1605 (1967).
- 123. R. J. Gillespie and T. Birchall, Can. J. Chem., 41, 148 (1963).
- 124. B. B. Wayland, R. S. Drago, and H. S. Henneike, J. Amer. Chem. Soc., 88, 2455 (1966).

